UNIVERSITÀ
DEGLI STUDI
DI PADOVA

Sede Amministrativa: Università degli Studi di Padova

Dipartimento di GEOSCIENZE

DOTTORATO DI RICERCA IN : SCIENZE DELLA TERRA
CICLO XXVIII

MORPHODYNAMIC EVOLUTION OF MEANDERING CHANNELS IN TIDAL LANDSCAPES: SEDIMENTOLOGY AND STRATAL ARCHITECTURE

Coordinatore : Ch.mo Prof. Fabrizio Nestola

Supervisore :Ch.mo Prof. Massimiliano Ghinassi

Co-supervisore :Ch.mo Prof. Andrea D'Alpaos

Dottorando : Lara Brivio

È proprio quando si crede che sia tutto finito,

che tutto comincia.

- Daneil Pennac -

It is just when you think it's all over,

that everything begins.

- Daneil Pennac -

TABLE OF CONTENTS

ABSTRACT

Meandering channels constitute one of the fundamental components of tidal systems, as related tidal point bars are ubiquitous features in lagoonal or estuarine sedimentary successions. Nevertheless, a limited number of studies analyzed their morphodynamic evolution, together with their planimetric shape and morphometric characteristics. Their internal architecture and sedimentary facies distribution are relatively unexplored, and commonly investigated using facies models developed for fluvial meander bends.

Focusing on differences, more than on similarities, between tidal and fluvial meanders, the present work aims at investigating the stratal architecture and sedimentary facies distribution of selected tidal point bars in the Venice Lagoon (Adriatic Sea, Italy). Three main issue were investigate by the present work: i) the role of low order tributaries in controlling the evolution of tidal meander bend; ii) the influence of salt marsh aggradation in shaping geometries of tidal point bars, iii) sedimentary process and morphodynamics changes acting on subtidal point bars. The morphodynamic evolution of tidal channels, and related sedimentary products, were analyzed using a multidisciplinary approach, which comprises the comparison of historical photos, the interpretation of high-resolution sub-bottom profiles, core logging analysis and 3D modelling.

The main results stemmed out form the study sites highlight that: I) lateral tributaries can strongly influence the evolution of bends modifying local mechanisms of sediment and flow distribution; II); the migration of tidal point bars occurs under aggradational conditions both in intertidal and subtidal setting; III) subtidal bars evolve under the strong interaction between wave and tidal currents.

RIASSUNTO

I canali meandriformi costituiscono una delle principali componenti dei sistemi tidali e, come le relative point bar, sono una caratteri ricorrenti all'interno delle successioni sedimentarie lagunari. Tuttavia, un numero limitato di studi hanno analizzato l'evoluzione morfodinamica e le caratteristiche morfometriche di canali meandriformi tidali. La loro architettura interna e la distribuzione delle facies sedimentarie sono relativamente inesplorate, e comunemente investigate utilizzando i modelli di facies sviluppati per i meandri fluviali.

Concentrandosi sulle differenze, più che sulle similitudini, tra i meandri tidali e fluviali, questo lavoro si propone di investigare le architetture stratali e la distribuzione delle facies sedimentarie delle point bar selezionate nella della Laguna di Venezia (Mare Adriatico, Italia). In questo lavoro vengono affrontate tre problematiche principali: i) il ruolo dei tributari di ordine inferiore nell'evoluzione dei meandri tidali; ii) l'influenza dell'aggradazione delle barene nella modellazione delle geometrie delle point bar tidali; iii) i processi sedimentari e le variazioni morfodinamiche agenti sulle point bar subtidali. L'evoluzione morfodinamica dei canali tidali, e i relativi prodotti sedimentari, sono stati analizzati utilizzando un approccio multidisciplinare, che comprende la comparazione di foto storiche, l'interpretazione di profili sub-bottom ad alta risoluzione, log di carote e modellazione 3D.

I risultati principali ottenuti dai tre siti in esame evidenziano che: I) gli affluenti laterali possono influenzare fortemente l'evoluzione dei meandri, modificando i meccanismi locali di distribuzione dei flussi e dei sedimenti; II) la migrazione delle point bar tidali avviene in contesti aggradazionali, sia in ambienti intertidali che subtidali; III) le barre subtidali evolvono sotto l'influenza della forte interazione tra correnti da onde e di marea.

CHAPTER 1
INTRODUCTION

1.1 OVERVIEW

This study deals with tidal meandering channels and related deposits and aims at investigate the internal architecture and morphodynamic evolution of tidal point bars in the Venice Lagoon (Italy). Sedimentary products deriving from the lateral migration of inter-tidal and sub-tidal meanders and their facies distribution were analyzed through a multidisciplinary approach, that couples remote sensing, sedimentological and geophysical analyses with numerical and 3D modeling.

1.2 STATE OF THE ART

Branching and meandering tidal channels, constitute the circulation system of lagoons and estuaries. They form the pathway for tidal currents to propagate and distribute sediments and nutrients, acting a primary control on the sedimentation and ecology of costal environments (Hughes, 2012). Tidal channels cut through tidal basins forming complex dendritic networks, in which minor creeks usually converge into a major channel (Ashley and Zeff, 1988; Fagherazzi et al., 1999). Sinuous channels are very common in tidal landscapes (Fig. 1.1), where they can occur either in the intertidal or the subtidal zone (Bartholdy, 2012), and be, therefore, either periodically or constantly submerged. Their morphodynamic evolution is governed by the complex interaction between several interconnected features, such as the tidal prism, tidal asymmetry, sediment texture, and vegetation (Garofalo, 1980; Gabet, 1998; Dalrymple et al., 1991; Fenies and Faugères,

1998; Marani et al., 2002; Lanzoni and Seminara, 2002; Solari et al., 2002; Fagherazzi et al., 2004; Garotta et al., 2006), which can limit or increase erosion, deposition and lateral migration.

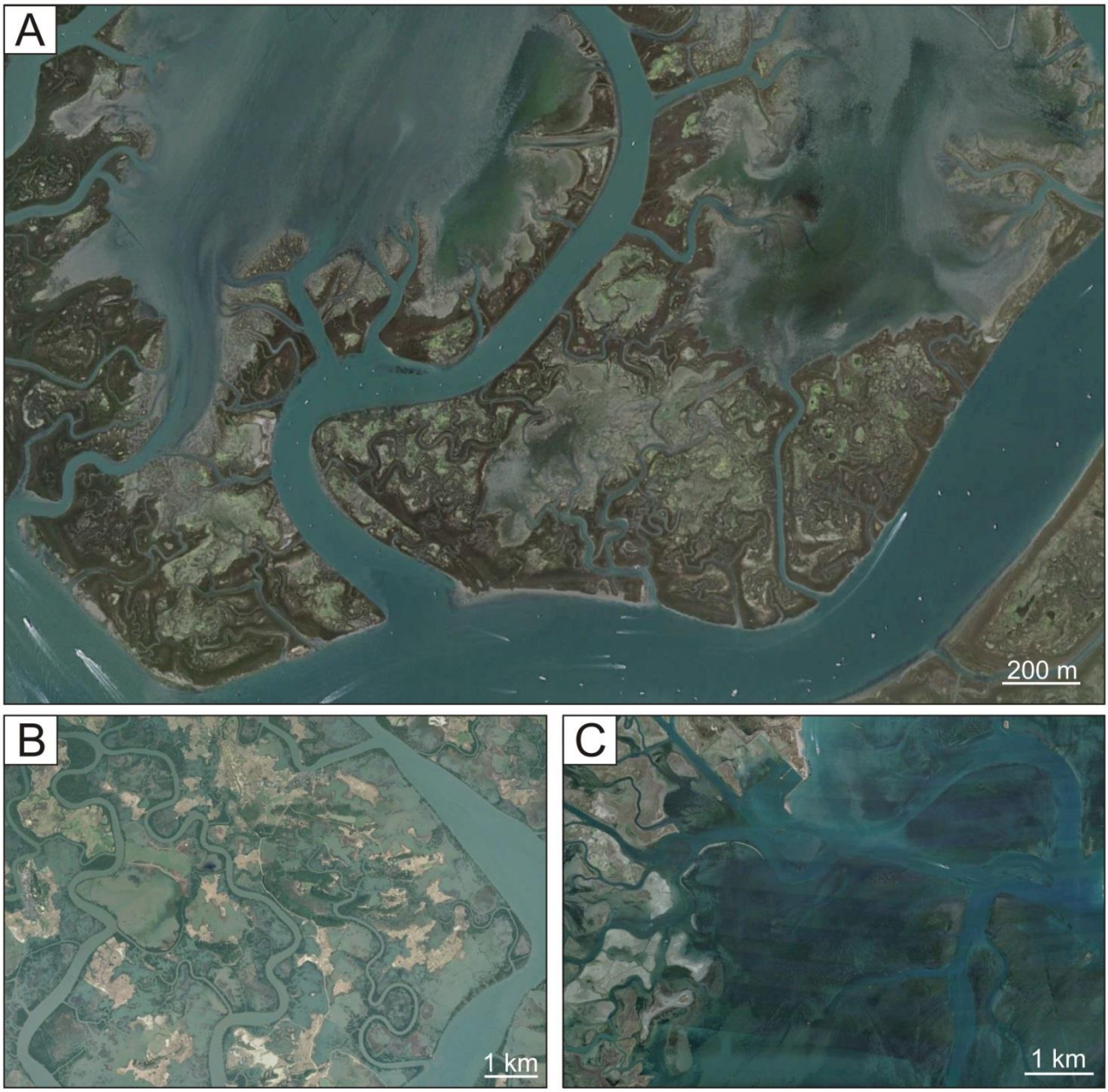

Figure 1.1: A) tidal channel network; B) meandering channels in intertidal setting; C) meandering channels in subtidal setting.

Although tidal meanders are ubiquitous features of the tidal landscape, very few studies analyses their hydrodynamics and morphodynamic evolution, together with their planimetric shape and morphometric characteristics (e.g. Marani et al., 2002; Solari et al., 2002; Fagherazzi et al., 2004).

The internal architecture and sedimentary features of tidal point bars is relatively unexplored, and mainly based on studies focused on intertidal channels crossing through modern tidal-flats (Land and Hoyt, 1966; Howard et al., 1975; Barwis, 1978; de Mowbray, 1983; Bridges and Leeder, 1976; Choi et al., 2004; Choi, 2011; Hughes, 2012), where overbank areas are generally exposed during low tide. This settings allow the morphology of the bars to be observed and the deposits to be easily investigated through trenching and coring. From these studies, an overall similarity between tidal and fluvial point bars emerged. As a consequence, the basic architectural and facies models developed for fluvial meander bends (Allen 1963; McGowen and Garner, 1970; Brice, 1974; Jackson, 1976; Nanson, 1980) are commonly used to detect tidal point bars in the fossil record (Díez-Canseco et al., 2014), by assuming that the abundance of mud, higher degree of bioturbation and bidirectional flows represent the main differences with the fluvial realm (Allen, 1982; Thomas et al., 1987), as shown in figure 1.2. and 1.3.

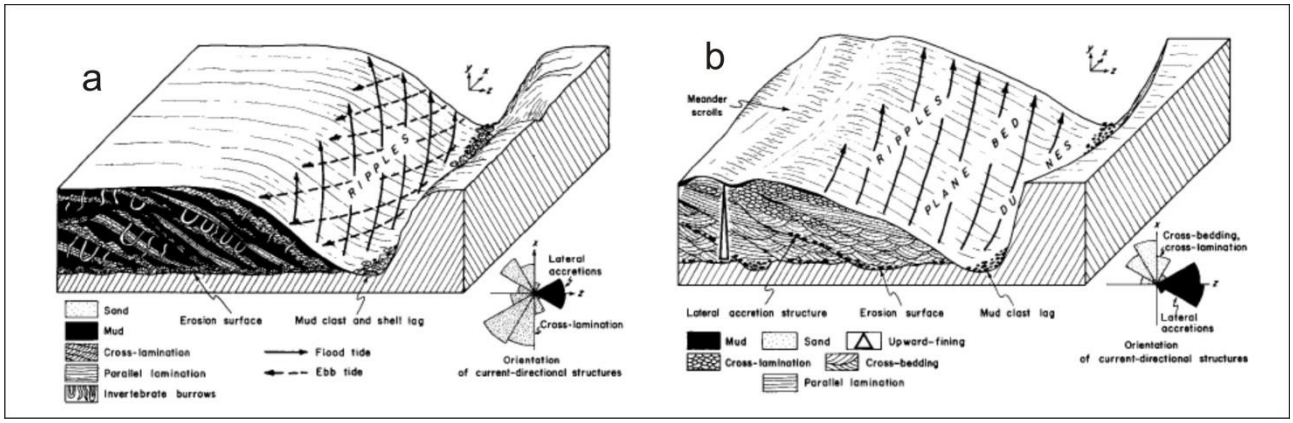

Figure 1.2: Models for the sequence of lithologies and sedimentary structures in point bars. a) Mixed mud-sand tidal gully. b) Sand-bed river. (Adapted from Allen, 1982).

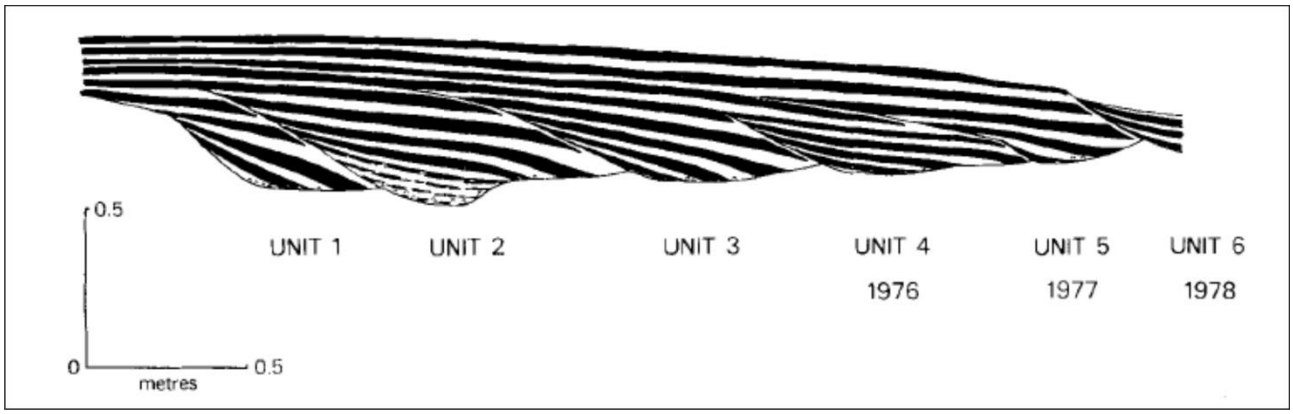

Figure 1.3: Lateral accretion deposits form a series of wedge-shaped units. Each unit represents one year's deposition, bounded by erosion scarps produced during successive winter. The point bar base shows a gradual aggradation, keeping pace with the build-up of the adjacent inter-channel flats (de Mowbray, 1983).

Nevertheless, further differences can arise from a comparison between tidal and fluvial meandering channels. Tidal channels generally form an intricate and complex network of channels, with numerous low order tributaries, which can interfere with the flow within the main channel, while fluvial channel networks are generally less articulated, with lower number of tributaries, especially near meander bends. Tidal channels, behind experiencing a daily reversion of flows, are characterized by highly variable discharges on the short term (Fig. 1.4), whereas they show an almost constant discharge on the long term, while rivers maintain a generally constant discharge on the short term and display variable discharges on the long term due to flood events, during which high velocities can be maintained for long time. Consequently, tidal discharge fluctuates within a defined range, whereas fluvial discharge can be characterized by a more marked variability. In fluvial channels, landscape forming discharges occur when water is at bankfull stage, whereas in tidal channels high-water level conditions are characterized by null velocities (Hughes, 2012).

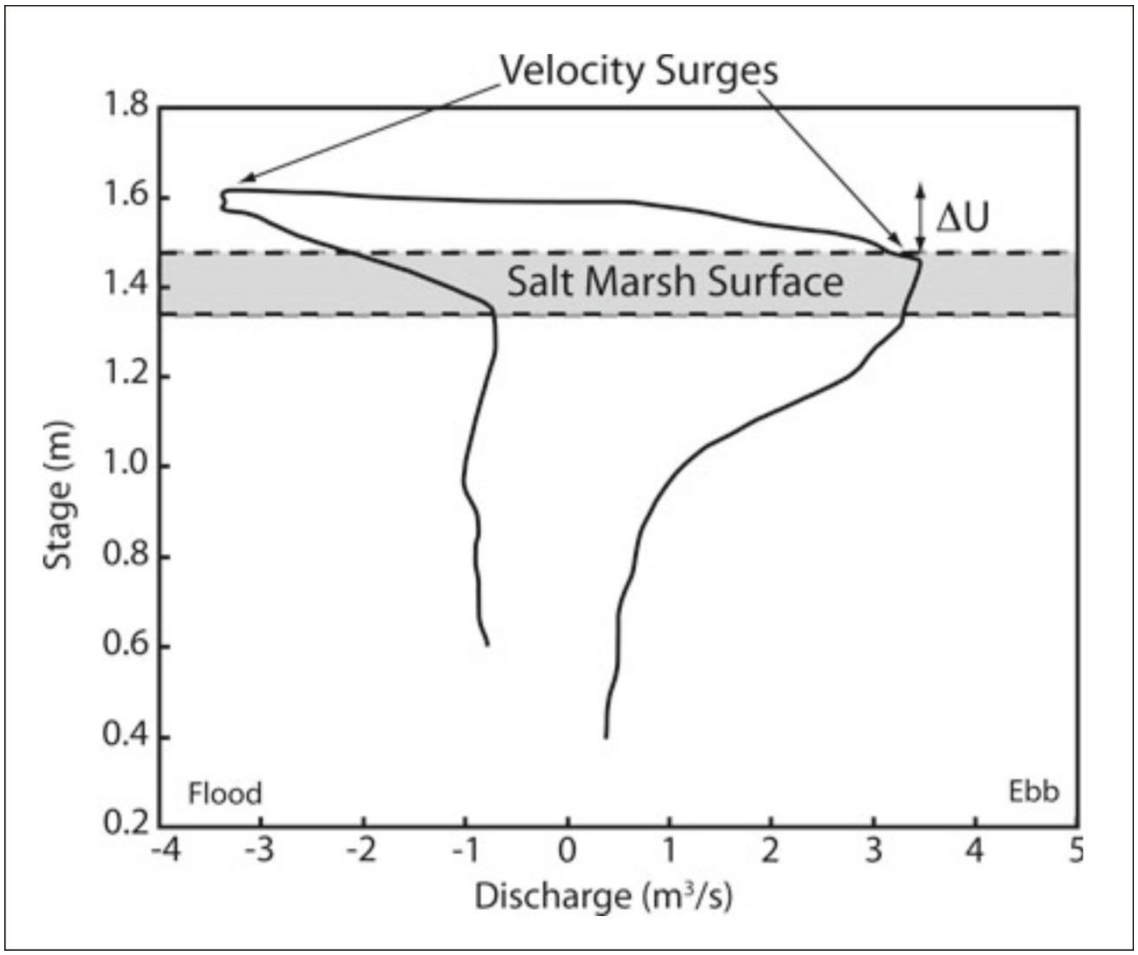

Figure 1.4: This graph shows the hysteresis observed in tidal velocity versus water depth (stage). Despite velocity is highly variable, two peaks are detectable in correspondence of flood (just above bankfull conditions), when the water level is the same of the marsh surface, and one during the ebb. In terms of symmetry around either high tide or the timing of bankfull conditions, the peak ebb velocities lag the flood transients, occurring later, at a lower stage of the tide, just below bankfull. (Adapted from Fagherazzi et al., 2008).

Differences between fluvial and tidal meanders appear to be even more evident considering subtidal channels which, unlike alluvial plains that can be inundated only during exceptional floods, are constantly submerged as well as their related overbanks. Subtidal channels hydrodynamic is extremely complex, since both minimum and maximum velocities of tidal currents are experienced when both the channel and related overbanks are flooded, and flow distribution within the channel can be influenced by currents developed in overbank areas. Further, in subaqueous setting, water-saturation of point bar deposits decreases the intergranular friction, promoting collapses along the bar flanks (Bridges and Leeder, 1976; Choi et al., 2013).

Additionally, in wide shallow lagoons, inter-channels areas can be affected by strong wind-induced wave winnowing, which can influence sediment distribution along the channels.

Such divergent features certainly produce differences in the morphodynamic evolution of fluvial and tidal meanders, as well as in stratal architectures, sedimentary deposits and facies distribution of related point bar deposits.

1.3 GOALS OF THIS STUDY

Focusing on differences, more than on similarities, between tidal and fluvial meanders, the present work aims at investigating the stratal architecture and sedimentary facies distribution of tidal point bars of the Venice Lagoon (Italy; Fig. 1.5) focusing on three main issues:

i) Tidal networks appear much more articulated and interconnected than fluvial once. Low order tributaries are widespread, and generally located in correspondence of main meander bends formed by the main channels. Such configuration is extremely rare in fluvial settings, where the number of tributaries is lower. **Can minor tributaries influence the morphodynamic evolution of tidal channel bends?**

ii) Vegetated, cohesive salt-marsh mud well resembles floodplain deposits and encourages a comparison between salt-marsh meanders and their fluvial counterparts. In fluvial setting, where the rate of channel migration is orders of magnitude higher than the rate of bed aggradation, bed aggradation do not significantly influence point bar and channel belt architecture. In salt marsh setting, the rate of channel migration is significantly lower than in fluvial setting, but aggradation rates are comparable. **Can the salt-marsh aggradation rate influence the morphodynamics of tidal meanders?**

iii) Sedimentology and stratal pattern of subtidal meanders are almost unknown. Hydrodynamic of these channels is extremely complex, since both minimum and maximum velocities of tidal currents are experienced when both the channel and related overbanks are flooded. Flow distribution within the channel can be influenced by currents developed in overbank areas, promoting a hydrodynamic configuration which can control times and modes of channel planform evolution. **How do subtidal meanders evolve and what are sedimentary products of their planform evolution?**

Figure 1.5: Map locations of the three study sites (yellow dots).

1.4 THESIS OUTLINE

The present work is presented by five chapters.

Chapter 2 analyzes the role of low order lateral tributaries in evolution of tidal meander bends. The internal architecture and morphodynamic evolution of an intertidal meander bend of

the northern Venice Lagoon has been reconstructed through high-resolution sub-bottom seismic data using a 3D modeling software. Results from sedimentological analyses have been also compared with those from numerical modeling. The main body of this chapter has been submitted to PNAS (PNAS-manuscript-2015-21482).

Chapter 3 focuses on the role of bed aggradation in shaping geometry of a point bar developed in a salt marsh of the northern Venice Lagoon. Basin on sedimentological analyses of core data and 3D modeling, the geometry of a tidal point bar has been defined and analyzed. Particular attention was paid to reconstruct the relationship between lateral migration of the channel and vertical accretion of the surrounding saltmarshes. A manuscript summarizing the main results stemming out from this investigation will be submitted to Sedimentary Geology.

Chapter 4 focuses on sedimentary features of a subtidal meander bend. The planform evolution of the study bend during the last century was obtained through the comparison between detailed historical maps, aerial photos and satellite images. High-resolution geophysical investigations along with the analysis of sedimentary cores allowed to depict the sedimentary facies and internal architecture of the point bar deposits and outer bank region.

Chapter 5 summarizes the main results of this thesis.

CHAPTER 2

OBSERVATIONAL STRATAL ARCHITECTURE CHALLENGES CURRENT UNDERSTANDING OF TIDAL MEANDER-MORPHODYNAMICS

2.1 OVERVIEW

The present chapter is a manuscript submitted to PNAS (manuscript#2015-21482) and deal with the role exerted by lateral tributaries in the morphodynamics evolution of a tidal meander bend of the northern Venice Lagoon. This work highlights that when the sediment discharge of tributaries exceeds the sediment transport capability of the main channel, sedimentation can occur at the outlet of tributary channels, forming prograding lobate units. In such cases, flux funneling within the main channel can generate local erosion, also in areas where classical facies models predict deposition.

2.2 PAPER

LARA BRIVIO[1], MASSIMILIANO GHINASSI[1], ANDREA D'ALPAOS[1], ALVISE FINOTELLO[1], LUCA CARNIELLO[2], MARCO MARANI[2,3], ALESSANDRO CANTELLI[4], NICK HOWES[4]

[1] *Department of Geosciences, University of Padova, Padova, Italy.*

[2] *Department of Civil, Environmental and Architectural Engineering, University of Padova, Padova, Italy.*

[3] *Department of Civil and Environmental Engineering and Nicholas School of the Environment, Duke University, Durham, USA.*

[4] *Shell Technology Center Houston, Houston, TX, US.*

2.2.1 Abstract

Meandering channel network exert a fundamental control on hydrodynamic and morphodynamic processes within tidal landscapes. However, the planform evolution of tidal meanders is currently inferred via observations and models of their fluvial counterparts. The present study addresses in tidal landscapes, the internal architecture and morphodynamic evolution of a tidal meander bend in the Venice Lagoon (Italy), through an approach integrating three-dimensional high-resolution geophysical investigations, bathymetric field surveys, aerial photographs, and numerical modeling. We find that lateral tributaries influence sedimentation patterns within the meander bend in such a way that their effects remain imprinted in the sedimentary record of meander deposits. We also find that the evolution of tidal channels is punctuated by abrupt changes in channel dynamics, that contrast with the predictable and monotonous rise and fall of the tides. Meander dynamics inferred from depositional architectures challenge current assessments of tidal meander morphodynamics. The critical role exerted by lateral tributaries on tidal meander migration, emerges in response to evolving landforming processes operating on comparable timescales. Key differences with fluvial meanders emerge. Specifically, the concept that meander wavelength and radial progression stem from free migrating modes excited by bottom or flow instabilities is insufficient to explain tidal meander evolution, as evidenced by its stratigraphic record. A more complex set of forcings, including the influence of lateral tributaries, must be invoked.

2.2.2 Significance

Sinuous channels are ubiquitous features of tidal landscapes and contribute to the distribution of water, sediments and nutrients in these landscapes. However, little is known about their morphodynamic evolution and related sedimentary products, and these meandering

channels are commonly studied following theories developed for their fluvial counterparts. Here we show that tidal meander evolution differs from that of fluvial ones and distinctive features characterize deposits formed in tidal bends. Specifically, we highlight the role of minor tributaries that allow sediment accumulation where traditional models predict erosion. This bears important consequences for the management of tidal landscapes and interpretation of tidal channel deposits in the fossil record.

Keywords: tidal meander, stratal architecture, morphodynamics, tidal landscapes, Venice Lagoon

A longstanding question in geomorphology is whether the morphology of a particular landscape is in balance with its current environmental forcings or if it contains distinct relict signatures of past ones. Clear examples of these two end-member cases exist (Rinaldo et al.,1995), but in contexts where the rates of change of the forcings are comparable with (the inverse of) adaptation timescales of physical or biological processes, the identification of equilibrium/disequilibrium features is not straightforward. Branching and meandering tidal channels, the essential circulation system of lagoons and estuaries, form the pathway for tidal currents to propagate and distribute clastic sediments and nutrients (e.g. Hughes, 2012; Coco et al.,2013), thus providing a primary control on tidal landscape ecomorphodynamics (Fagherazzi et al., 2012). Although meandering patterns are ubiquitous features of the tidal landscape, very few studies have analyzed their planimetric shape, morphometric characteristics, and their morphodynamic evolution (Gabet, 1998; Marani et al., 2002; Solari et al., 2002; Fagherazzi et al., 2004). The depositional architecture of tidal meander bends has received even less attention, and is commonly approached using facies models (Barwis, 1978; De Mowbray, 1983; Choi and Jo, 2015) developed from the comparison with their fluvial counterparts (Jackson, 1976; Brierley,

1991), and by assuming that the abundance of mud and bidirectional flows represent the main differences with the fluvial realm (e.g. Thomas et al., 1987).

Quantifying the sediment transport dynamics in tidal channel bends and its impact on meander-bend architecture is a fundamental step towards an improved understanding of the role of tidal channels in the ecomorphodynamic evolution of lagoonal and estuarine systems. The present study addresses, for the first time in tidal landscapes, the internal architecture and morphodynamic evolution of a tidal meander bend in the Venice Lagoon (Italy, Fig. 2.1) by coupling three-dimensional, high-resolution geophysical investigations with geomorphological information from bathymetric field surveys, aerial photographs and numerical modeling.

Theoretical investigations (Marani et al., 2002; Solari et al., 2002; Fagherazzi et al., 2004) posit that locally the relevant dynamics follows from bend assessments for fluvial meanders (Seminara, 2006). Specifically, field evidence (Marani et al., 2002) shows that tidal meanders develop a characteristic spatial wavelength of about 10-15 channel widths, an observation that is consistent across channels of different widths, varying up to two orders of magnitude. This suggests that the mechanism of meander evolution is controlled by processes acting at the scale of a few channel widths. This observation has motivated notable attempts to interpret the above process on the basis of a planimetric instability theory, of the type established for fluvial meandering (Ikeda et al., 1981; Parker et al., 2011). Here we show, on the contrary, that sediment pulses delivered to the main channel through lateral tributaries, substantially influence meander evolution, by promoting the formation of atypical sedimentary bodies with sediment accumulation along the outer bank, where erosion is expected for fluvial meanders. This results from a concurrent evolution of the sediment supply and landforming discharges, tied to an ever-changing competition for relevant tidal prisms driving channel morphologies, co-evolving with RSL changes and the related ecological adaptations. Typical characteristic timescales are argued to be

comparable, thus leading tidal landforms to a perennial transient state whose imprintings are long-lived. Landforms in equilibrium with the current forcing and relict features are argued to perennially coexist in the tidal landscape.

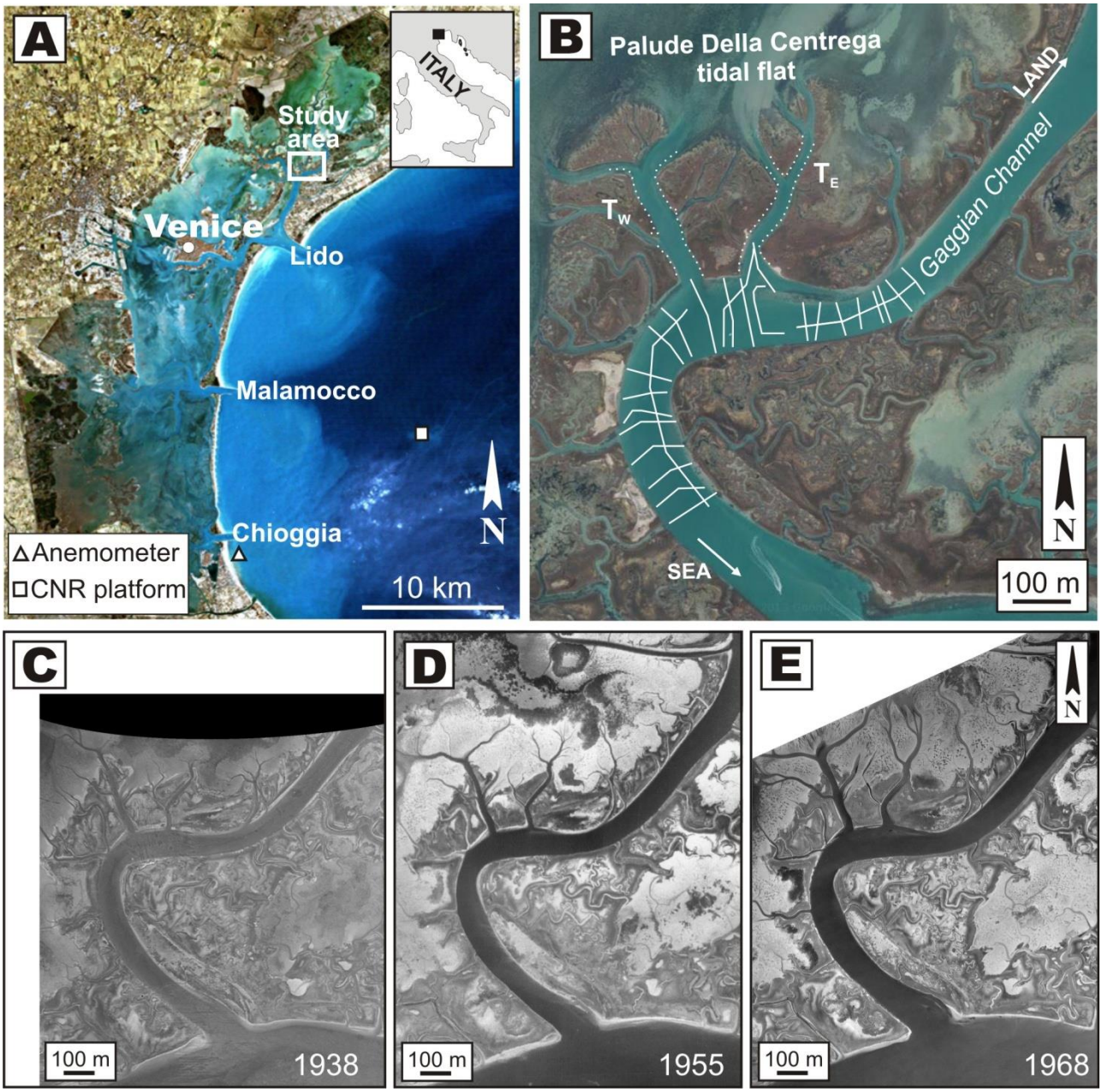

Figure 2.1: The study site. (A) Geographic location of the study area, in northeastern portion of the Venice Lagoon, Italy. (B) Satellite image (2012) of the Gaggian channel showing acquisition scheme of sub bottom profiles (white lines). (C – E) Digitalized orthophotos of the Gaggian channel in: 1938 (C), spatial resolution of 600 dpi (1pixel = 0.897 m); 1955 (D), resolution of 600 dpi (1pixel = 1.124 m); 1968 (E), resolution of 600 dpi (1pixel = 0.599 m).

2.2.3 Geomorphological Setting

We analyzed a meander bend of the Gaggian Channel, located in the Northern, and best naturally preserved, part of the Venice Lagoon (Fig. 2.1A). The Venice Lagoon, which formed over the last 7500 years covering alluvial Late Pleistocene deposits locally known as Caranto (Zecchin et al., 2008), is the largest Mediterranean brackish water body, with an area of about 550 km^2. It is connected to the Adriatic Sea through three inlets (Lido, Malamocco and Chioggia) and is subjected to a semidiurnal tidal regime, with an average tidal range of about 1.0 m and peak tidal amplitudes of about 0.75 m around Mean Sea Level (MSL). The study site is a 900 m long meander bend, which develops around a point bar with a mean radius of curvature of about 200 m (Fig. 2.1B). The channel is about 100 m wide, up to 8 m deep and receives tributaries, on both the inner and the outer banks. We focus specifically on the two main tributaries along the outer bank, named hereafter as T_w (Western Tributary) and T_e (Eastern Tributary), which enter the Gaggian channel near the bend apex an connect it with the Palude della Centrega tidal flat to the North (Fig. 2.1B). Medium to coarse-grained sand is common in the deepest part of the Gaggian channel, whereas fine-grained silty sand occurs in shallower areas and along the thalweg of the T_w and T_e tributaries.

The T_w and T_e tributaries, which are about 40 and 30 m wide and 3.6 and 3.0 m deep, respectively, branch northward into a number of minor channels which cut through the 0.55 m deep Palude della Centrega tidal flat. Historical aerial photos (Fig. 2.1C, D, E) show that between 1938 and 1968 the T_w and T_e tributaries were narrower than they are today and used to drain a salt-marsh platform, thus conveying smaller water and sediment fluxes into the Gaggian channel compared to modern conditions.

2.2.4 Results of Geophysical Investigations

Geophysical data (Fig. 2.2) show that the basal erosive surface of the Gaggian channel deposits locally occurs between 7 and 12 m below MSL, and overlies alluvial Late Pleistocene deposits. In-channel deposits are split into three sedimentary Units (hereafter called Unit 1, 2 and 3) by two distinctive and laterally extensive surfaces (Fig. 2.2), which show streamwise changes from erosive to depositional features.

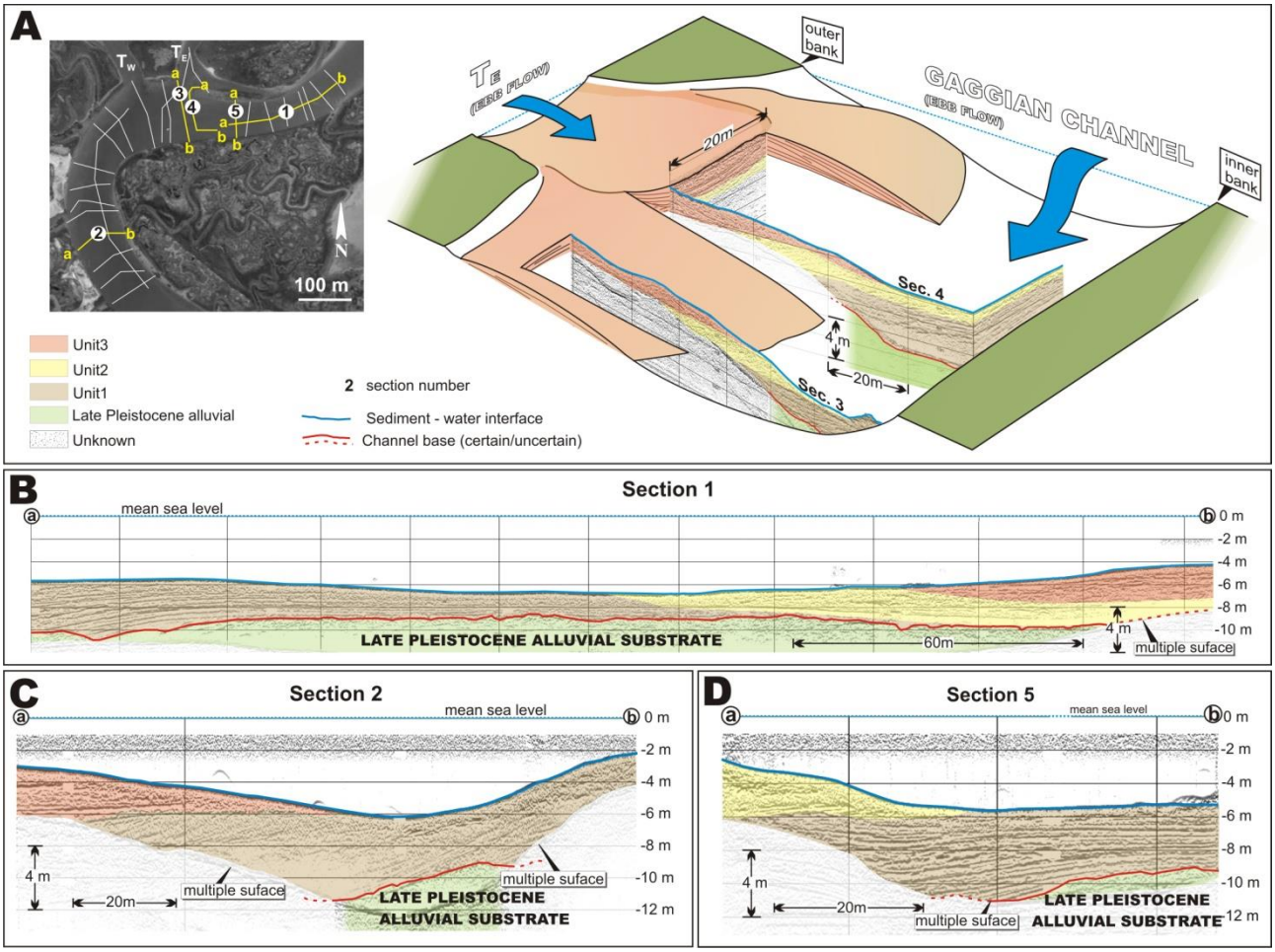

Figure 2.2: Interpretation of the most representative seismic sections. (A) Sections 3 and 4 in a sketch depicting the lobe fed by the T_E tributary. (B) Longitudinal section along the landward portion of the Gaggian channel showing ebb-oriented inclined deposits of Unit 1. (C) Inclined deposits of Unit 1, dipping 10-20° toward the outer bank, overlain by deposits of Unit 3. (D) Inclined deposits of Unit 1 and 2 dipping toward the outer bank, together with minor erosive truncations and gravitative deformations.

Unit 1 overlies the channel basal surface and reaches 6 m in thickness along the seaward side of the inner bank, whereas it becomes thinner in the landward side (Fig. 2.2B). Unit 1 consists

of inclined deposits dipping 10 – 20° toward the outer bank (Fig. 2.2C, D), as commonly expected in channel bends. Minor erosive truncations and gravitational deformations occur in the central and upper portion of the inclined beds (Fig. 2.2D). Unit 1 developed during the first stage of meander bend evolution, when sedimentation occurred along the inner bank due to the occurrence of a bend-apex helicoidal flow, as usually expected for fluvial patterns (Seminara, 2006). The thickness of deposits of Unit 1 is relatively constant along the bar, although its asymmetric planform profile suggests dominance of ebb currents.

Unit 2 mainly occurs in the landward side of the bend, where it erosionally overlies Unit 1 and locally the Caranto deposits, reaching the maximum thickness of about 4 m. Inclined beds dip toward the outer bank at about 10 – 15° and show minor internal truncations (Fig. 2.2A, D). Locally, the basal surface of this Unit is characterized by 1.0 – 1.5 m deep scours, which are filled with cross-stratified deposits fed by seaward-directed flows. Unit 2 testifies the seaward propagation of a sediment wave, which mainly accreted above Unit 1 along the landward side of the inner bank. Cross-stratified deposits agree with dominance of ebb currents (see Fig. 2.S1 in the Supplementary Information). The erosive nature of the basal surface suggests an increase in the landscape forming water discharge, which heralded the propagation of the aforementioned sediment wave.

Finally, Unit 3 which is up to 3.5 m thick, is erosively based and is distributed along the outer bank of the meander bend. Beds dip at about 10° toward the inner bank (see Section 3 and 4 in Fig. 2.2A) and define two lobes at the outlet of the T_w and T_e tributaries. The proximal part of these lobes includes channelized deposits (see Section 4 in Fig. 2.2A). The surface capping Unit 3 defines the present-day bend morphology, which is characterized by the erosion of the inner bank, where deposits of Unit 1 are exposed on the channel bottom (see Section 3 in Fig. 2.2A). Unit 3 documents the onset of accumulation at the outlets of the T_w and T_e tributaries, which fed two

main sedimentary lobes in the Gaggian channel. Accumulation of these lobes likely promoted a migration of tidal currents towards the inner bank of the main channel, triggering its erosion.

2.2.5 Discussion and Conclusions

Unit 1 to 3 document the occurrence of three distinct stages of meander bend evolution, named as Stage 1 (older) to 3 (younger) in Fig. 2.3. These stages are characterized by a transition from inner to outer bank accumulation. During the first and second stages of bend evolution, sediments were mainly stored along the inner bank (Fig. 2.3A, B). During the third stage of bend evolution (Fig. 2.3C), the occurrence of sedimentation along the outer bank and erosion along the inner bank is the dominant morphodynamic feature. These atypical sedimentary patterns are associated to the development of the lobes at the outlets of the T_w and T_e tributaries (Fig. 2.3C), which suddenly delivered to the main channel an amount of sediment that exceeded its maximum sediment transport capacity. This abrupt increase in sediment supply from the T_w and T_e tributaries was triggered by increasing sediment erosion over the Palude della Centrega tidal flat, which is connected to the Gaggian Channel by the T_w and T_e tributaries. The Venice Lagoon experienced a strong erosional trend over the last century (Carniello et al., 2009), which led to an increase in the average water depth of about 0.60 m in the Palude della Centrega tidal flat (see Fig. 2.S2 in the Supplementary Information). The positive feedback between tidal-flat deepening and wind-wave induced erosion (Fagherazzi et al., 2006) results in high values of the suspended sediment concentration during storm events. The sediment suspended by wind waves in the Palude della Centrega tidal flat was therefore routed into the Gaggian channel (Fig. 2.3F) by the ebb currents, which increased flow velocity and the related sediment transport capability (see Fig. 2.S1 in the Supplementary Information) triggering erosion and bypass along the tributaries. Mutually evasive currents, documented in tidal bends, contribute to storing sediment along the

outer bank (Hughes, 2012; Li et al., 2008). The effect of these currents here is however overwhelmed by the sediment supply of lateral tributaries as emphasized by the development of lobate units at the outlet of the tributaries (Fig. 2.3C), which causes a shift of the pool scour toward the inner bank zone.

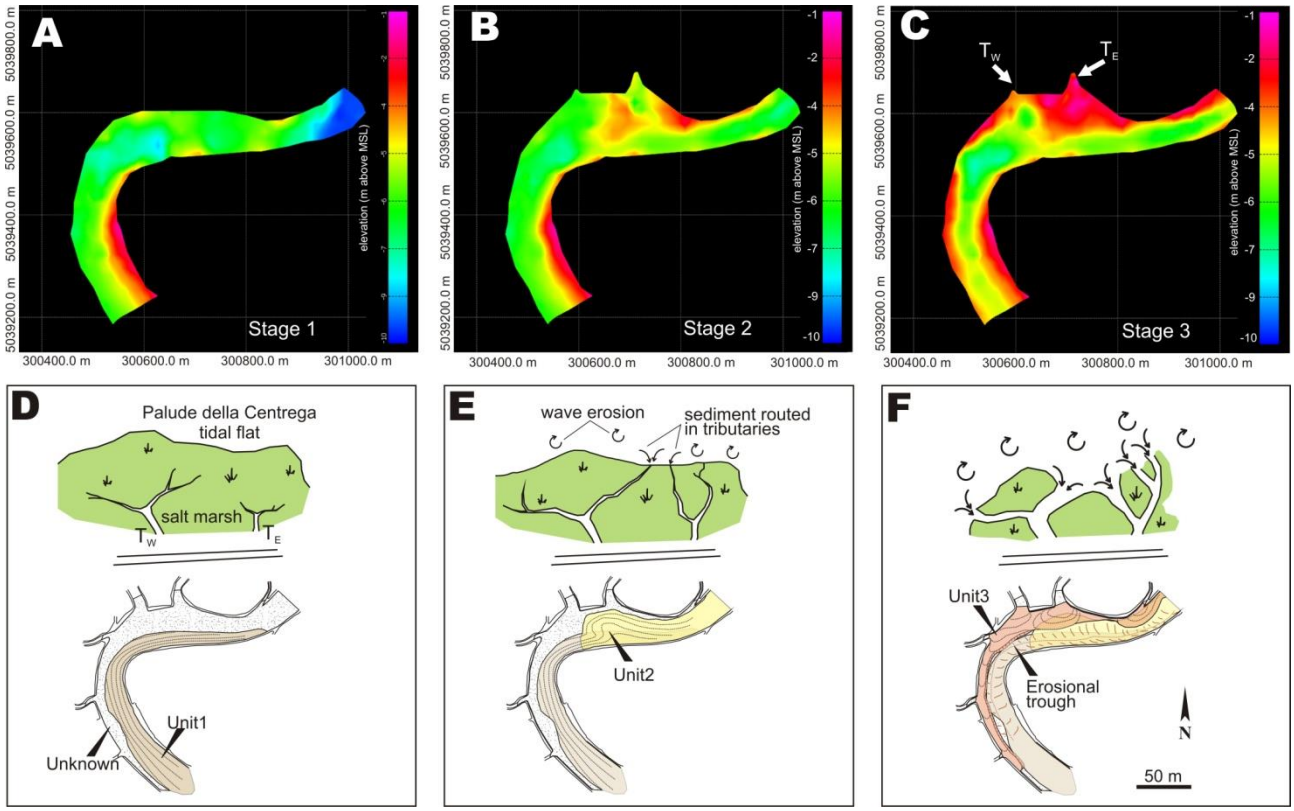

Figure 2.3: Morphological evolution of the Gaggian channel. (A - C) Top morphologies of Unit 1 to 3 as they emerge from the spatial interpolation of seismic profiles obtained through a kriging procedure. Panels A – C highlight the development of lobes at the tributary outlets and the related deposition patterns along the outer bank. (D – F) Conceptual model portraying the three stages of the Gaggian channel evolution. (D) TW and TE tributaries do not receive sediment from the Palude della Centrega tidal flat and the Gaggian channel bend is dominated by inner bank deposition. (E) Ongoing inner bank sedimentation , which is mainly concentrated along the landward side of the inner bank. (F) Sediments resuspend by wind waves in the Palude della Centrega are routed into the Gaggian channel through the TW and TE tributaries causing accumulation along the outer bank.

The analysis of aerial photographs and the results of numerical modelling (see the Material and Methods for details), confirms the above scenario (Fig. 2.4). A comparison of the 1938 and 2007 channel planforms and bathymetries (Fig. 2.4A, B) indicates that the Gaggian Channel and the two lateral tributaries experienced an increase in their width and depth. This was due to the

increase in the tidal prisms shaping their cross sections (D'Alpaos et al., 2010), triggered by the vertical erosion of the tidal flat surfaces drained by these channels due to wind-wave induced erosion processes (Carniello et al., 2009). When the model is forced with the same tidal levels and wind velocities and directions for both configurations (Fig. 2.4C), results show that both hydrodynamics and sediment transport processes experienced important changes (Fig. 2.4D-I). The erosion of the landward tidal-flat and salt-marsh surfaces led to an increase in the landscape-forming discharges (Figs. 2.4D, E), whereas the amount of mud (Figs. 2.4F, G) and sand (Figs. 2.4H, I) routed towards the main channels along the two tributaries largely increased, yielding two lobate structures at the confluences. Interestingly, although discharges routed through the Gaggian Channel experienced a 60% increase between 1938 and 2007, the resulting velocities were not strong enough to remove these intra channel sedimentary bodies, which therefore represent the fingerprint of transient sediment dynamics and reflect patterns operating at a larger spatial scale than the single bend scale.

The occurrence of erosively-bounded sedimentary Units emphasizes that tidal channels evolve under the control of significant changes in local hydrodynamics, which apparently contrast with the predictability of channel discharge dictated by specific ranges of tidal excursion. The evolution of the tributary network plays a key role in driving the above described morphodynamic changes. Although tidal and fluvial meanders seem to be characterized by a similar planform morphology (Marani et al., 2002; Solari et al., 2002), the governing mechanisms, documented by the Gaggian stratigraphic record, lead to the establishment of sediment patterns which differ in the two considered cases. Accumulation in the outer bank zone is observed in tidal bends thanks to mutually evasive currents (Hughes, 2012) but is locally overwhelmed by the discharge from lateral tributaries, that can produce confluence bars. Differently from fluvial confluence bars

(Biron et al., 1993), which are commonly removed during flood events, tidal confluence bars are much more likely preserved in the stratigraphic record.

Our results suggest that tidal meander bends are commonly affected by abrupt variations in sediment and water discharge, which trigger alternation between growth and degradation of channel bars as a result of evolutionary timescales subsumed by variations in the tidal prism, an effective proxy of landscape morphology. We show that lateral tributaries exert a critical role on tidal meander evolution because they control the amount of water and sediment provided to the main channels. When the sediment discharge of tributaries at the outer bank exceeds the sediment transport capability of the main channel, sediment accumulation at the outlet of tributary channels forms prograding lobate units. This causes flux concentration against and erosion of the inner bank, where both fluvial and tidal classical facies models predict deposition. Overall, we find that current landforms in the tidal landscape bear the signatures of processes occurring at larger spatial scales, prompting alternating sediment production and dissipation, watershed capture and migration, channel advancement and retreat, saltmarsh and tidal flat construction and reflected in varying evolutions of tidal meanders. Our main results call for a paradigm shift in the theory of tidal meanders and in the interpretation of tidal geomorphology from theories derived from their fluvial counterparts (Barwis, 1978; De Mowbray, 1983; Choi and Jo, 2015) to new approaches specifically developed for tidal landscapes.

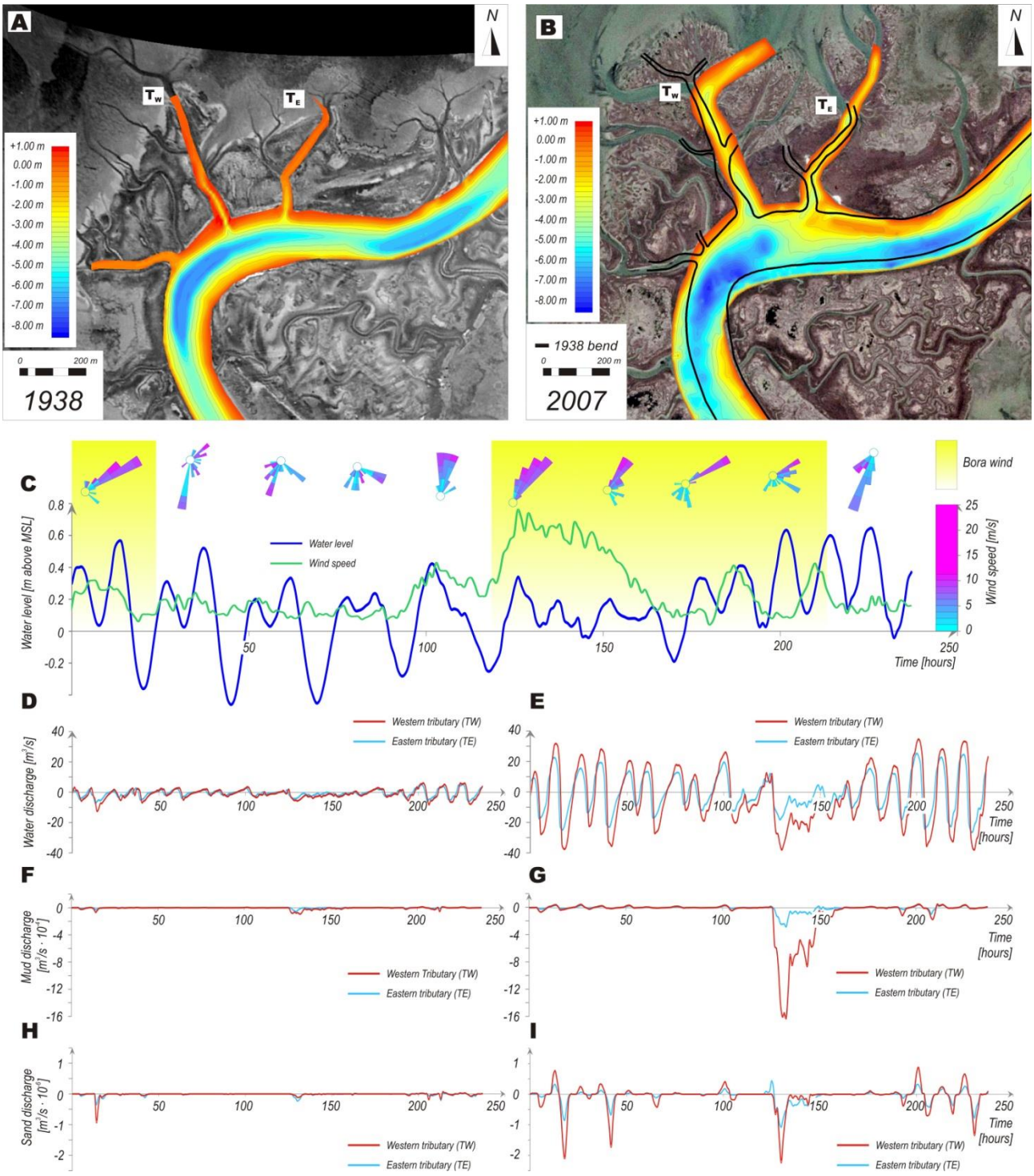

Figure 2.4: Results of the numerical model. (A, B) Orthophotos of the Gaggian channel configuration in 1938/2007 over which bathymetric surveys of 1930/2012, respectively, are overlapped. (C) Observed water levels and wind velocities and directions used to force the sediment transport model. Water (D,E), mud (F,G), and sand (H,I) discharges through the T_W (red line) and T_E (light blue line) tributaries computed for the 1938/2007 configurations, respectively.

2.2.6 Materials and Methods

2.2.6.1 Geophysical data

In April 2011 two longitudinal sub-bottom profiles and 25 transverse profiles were collected within the Gaggian channel (Fig. 2.1B). These profiles were acquired by using a Innomar SES – 2000 Compact, a parametric sub-bottom profiler, equipped with a SES 2000 transducer. During the acquisition, low frequencies were used to investigate the subsurface architectures.
An 8 kHz frequency was used and varied locally in the range of 5-10 kHz in order to increase the penetration (5 kHz) of the signal and to improve the resolution (10 kHz).

Data processing was carried out by means of SES Innomar software, using a signal velocity of 1509 m/s determined on the basis of contemporary temperature and salinity measurements. Position data were recorded through GPS (two TOPCON GR-3 receivers – dual frequency (L1/L2) and dual constellation (NavStar/Glonass), with integrated Tx/Rx UHF radio were used) and processed through the Geo Office software (Leica). The main bounding surfaces separating different sedimentary units were defined on the basis of onlap, downlap, and toplap geometries. The Move 2013.1^{TM} software was used to correlate interpreted seismic sections through a kriging procedure, with the goal of defining the paleo-morphology of the meander bend at different depositional stages.

2.2.6.2 Mathematical modelling

A series of aerial photographs (Fig. 2.1B, C, D, E) and bathymetric data, obtained from the 1932 and 2013 bathymetries (see, Carniello et al., 2009 for details), were used to determine morphological changes of the Gaggian channel and its lateral tributaries.

A numerical morphodynamic model was used to analyze changes in water and sediment fluxes occurred along the considered bend. The model describes tidal and wave hydrodynamics

and sediment transport processes to determine the related bed evolution in shallow tidal basins (Carniello et al., 2012, the reader is referred to the original paper for full derivations). A hydrodynamic model, which solves the 2D shallow water equations (see, D'Alpaos and Defina, 2007) is fully coupled to a wind-wave model (Carniello et al., 2011) that solves the wave-action conservation equation parameterized using the zero-order moment of the wave action spectrum in the frequency domain. Tidal currents and wind waves determine the hydrodynamic field used to solve an advection-diffusion equation and the related sediment resuspension, transport, and deposition that control bed evolution accounting for the simultaneous presence of both cohesive (mud) and non-cohesive (sand) sediments (Carniello et al., 2012). Numerical simulations were carried out on different computational grids representing the Venice Lagoon in its 1932 and present configurations (see Fig. 2.S1 in the Supplementary Information). In all simulations, the model was forced by using 30 days (from 11/16/2005 to 12/16/2005) of hourly tidal levels measured at the CNR Oceanographic Platform, located in the Adriatic Sea in front of the Venice Lagoon, and wind velocities and directions observed at the Chioggia anemometric station (Fig. 2.1A).

2.2.7 Supplementary Information

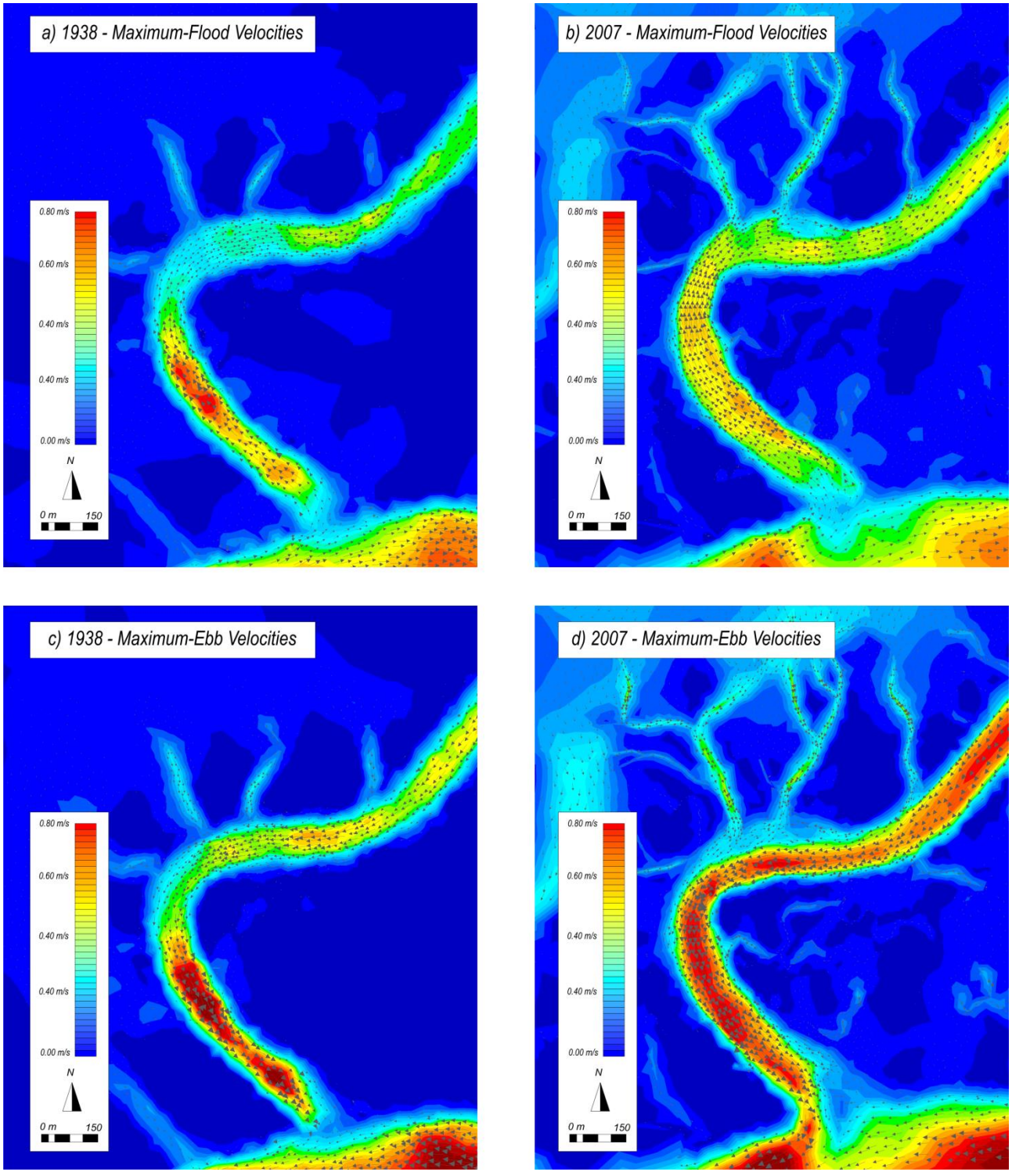

Figure 2.S1: (A,B) Maximum flood and (C,D) maximum ebb velocities for the 1938 and 2007 configurations, respectively, when the model is forced by the observed water levels and wind velocities and directions shown in Fig. 2.4C.

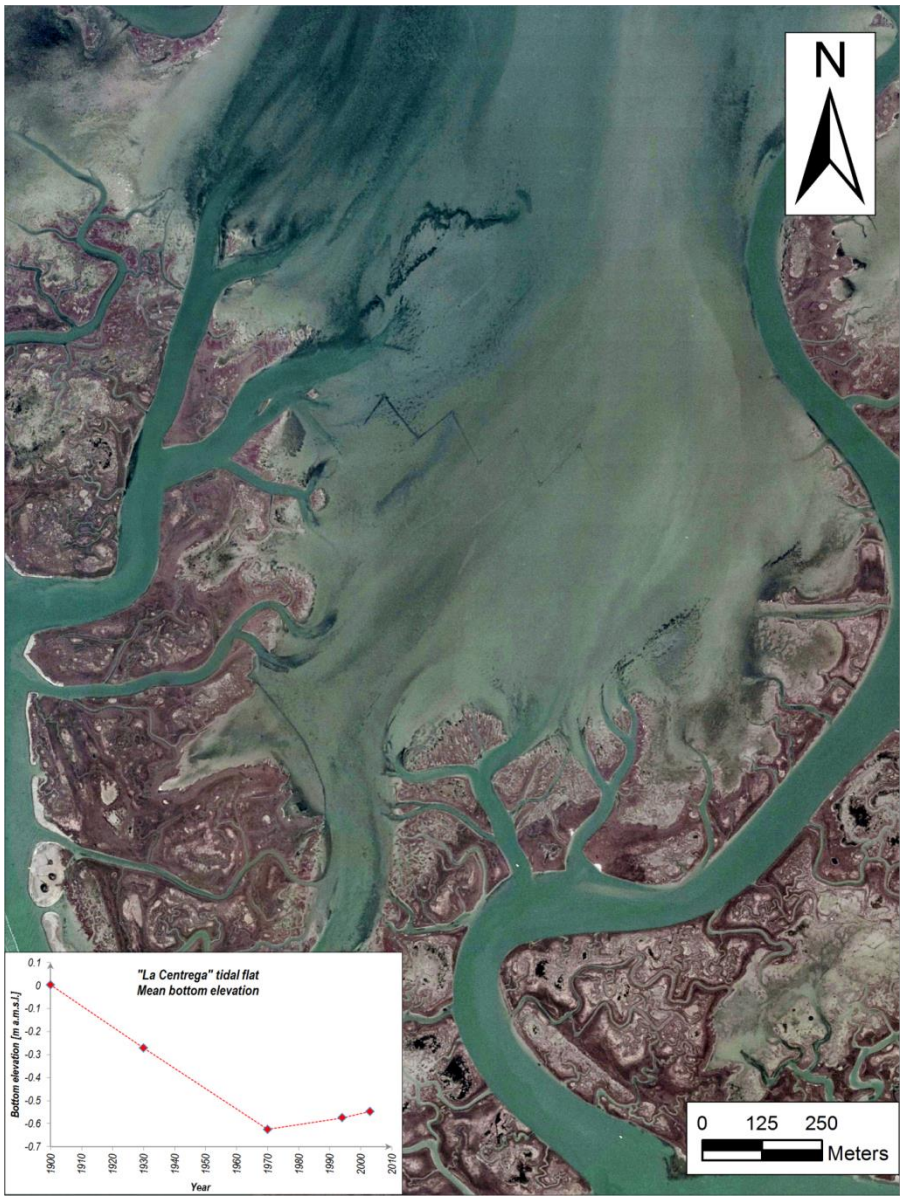

Figure 2.S2: Orthophoto of the Gaggian channel in 2007 and evolution in time (inset) of the average bottom elevation of the Palude della Centrega tidal flat, which is drained by T_W and T_E tributaries.

CHAPTER 3

INTERACTION BETWEEN AGGRADATION AND LATERAL MIGRATION SHAPES GEOMETRY OF A TIDAL POINT BAR: AN EXAMPLE FROM SALT MARSHES OF THE NORTHERN VENICE LAGOON (ITALY)

3.1 OVERVIEW

This chapter is a manuscript ready to be submitted to Sedimentary Geology and focuses on a tidal point bar developed in salt marshes of the northern Venice Lagoon. This work is based on sedimentological core data and 3D architectural modeling, and highlights that during lateral accretion the point bar sedimentary body is affected by a progressive thickening that is associated by lowering of the channel thalweg and rising of the channel banks. Lowering of the thalweg is due to increase in channel sinuosity and efficiency of the secondary circulation. Rising of the banks is induced by the continuous aggradation of salt marshes surrounding the channel.

3.2 PAPER

LARA BRIVIO[1], MASSIMILIANO GHINASSI[1], ANDREA D'ALPAOS[1], ALVISE FINOTELLO[1], ALESSANDRO FONTANA[1], MARCELLA RONER[1], NICK HOWES[2]

[1] *Department of Geosciences, University of Padova, Padova, Italy.*

[2] *Shell Technology Center Houston, Houston, TX, US.*

3.2.1 Abstract

Although meanders are ubiquitous features of the tidal landscape, the architectural geometries of tidal point bar deposits are relatively unexplored and commonly investigated on the

basis of facies models developed for their fluvial counterparts. The present study aims at improving current understanding of tidal point bar deposits developed in salt-marsh setting, by investigating an abandoned intertidal meander loop, located in the Northern part of the Venice Lagoon (Italy). The study channel is 6 m wide and its radius of curvature is approximately 13 m. It was active until the 50's when it was deactivated as consequence of a neck cut-off. A total number of 150 cores were recovered from the meander loop and used to define the sedimentary features of the bar and the geometries of its main stratal surfaces. The bar is cut on a subtidal platform of sand and mud and is covered by both channel fill and salt-marsh mud. It is floored by a shell-rich sandy lag and consists of stratified fine sand grading upward into sandy mud. The outer bank of the study bend is characterized by well-developed, sand-rich levee deposits. Sediment grain size distribution shows slight changes along the bar, suggesting that seaward and landward side of the point bar experience comparable changes of bed shear stress as a consequence of alternation between flood and ebb currents. Spatial interpolation between key stratal surfaces shows an overall thickening of the bar from 1.2 to 1.7 m in the direction of channel migration. This thickening, associated with both lowering of bar base and rising of its brink, occurs in parallel with an increase in channel cross-sectional area, to progressively accommodate the increasing tidal prism shaping the channel. Interestingly, we find that the bar top surface is characterized by a spoon-shaped geometry stemming out from a combination between lateral migration (8-10 cm/yr) and vertical aggradation (2.5-3 mm/yr). This peculiar bar top geometry is quite uncommon in fluvial meanders, where the high rate of lateral migration causes the cutoff to be reached before substantially thick deposits are accumulated on the bar top.

Keywords: tidal point bar, salt marsh, neck cut-off, morphodynamics, aggradation, lateral migration, Venice Lagoon

3.2.2 Introduction

Tidal channels play a key role in the evolution of coastal environments and constitute the pathway for the propagation of tides, sediments and nutrients within these environments (e.g. Hughes, 2012). The morphodynamic evolution of these channels is governed by the complex interaction between several interconnected features, such as the tidal prism, tidal asymmetry, sediment texture, and vegetation presence (Garofalo, 1980; Gabet, 1998; Dalrymple et al., 1991; Fenies and Faugères, 1998; Marani et al., 2002; Lanzoni and Seminara, 2002; Solari et al., 2002; Fagherazzi et al., 2004; Garotta et al., 2006). Although the sedimentary products deriving from the lateral migration of tidal meanders have been explored by a few works (Land and Hoyt, 1966; Howard et al., 1975; Barwis, 1978; de Mowbray, 1983; Bridges and Leeder, 1976, Choi et al., 2004; Choi, 2011), it is commonly assumed that stratal geometries of these deposits show marked similarities with those of their fluvial counterparts. Accordingly, the basic architectural and facies models developed for fluvial meander bends (e.g. Allen, 1963; McGowen and Garner, 1970; Brice, 1974; Jackson, 1976; Nanson, 1980) are commonly used to detect tidal point bars in the fossil record (e.g Díez-Canseco et al., 2014), commonly considering that the latter shows evidence for bidirectional currents along with a higher mud content and degree of bioturbation (Allen, 1982). Nevertheless, a number of features highlight relevant differences between the morphodynamics of tidal and fluvial meanders. Rivers maintain a generally constant discharge on the short term and display variable discharges on the long term due to flood events, during which high velocities can be maintained for long time. Tidal channels, behind experiencing a daily reversion of flows, are characterized by highly variable discharges on the short term, whereas they show an almost constant discharge on the long term. Additionally, in fluvial channels landscape forming discharges occur when water is at bankfull stage, whereas in tidal channels high water level conditions are characterized by null velocities (Hughes, 2012).

Sedimentary facies models for tidal meanders mostly derived from modern mudflats (de Mowbray, 1983; Bridges and Leeder, 1976; Choi et al., 2004; Choi, 2011), while scarce attention was paid to meandering channels cutting through salt-marsh surfaces. Vegetated, cohesive salt-marsh mud well resembles floodplain deposits and encourages a comparison between salt-marsh meanders and their fluvial counterparts. In unconfined floodplains, fluvial meanders commonly evolve increasing their sinuosity ("expansional planform evolution" *sensu* Jackson, 1976), with a rate of lateral migration in the order of m/yr (van de Lageweg et al., 2015). In the fluvial realm, bed aggradation is not expected to influence channel belt architecture, since the rate of channel migration is orders of magnitude higher than the rate of bed aggradation. Nevertheless, numerical simulations show that high bed aggradation rates (i.e. >10 mm/yr) can impact on the architecture of channel-belt deposits (van de Lageweg et al., 2015), as also highlighted by outcrop evidence (Ghinassi et al., 2014). Salt-marsh meanders are characterized by rates of migration which rarely exceed 0.5 m/yr (Garofalo, 1980; Gabet, 1998) therefore the rate of bed aggradation, which can also exceed 5-10 mm/yr, is expected to have major effects on point bar sedimentation.

Towards the goal of providing new insight into tidal meander bend sedimentation, the present study investigates the morphodynamic evolution and the internal architecture of a point bar, developed in a salt marsh of the Northern Venice Lagoon (Adriatic Sea, Italy; Fig. 3.1). The study site is represented by an abandoned meander bend, consisting of sandy point bar and related muddy channel fill. Using closely-spaced sedimentary cores to define a high-resolution 3D model, the present study aims at investigating facies distribution and architecture of the point bar deposits. The geometry of the point bar body is analyzed here as function of the ratio between vertical aggradation and lateral migration, and a comparison with a fluvial bar of similar size is discussed.

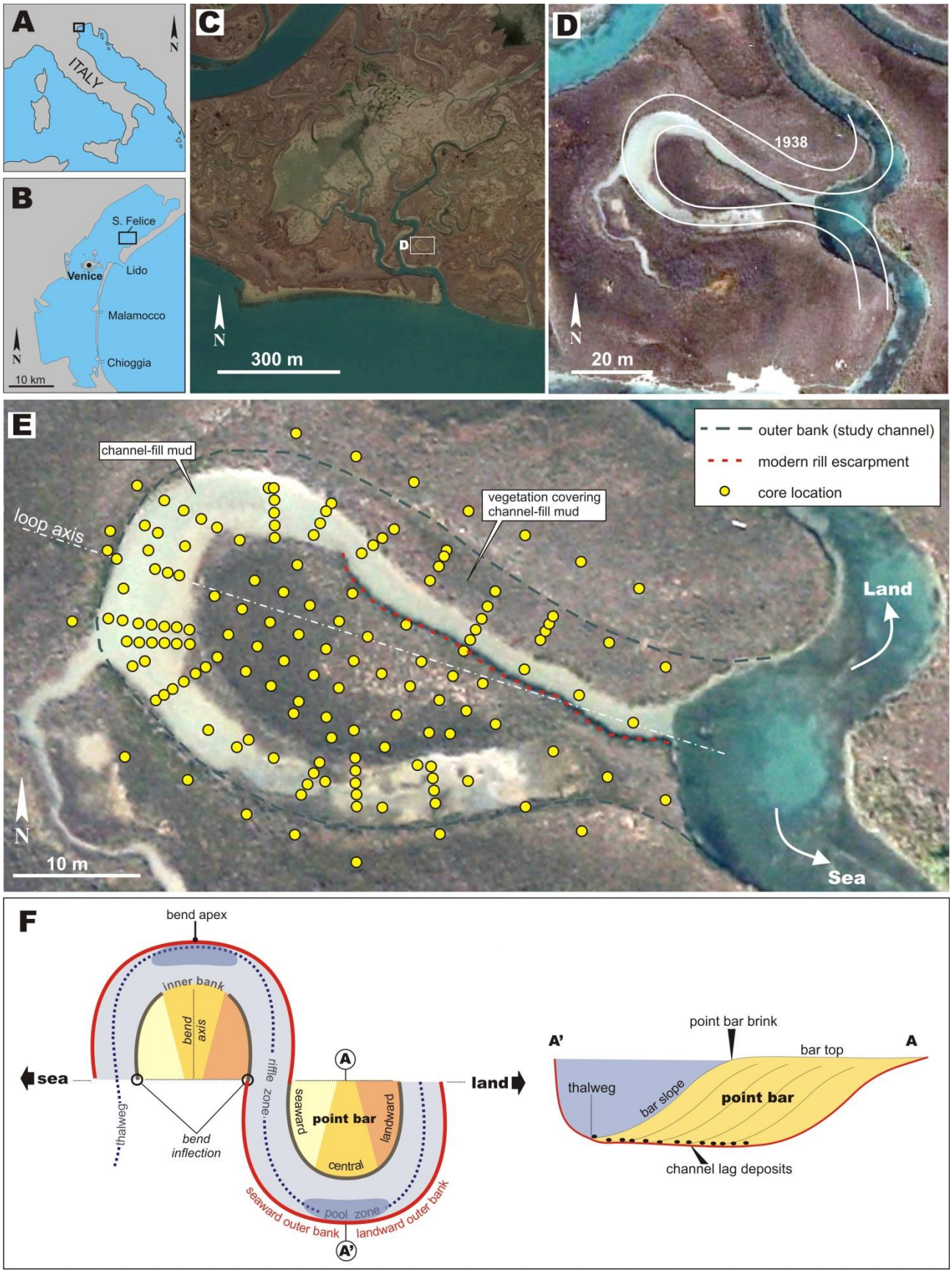

Figure 3.1: Geographic location of the study site and terminology used in the present work. (A) Location of the Venice Lagoon in the Mediterranean Sea. (B) Position of study site in the northern part of the Venice Lagoon. (C) Complex network of tidal meandering channels characterizing salt marshes of the S. Felice area. (D) Satellite image

(from Google™ Earth) showing the study meander loop. White line indicate location of the channel in 1938 (Modified after Rizzetto and Tosi, 2011). (E) Location of the 150 sedimentary cores recovered from the study site. (F) Descriptive terminology for tidal meander bends and point-bar architecture.

3.2.3 Geological Setting

3.2.3.1 The Venice Lagoon

The Venice Lagoon, located in the NE part of Italy (Fig. 3.1A), is hosted in the Venetian basin, a foreland basin that developed between the Apennine and South-Alpine chains since the Late Oligocene (Massari et al., 2009). After experiencing deep-water deposition, during the Early Pleistocene, the basin was filled up with ca. 750 m of shallowing-upward deposits, spanning from turbidites to shallow marine (Massari et al., 2004). The modern Venice Lagoon (Fig. 3.1B), forms an elongated body oriented NE-SW, that with a length of about 50 km and a width of 10 km, represents the largest Mediterranean brackish water body (total surface are of about 550 km^2). The Lagoon is characterized by an average depth of about 1.5 m, is connected to the Adriatic Sea through three inlets (Lido – San Nicolò, Malamocco and Chioggia; Fig. 3.1B), and is subjected to a semidiurnal tidal regime, with an average tidal range of about 1.0 m and peak tidal amplitudes of about 0.75 m (D'Alpaos et al., 2013) around Mean Sea Level (MSL). The Venice Lagoon formed during the last 7500 years as a consequence of the Holocene transgression, which promoted formation of lagoon – estuarine – barrier systems in the Northern epicontinental Adriatic shelf through the flooding of late Pleistocene alluvial-plain deposits (Zecchin et al., 2009). Salt marshes and tidal flats of the Venice Lagoon are drained by a dense network of sinuous channels, which progressively decrease in cross-sectional area as moving from the inlets towards the land.

3.2.3.2 The study site

The study site is located in the San Felice salt marsh (Fig. 3.1B, C), which is colonized by dense halophytic vegetation species (such as *Limonium, Juncus and Salicornia*) and represents one

of the most naturally preserved portions of the Venice Lagoon (Marani et al., 2003). During winter time, strong winds from NE (Bora) can generate waves which impact against salt-marsh margins and contribute to the flooding of salt-marsh surfaces (Carniello et al., 2011; Marani et al., 2011).

The present study focuses on point bar deposits associated with an abandoned meander loop (Fig. 3.1D), that was formed by a 6 m wide channel cutting through the salt marsh. The analysis of historical photos reveals that the meander (neck) cut-off occurred during the 50's (Rizzetto and Tosi, 2012) and caused progressive filling of the channel with muddy deposits. The meander loop, oriented NW-SE, shows a "simple symmetrical planform" according to the nomenclature proposed by Hooke (2013) and has a radius of curvature of about 13 m (Fig. 3.1E). In the northern sector of the meander loop, channel fill deposits are colonized by halophytic vegetation and locally drained by a small rill (Fig. 3.1E and 3.2A), which slightly erodes bar deposits.

3.2.4 Methods and Terminology

An elevation map of the site (Fig. 3.2A) was defined by measuring (GPS device: TOPCON GR-3 receivers – dual frequency (L1/L2) and dual constellation (NavStar/Glonass) with integrated Tx/Rx UHF radio) the geographic location and elevation of points forming a 1m-spaced grid.

A number of 150 georeferenced cores were recovered (Fig. 3.1E) using a hand auger core sampler, which prevents sediment compaction. A total number of 91 cores were recovered within the abandoned channel, whereas 19 and 40 cores were recovered from the outer and inner bank areas, respectively. Coring depth spans from 1 to 3 m and cores are 3.5 cm in diameter. Collected cores were kept humid in PVC liners and successively cut longitudinally, measured and photographed. Core logging was carried out following the basic principles of facies analyses, highlighting sediment color and grain size, presence of sedimentary structures, vertical grain-size

trends, degree of bioturbation and presence of vegetal and/or shell remains. Sedimentary features and core location allowed the definition of five main types of deposits, which will be described and interpreted in the next section.

The high-resolution sedimentary logs were placed in a virtual space and correlated using the software Move™ 2014.2 (Midland Valley), which allows to obtain a the three-dimensional representation of all cores in a georeferenced space. The boundaries between different deposits were interpolated among cores in order to define the spatial geometry of the main sedimentary units.

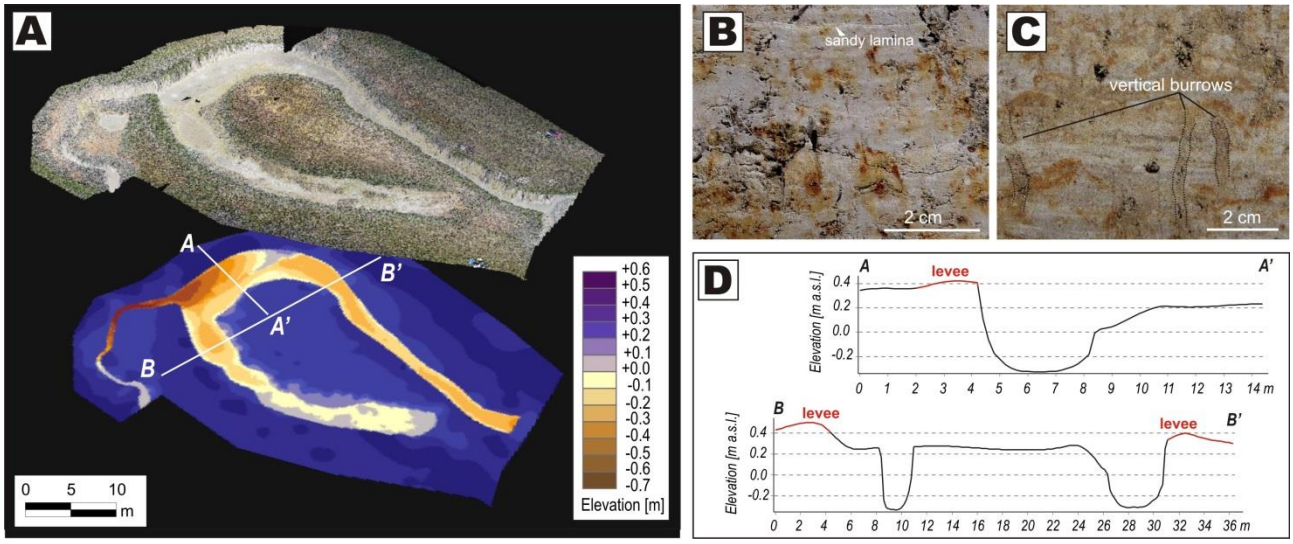

Figure 3.2: The study site. (A) Elevation model of the study area. Note the well-developed levee occurring along the outer bank zone of the channel. (B) Mid-rich salt marsh deposits forming the distal fringes of the levee. (C) Sand-rich deposits forming the proximal part of the levee. (D) Cross-sectional profiles across levee deposits.

The terminology used in the present work (Fig. 3.1F) is similar to that used for fluvial point bars and related deposits, although some modifications were required. Given the bidirectional nature of tidal currents along the meander bend, the upstream and downstream sides of the point bar are named here landward and seaward side, respectively (Fig. 3.1F). The point-bar brink (Fig. 3.1F) is named here as the rim separating the top of the bar from its slope.

3.2.5 Results

3.2.5.1 The study deposits

Salt-marsh deposits

These deposits occur just below the soil surface in overbank areas and overlay both point bar and subtidal platform deposits. They range in thickness between 0.2 and 1.3 m and consist of a horizontally-laminated, oxidized mud, with a variable amount of fine to very fine sand (Fig. 3.2B, C). *In situ* roots, wood fragments and bioturbation are common (Fig. 3.2B, C). Plant debris and organic matter are seldom present within dark laminae (1-2 mm thick). Sand forms 1-3 mm thick horizontal laminae, which are characterized by a remarkable grain-size sorting. Along the outer bank of the channel, where the elevation of the salt-marsh surface is higher than the surrounding areas (Fig. 3.2A, B), these deposits are sandier and tend to fine moving away from the channel bank.

These deposits accumulated in salt marsh environments (c.f. Allen, 2000) according with the presence of abundant root traces and sediment oxidation. Sedimentation occurred, therefore, in the highest portion of the intertidal zones that is commonly affected by subaerial exposure, as also suggested by a widespread sediment oxidation. Mud settled down during high water slack, at the transition between flood and ebb tide. Organic-rich laminae were associated with slightly reductive conditions, probably due to the presence of stagnant water developed in small ponds. Sandy laminae are interpreted to be generated during storm events in high tide conditions. In this setting, wind-induced waves winnow the salt marsh surface, suspending mud and remobilizing sand under tractional conditions. Textural sorting of sandy laminae and lack of a muddy matrix strongly support this hypothesis. Sediment ridges distributed along the outer bank edge are interpreted as levee, accumulated as consequence of the baffling of flow speeds due to vegetation (Bartholdy, 2012; Hugues, 2012).

Sub-tidal Platform deposits

These deposits represent the substrate of the study sedimentary unit and can be recognized in the lower portion of almost all the cores, between a depth of 1.3 and 3 meters (Fig. 3.3A). They reach a maximum thickness of 1.7 m, although their basal surface was not reached by any core. These deposits consist of alternating dark grey sand and mud that form beds up to 20 and 5 cm thick respectively. Sand is medium to fine in grain size and contains isolated mud clasts, sparse shells and shell fragments (Fig. 3.3B). Articulated bivalves locally occurs (Fig. 3.3E). Plant debris are very common and locally form 1-3 mm thick layers. Sand is commonly massive, due to the intense bioturbation, although traces of a primary plane-parallel stratification can be locally detected. Mud is mainly massive and contains scattered shells and wood fragments (Fig. 3.3D).

The dark color and abundant organic matter suggest that these deposits accumulated in a submerged and scarcely oxidized environment, which can be labeled as a sub-tidal platform (cf. Marani et al., 2007). The lack of root traces strongly support this interpretation. Sandy beds were originated during storm events, when the lagoon floor was deprived of fine-grained deposits as consequence of wave winnowing (Carniello et al., 2009). Part of these sands could also have been emplaced as distalmost fringes of washover fans, although the abundance of plant debris could also suggest they were fed by riverine flood flows that entered the lagoon after main rainstorm events. Muddy layers accumulated during fair-weather condition, especially after storm events, when suspended mud settled to the bottom.

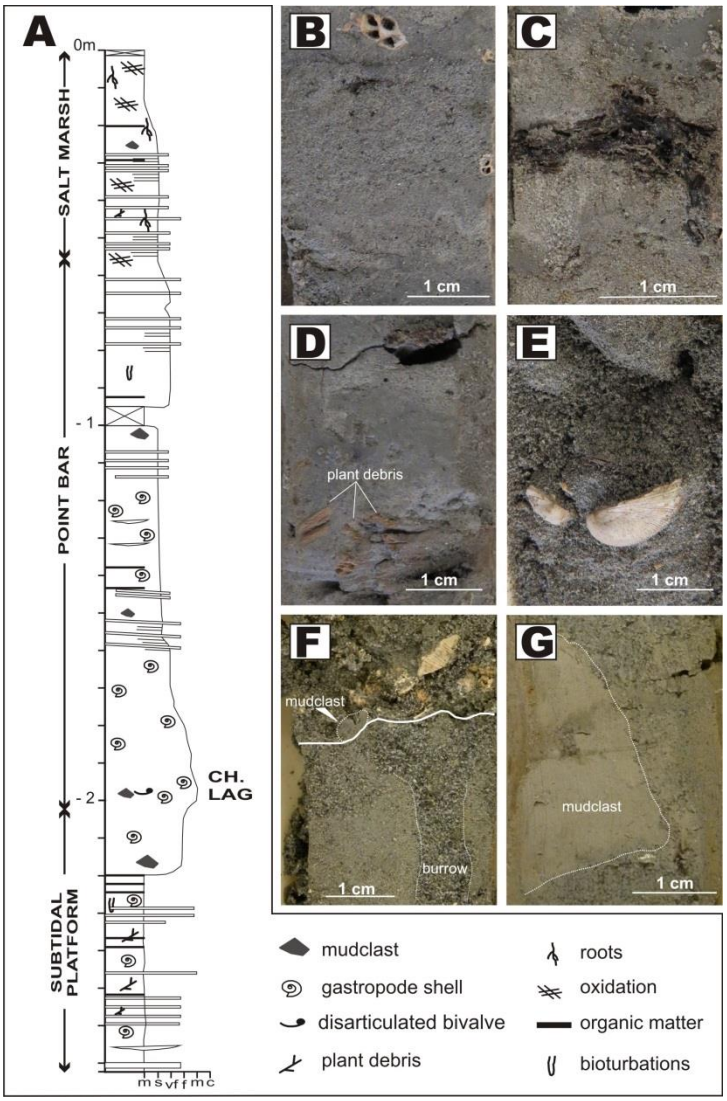

Figure 3.3: Sedimentary features of overbank and channel lag deposits. (A) Sedimentological log showing subtidal platform deposits overlain by channel-lag, point bar and salt marsh sediments. (B-E) Subtidal platform deposits. (F) Shell-rich, channel lag sand overlaying bioturbated subtidal platform deposits. (G) Pebble-sized, subrounded mudclast in the uppermost part of channel lag sand.

Channel-lag deposits

These deposits occur in 20 cores and are up to 0.4 m thick. They consist of massive grey-bluish medium sand overlying an erosional surface, cut onto the sub-tidal platform deposits (Fig. 3.3A, F). They usually contain abundant shells and shell fragments (Fig. 3.3F), wood debris and mud clasts (Fig. 3.3F, G), that are up to 5 cm in diameter. Vertical burrows locally cut through the sand and underlying subtidal platform deposits (Fig. 3.3F).

These deposits accumulated as channel lag in the deeper part of the channel (cf. Barwis and Hayes, 1979; Terwindt, 1988; Rieu et al., 2005), where water flow reaches its maximum velocity causing erosion and bypass. This process causes deposition of the coarser sediments, which are accumulated along with shell fragments. Pebble-sized mud clasts derive from fragmentation of blocks collapsed from the channel banks (Klein, 1977; Terwindt, 1988). Although transport occurs under tractional conditions, repeated scouring and intense bioturbation contribute to produce structureless deposits.

Point bar deposits

These deposits are up to 1.7 m thick and are found in most of the cores located within the meander loop. They cover the channel-lag sand and are overlain by salt marsh (Fig. 3.4A) or channel-fill (Fig. 3.5A) deposits. They show a clear fining-upward (FU) grain size trend, defined by the vertical stacking of two main intervals (Fig. 3.4A). The basal interval, 0.8 – 1 m thick, consists of a grey-bluish medium to fine sand. This sand is mainly massive, contains scattered shells and rare mud clasts (Fig. 3.4D). Local occurrence of millimetric muddy laminae highlights plane-parallel stratifications, that can be up to 30° inclined (Fig. 3.4C). Bioturbation is common and in some cases can lead to the complete obliteration of primary sedimentary structures. The upper interval, 0.5 – 0.8m thick, consists of massive mud with millimetric laminae of well-sorted fine to very-fine sand. These laminae range from inclined (18°) to sub-horizontal moving upward in the interval (Fig. 3.4B). Bioturbation is common, whereas shells or shell fragments are rare. In the uppermost part of the interval, close to the transition with salt marsh deposits, organic-rich mud can locally occur.

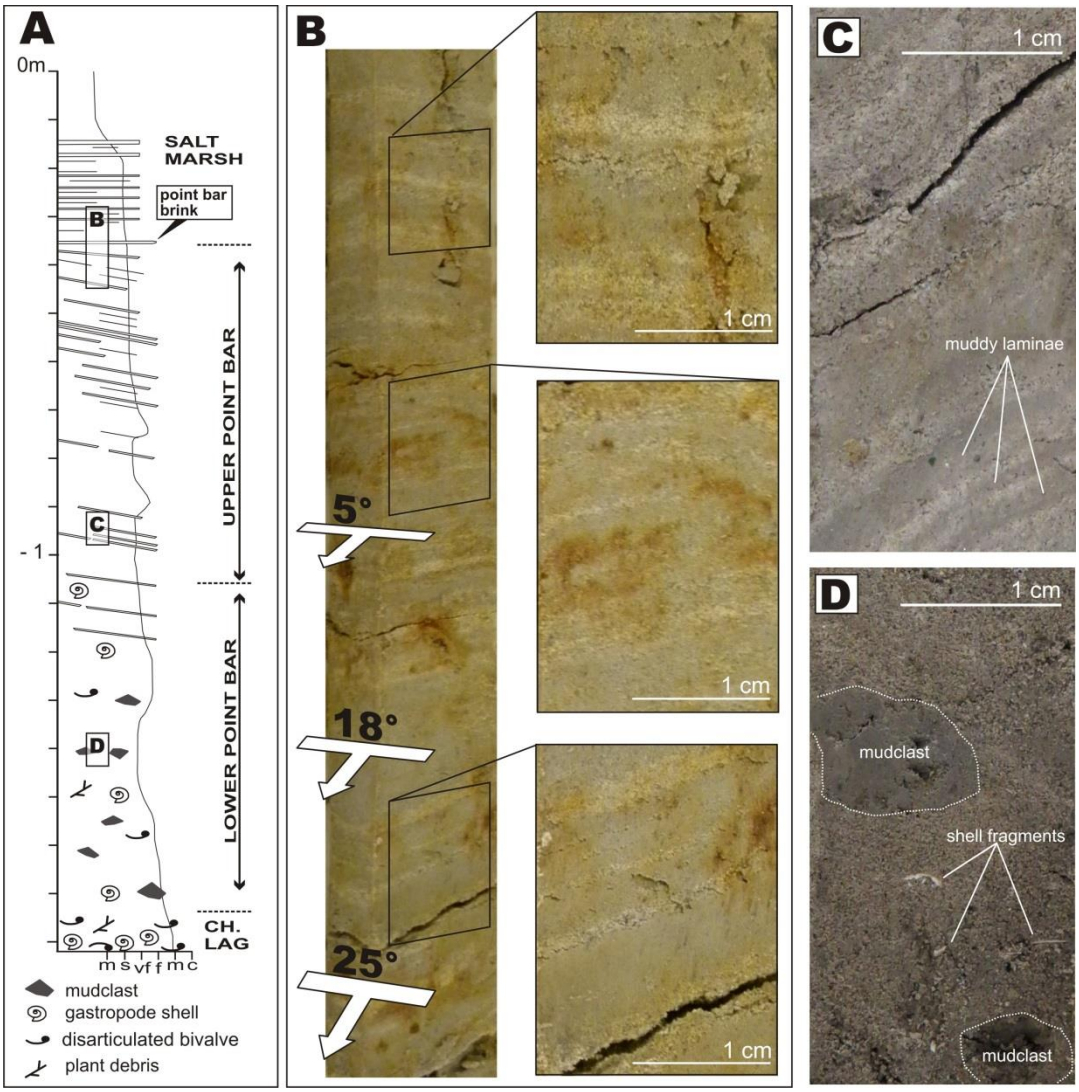

Figure 3.4: Sedimentary features of point-bar deposits. (A) Sedimentological log across point bar and overlaying salt marsh deposits. (B) Point bar brink deposits showing a decrease in depositional angle marking the establishment of salt marsh sedimentation. (C) Laminated sand with muddy laminae in the central part of the bar. (D) Massive sand with shell fragments and isolated mudclasts in the lower part of the point bar.

The fining-upward grain size trend and location of these deposits within the meander loop allow to interpret them as a point bar (cf. Rieu et al., 2005; Santos and Rossetti, 2006). Dominance of sand in the lower interval indicates that mud, accumulated on the bar during slack water phases, was removed by currents during both ebb and flood tide. The presence of sporadic muddy laminae may reflect settling during ebb or flood slough water, possibly during exceptional conditions such as during spring tides. Steeply inclined laminae would suggest gravitational deformations or minor collapses (Bridges and Leeder, 1976). In the upper part of the bar, the

dominance of silt indicates that sedimentation mainly occurred at flood peak, when fine-grained sediments settled from high water slack conditions. Millimetric laminae of well sorted sand formed during storm events, when salt marshes and bar top were winnowed by waves (cf. Fruergaard et al., 2011). The upward decrease in inclination of sandy laminae reflects the flattening of the bar morphology moving from bar slope to bar top.

Channel-fill deposits

These deposits, up to 1.9 m thick, occur in all the cores distributed along the oxbow lake and overlay the channel lag or point bar deposits (Fig. 3.5A). They consists of dark, organic-rich, massive mud (Fig. 3.5B) and contain bivalves in life position (Fig. 3.5C). Close to their base, they are slightly richer in fine sand and contain scattered plant fragments (Fig. 3.5D), whereas their uppermost part is locally characterized by oxidation (Fig. 3.5E).

Location and sedimentary features of these deposits suggest that they settled down in the abandoned channel after its cutoff. The presence of a sandy fraction in the lower part of the channel-fill succession suggests that the channel was not abruptly deactivated, and a minimum amount of water flowed along the bend just after the cutoff event. After the final abandonment, mud settled down and caused the complete infill of the channel. Local presence of oxidation in the uppermost part of the channel fill indicates that mud was affected by subaerial exposure, heralding colonization from salt marsh halophytic vegetation.

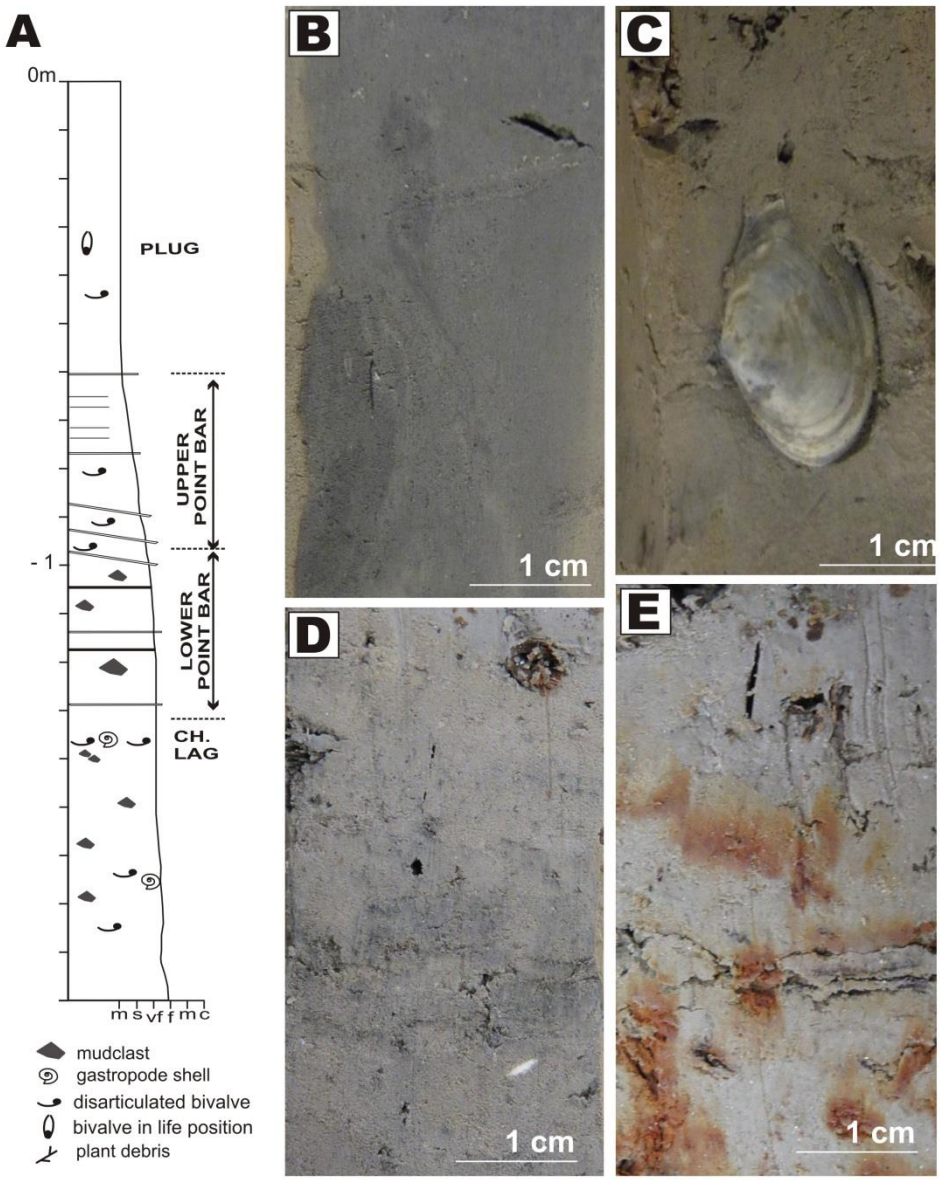

Figure 3.5: Sedimentary features of channel-fill deposits. (A) Sedimentological log showing the gradual transition from point bar sand to channel-fill mud. (B) Massive channel fill mud. (C) Bivalve in fife position in muddy deposits. (D) Sandy mud at the transition between point bar and channel fill deposits. (E) Oxidized uppermost channel fill mud.

3.2.5.2 Sediment distribution and stratal geometries

The study bar and its basal lag overlay subtidal platform sediments and are covered by both channel-fill and salt-marsh deposits (Fig. 3.6). Thickness of the channel lag deposits reaches its maximum in the bend apex zone, where the coarsest sand fraction is also concentrated. The overall fining upward grain size trend of the bar is well-developed, although the landward side

appears to be slightly sandier and coarser than the seaward one. Sandy laminae that typify the upper part of the bar occur in different portions of the bar, with similar frequency and thicknesses, without showing any specific distribution. Cross sections oriented both parallel and transverse to the point bar axis (Fig. 3.6A) show that bar deposits thicken toward the bend apex and the inflection points, and that thickening of the bar occurs in parallel with thinning of the overlying salt marsh deposits.

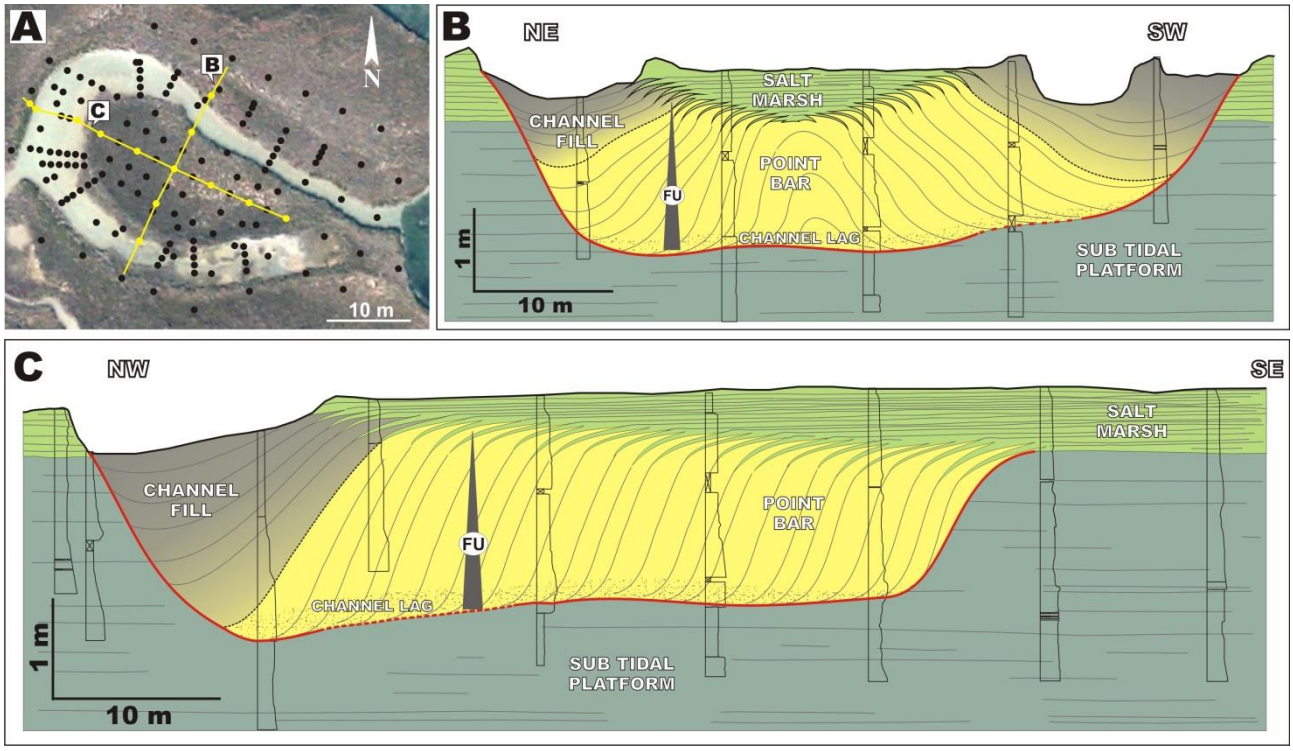

Figure 3.6: (A) Cross sections across the study point bar. (B) Section transverse to the point bar axis. Note that the bar top surface show a concave-upward geometry. (C) Section parallel to the point bar axis showing the progressive progressive channelward thickening of the bar deposits.

Spatial interpolation of core data allowed us to define geometry of three key surfaces: i) point- bar base; ii) point-bar top and iii) channel-fill base.

The point-bar base (Fig. 3.7A) is represented here as the erosive surface capping the sub-tidal platform deposits and flooring the channel-lag or, where it is missing, the point-bar sand. This surface is relatively smooth and has a lunate plane-view shape. It dips (4 – 6°) radially toward the thalweg zone, and, in a section parallel to the bend axis, it lowers down of about 0.8 m. In the

bend apex zone, the point bar basal surface defines a localized, elongated depression that follows the orientation of the channel. The point bar top surface divides the point bar body from the overlying salt-marsh and channel-fill deposits (Fig. 3.7B). This surface shows an overall topographic relief of about 1.9 m and is characterized by a lunate plan-view shape. The portion of this surface that is covered by salt marsh deposits shows a concave-upward, spoon-shaped geometry, whose axis is parallel to that of the channel bend. This depression has a topographic relief of about 0.6 m, and its rim corresponds to the point bar brink (i.e. inner bank of the abandoned channel; Fig. 3.7B).

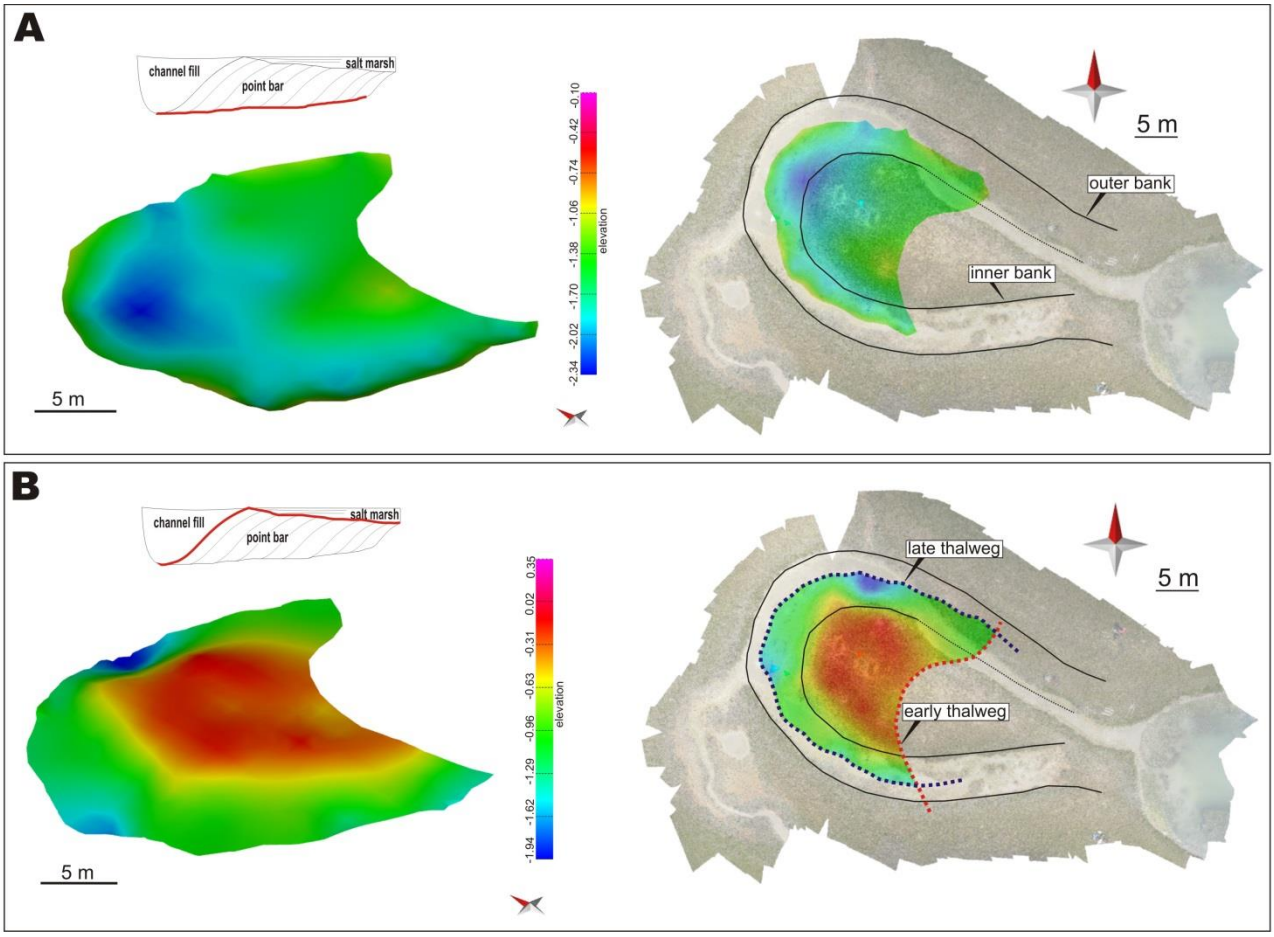

Figure 3.7: Point bar geometries. (A) Elevation model of the point bar basal surface showing the elongate scour depression formed by lateral migration of the pool zone. (B) Elevation model of the point bar morphology. Note the depression (yellow surrounded by red color) occurring on the bar top area.

The channel base is defined by the surface flooring the channel-fill deposits (Fig. 3.8A). The topographic relief of this surface reflects the depth of the abandoned channel. It spans from 1 m,

in the riffle zones, to about 2 m, in correspondence of the bend apex, where an elongate pool depression (Fig. 3.8A) is characterized by the occurrence of two main scours, located just landward and seaward of the bend apex (Fig. 3.8B). The seaward and landward scours are 1.7 and 1.9 m deep, respectively, and their distance is about 15m (Fig. 3.8C). Basing on the morphology of this surface, the related channel was characterized by a width-to-depth ratio of 3 and 4 in the pool and riffle zone, respectively.

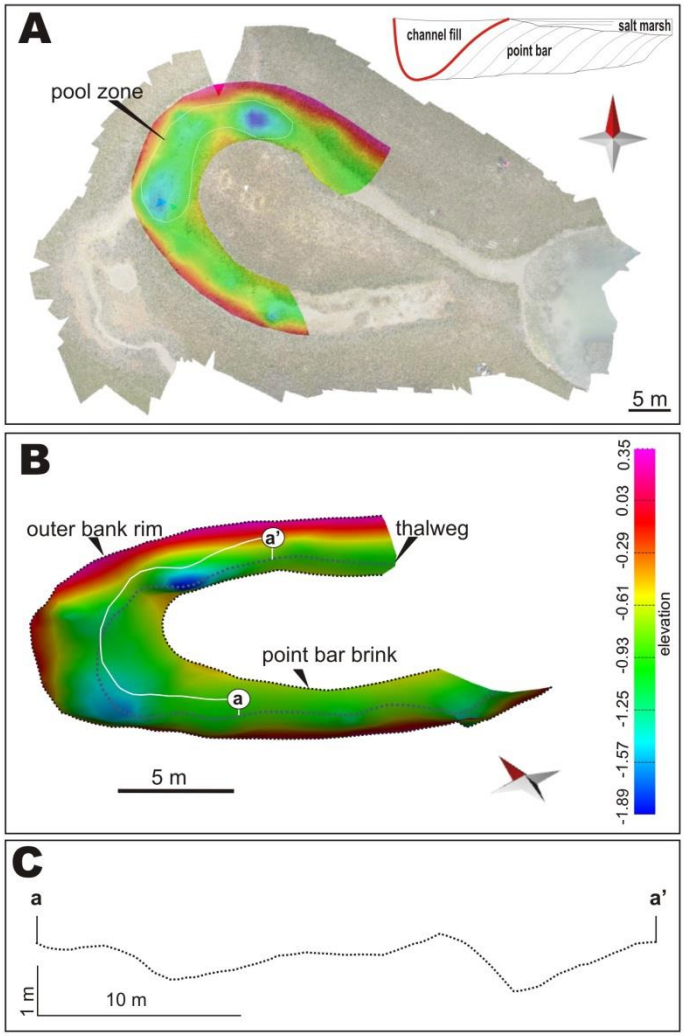

Figure 3.8: Channel-fill geometries. (A) Plane view of the relief map showing distribution of the deeper areas of the channel base. (B) Elevation model of the channel basal surface. (C) Cross section along the thalweg in the pool zone. Note the occurrence of two main scours probably associated with activity of the ebb and flood secondary cells.

3.2.6 Discussion

3.2.6.1 Sediment distribution along the bend

The occurrence of the point bar body between sub-tidal platform and salt-marsh deposits (Fig. 3.6) suggests that the study channel started to develop in the lower part of the intertidal zone, which then evolved into a salt marsh platform and was progressively colonized by vegetation, as attested by the widespread diffusion of root remains in the uppermost 0.6 m of the overbank succession (Fig. 3.3A and 3.6). The establishment of a salt marsh environment corresponds to the onset of bar growth, suggesting that development of vegetation stabilized the channel banks, promoting lateral migration of the channel bend (cf. Peakall et al., 2007). Sediment distribution and geometries of point-bar body suggest a number of similarities between tidal and fluvial point bars, such as the "classical" fining upward grain-size trend (McGowen and Garner, 1970; Brice, 1974; Jackson, 1976; Nanson, 1980), or the development of levees along the outer bank (Kolb, 1963; Cazanacli and Smith, 1996; Houdson et al., 2003). On the other hand, several differences can be also noted, such as the absence of crevasse-splay deposits along the outer bank and the uniform distribution of sediment grain size along the bar. Crevasse splay deposits represent a distinctive feature of overbank areas in alluvial plain settings (Smith et al., 1989; Mjos et al., 2009; Ielpi and Ghinassi, 2014); they commonly develop along the outer bank of open bends, where the flood flow impinges and break through the bank at the bankfull stage. In salt marsh channels, development of crevasse splay would be potentially triggered only by flood flows, but their formation is hindered by the absence of long-lasting, exceptionally-high discharges resembling fluvial floods.

The depth-averaged flow velocity and the related bed shear stress play a key role in determining mean grain size distribution along channel bends. In fluvial meanders, these quantities reach higher values along the upstream portion of the point bar, and along the outer

bank at the downstream end of the bend (Dietrich and Smith, 1983; Frothingham and Rhoads 2003; Kasvi et al., 2013). Accordingly, grain size significantly fines downstream along fluvial point bars (Jackson, 1976; Smith et al., 2009; Hubbard et al., 2011; Labrecque et al., 2011; Ielpi and Ghinassi, 2014). The overall nearly symmetric distribution of sediment grain size along the study bar, highlights that its seaward and landward sides behaved cyclically as upstream and downstream bar sectors, experiencing similar changes in the intensity of bed shear stresses. Although salt marsh channels are usually dominated by ebb currents (Bayliss-Smith et al., 1979; Fagherazzi et al., 2008; Hughes, 2012), this asymmetry was not strong enough to be significantly reflected in the grain-size distribution along the bar, and is possibly documented by the occurrence of slightly coarser sand along the landward side of the bar. A further effect of the current reversal is the cyclic relocation of the flow impingement point (Hughes, 2012) along the outer bank. This causes development of two distinct helicoids (i.e. flood and ebb helicoids) that act at different times and different areas of the bend apex zone. Such a flow configuration is responsible for the elongated shape of the pool zone (Fig. 3.8A), where the two scours are thought to reflect localized erosion, triggered by flood and ebb helicoids.

3.2.6.2 Bed aggradation and bar geometry

Surfaces bounding the base (Fig. 3.7A) and the top (Fig. 3.7B) of the study bar diverge toward the outer bank zone in correspondence of the bend apex, causing an overall thickening of the bar from 1.5 to about 2 m (Fig. 3.6C). The basal surface of the bar represents the trajectory along which the channel lag moves during the meander bend evolution. The lowering of the basal surface during channel migration, results from the progressive increase in sinuosity of the channel, that increases the erosion by the helicoidal flow, which in turn downcuts deeper in the bend apex zone (Willis and Tang, 2011). The bar top surface is shaped by the progressive lateral and upward

shift of the point bar brink. The intersection between this surface and the axial plane of the bend defines the brinkpoint trajectory (Fig. 3.9). In both transverse and longitudinal sections (Fig. 3.6), the bar top surface rises, indicating that channel migration occurred during aggradation of surrounding salt marshes. In equilibrium conditions, like those occurring in the S. Felice area (Roner et al., 2015), the rate of salt marshes aggradation keeps pace with the rate of relative sea level rise, through organic and inorganic sediment accumulation (Morris et al., 2002; D'Alpaos et al., 2007; Mudd et al., 2010). As a result, channel banks rise causing a progressive channel deepening, that is further enhanced by the aforementioned lowering of its basal erosional surface. Lateral migration of the channel is, therefore, associated with an increase in its cross-sectional area, which adapts to the progressively increased tidal prism (D'Alpaos et al., 2010). A similar process is documented in Holocene tidal channels, offshore of western Netherlands (Rieu et al., 2005), where the increase of tidal prism is entirely accommodated by the basal scouring of the channel. Progressive rise of basal channel surface, as that documented by deMowbray (1983), would therefore suggest a subtle increase of the tidal prism, that forces the channel cross-sectional area to remain constant through in-channel aggradation.

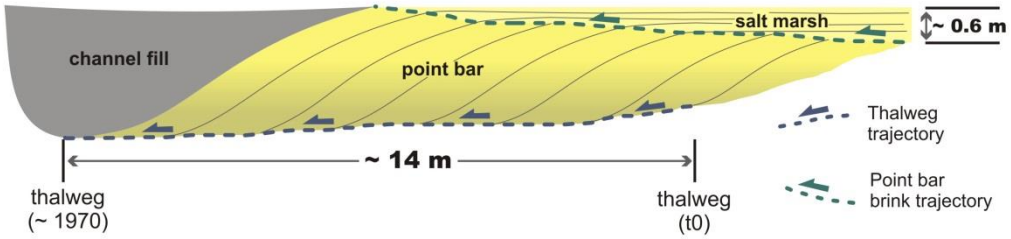

Figure 3.9: Schematic cross section parallel to the meander bend axis. Note the rising trajectory of the bar brink zone and lowering of the basal point bar surface.

Bar top aggradation contributes also to explain the absence of a scroll-bar morphology on top of tidal point bars. In fluvial settings scroll-bar morphology develops during large flood events (Nanson, 1980; Nanson and Hickin, 1983), when a large amount of sediment is pushed on the bar by the secondary circulation. In tidal settings, the absence of a sustained secondary circulation

during most of the tidal cycle along with the limited range of flowing discharge (Fagherazzi et al., 2008; Hughes, 2012) hinders this process. Additionally, the salt marsh accretion on bar top rapidly smooths all the possible subtle scroll-bar morphologies.

The mean vertical aggradation rate of the San Felice salt marsh is about 2.5-3 mm/yr (Bellucci et al., 2007; Rizzetto and Tosi, 2011). This suggest that the 60 cm thick salt marsh deposits covering the oldest part of the bar (Fig. 3.9) started accumulating around 200-240 years ago. The lifespan of the bar is about 135-175 years, since aerial photos show that cutoff occurred at the beginning of the 50's (Rizzetto and Tosi, 2012). It follows that the average lateral migration rate of the study meander was about 8-10 cm/yr, being the distance covered by lateral migration of 14 m (Fig. 3.6 and 3.9). This rate of channel migration is consistent with other studies (Garofalo, 1989; Gabet, 1998), and specifically with rates obtained by recent works on channels of the Venice Lagoon (Finotello et al., 2015). The occurrence of medium pebble-sized mud clasts in channel lag deposits is consistent with a slow migration rate. Their presence suggests that large blocks, collapsed from channel banks (c.f. Gabet, 1998; Fagherazzi et al., 2004), remained for a long time in the thalweg zone, where they are comminuted before to be buried the adjacent laterally migrating bar. This scarce mobility of the channel can be partially explained by the stabilizing effect of vegetation and cohesive sediments (Hooke, 2013; Marani et al., 2002), although a relevant contribute to hindering lateral migration is certainly provided by the absence of long-lasting, high-discharge events, like those affecting river meanders (Moody and Meade, 2014).

Research studies on floodplain sedimentation (e.g. Middelkoop and Asselman, 1998; Erkens et al., 2011; Stouthamer et al., 2011) show that the rate of fluvial overbank aggradation is comparable with that of the study case. The scarce documentation of geometries, like those highlighted in the present study, suggests that in fluvial realm the effects of overbank aggradation are commonly nullified by high rates of lateral migration (Hickin and Nanson, 1975; 1984; 1986;

Brice, 1977; Biedenham et al., 1989; Lagasse et al., 2003; 2004; Moody and Meade, 2014), which are known to be at least an order of magnitude higher than in tidal setting (Allen, 2000). A fluvial channel with the same geometry (i.e. width and radius of curvature) of the study bend, might migrate over the same distance within about 20-25 years (Hickin and Nanson, 1985; Hooke, 1997; 2007; Biedenham, 1984), producing, with a bed aggradation of about 2.5-3 mm/yr, a negligible rise of the point bar brink trajectory (c.a. 6 cm). This suggests that outcrop examples, where the effects of bed aggradation on meander belt geometries is manifested (Ghinassi et al., 2014), are associated with floodplain aggradation rates of centimeters per year, as also demonstrated by numerical simulations (van de Lageweg et al., 2015).

3.2.7 Conclusions

Stratal architecture and sedimentary features of a meander bend in the northern Venice Lagoon provided insights to understand the morphodynamic evolution of tidal point bars, and to compare them with their fluvial counterparts. The highlights of the present study are graphically summarized by figure 3.10 and can be listed as follows:

1) Tidal meander bends are characterized by well-developed, sand-rich levee deposits. Differently from fluvial setting, limited range of flowing discharge prevents levee breaching and formation of crevasse splays.

2) In a symmetric tidal meander bend, during a tidal cycle, the seaward and landward sides of the tidal point bar act as upstream and downstream bar sectors and experience bed shear stresses of similar magnitude. In the studied bar, this causes an overall symmetric distribution of sediment grain size along the bar.

4) The bi-directionality of tidal currents causes secondary circulations to cut an elongated pool scour, that can be characterized by two minor depressions possibly associated to ebb and flood secondary cells.

5) The bar migrated laterally and increased its cross-sectional area both scouring its base and lifting up its banks. This allowed the channel to compensate the progressive increase in the tidal prism.

6) Combination between lateral migration (8-10 cm/yr) and vertical aggradation (2.5-3 mm/yr) provided a spoon-shaped geometry to the bar top surface. Although meandering rivers can be affected by comparable rates of floodplain aggradation, development of similar geometries is hindered by their high lateral migration rate, that allows the cutoff to be reached before that a significant thickness of deposits is accumulated on the bar top.

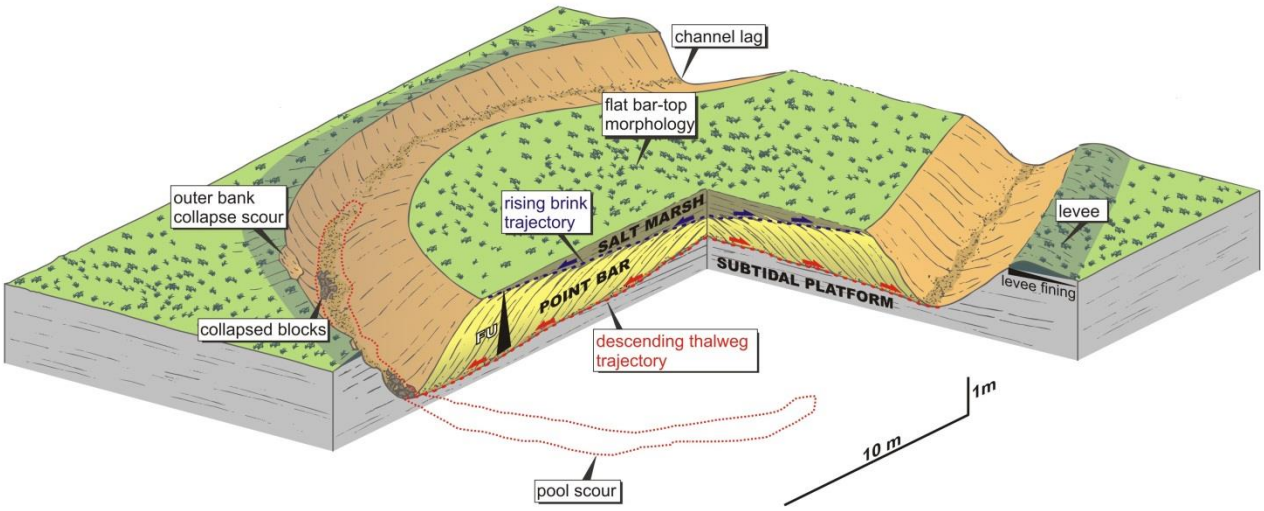

Figure 3.10: Block diagram summarizing the main architectural and sedimentological features of the study bar.

CHAPTER 4

MORPHODYNAMICS, STRATAL PATTERNS AND SEDIMENTARY PROCESSES OF A SUBTIDAL POINT BAR

4.1 OVERVIEW

This chapter represents a journal paper in preparation. It deals with sedimentary processes and planform evolution of a subtidal channel in the southern Venice Lagoon. This work is based on the interaction between remote sensing, seismic and sedimentological data. The results stemming out from this work show that the study channel evolves under the interaction between tidal and wave currents, and that lateral accretion occurs in parallel with top bar and overbanks aggradation.

4.2 PAPER

LARA BRIVIO[1], MASSIMILIANO GHINASSI[1], ANDREA D'ALPAOS[1], ALVISE FINOTELLO[1]

[1] *Department of Geosciences, University of Padova, Padova, Italy.*

4.2.1 Abstract

Facies models for tidal meander bends are essentially based on modern channels developed in the intertidal zone, whereas limited attention has been paid to sedimentary processes and stratal architecture characterizing subtidal channels. The present study aims at improving our understanding of subtidal point bars formed in a lagoon affected by microtidal regime, analyzing a submerged meander bend in the southern part of the Venice Lagoon (Italy). The study channel is 70-100 m wide, has radius of curvature of about 260 m and develops on a

constantly submerged subtidal platform. Water depth ranges from 1 to 5 m above the mean sea level on the subtidal platform and channel thalweg, respectively. The present work is based on coupling of remote sensing (i.e. comparison between historical maps, aerial photos and satellite images), sedimentological (i.e. core logging) and geophysical analyses (i.e. sub-bottom profiles). Differently from classical model developed for tidal point bars, sedimentation in the study bar stemmed out from the interaction between the in-channel secondary helical flow and wave winnowing of the overbank areas. The helical flow redistributed sediment from the channel thalweg to the bar top and contributed to development of the "classical" fining-upward grain size trend of point bar deposits. Wave-winnowing of the overbank areas drifted sediment into the channel, forming peculiar apron-like accumulations both along the outer and inner bank. Coupling between remote sensing data and sub-bottom profiles shows that, over the past century, sedimentation was not uniform in different sectors of the meander bend. Maximum values of channel migration rate (dm/yr), nevertheless, are still in the range of those measured for tidal channels. The sector of the bar affected by major lateral shift was also affected by strong vertical aggradation (ca. 1 cm/yr). In this zone, the rising and flattening bar brink point trajectory indicates the progressive decrease in aggradation rate, which is associated with reduction of sediment supply affecting the lagoon over the past century.

Keywords: subtidal meander, tidal currents, morphodynamics, aggradation, lateral accretion, Venice Lagoon

4.2.2 Introduction

Tidal channels constitute the pathway for propagation of tides and sediments and act a primary control on the sedimentation and ecology of lagoons and estuaries (Hughes, 2012). Tidal

channels cut through the tidal basin forming complex dendritic networks, in which minor creeks usually converge into a major channel (Ashley and Zeff, 1988; Fagherazzi et al., 1999). Meandering channels are very common in tidal setting, and they can be located either in the intertidal or the subtidal zone (Bartholdy, 2012) and, therefore, they can be either periodically or constantly submerged by water. Geomorphological and sedimentological models for tidal meanders entirely derive from modern intertidal, tidal flat channels (Land and Hoyt, 1966; Howard et al., 1975; Barwis, 1978; de Mowbray, 1983; Bridges and Leeder, 1976; Choi et al., 2004; Choi, 2011; Hughes, 2012), where overbank areas are generally exposed during low tide. Such meanders usually develop on muddy or sandy substrates, on which the vegetation cover can range from absent to widespread. Point bars associated with intertidal meanders show an overall architecture which is comparable with their fluvial counterparts (Allen, 1963; McGowen and Garner, 1970; Brice, 1974; Jackson, 1976; Nanson, 1980), because channels are characterized by similar sinuosity, and accretional and erosional processes along the inner and outer bank respectively (e.g. Allen, 1982; Solari et al., 2002; Seminara et al., 2002). Beyond such affinities, sedimentary facies distribution would be different in tidal and fluvial point bars since: 1) tidal channels are affected by flow reversal; 2) tidal discharge fluctuates within a defined range, whereas fluvial discharge can be characterized by a more marked variability; 3) tidal channels experience condition of slack water even without be abandoned; 4) expansion of tidal channels is commonly associated with an increase in channel width, whereas the width of fluvial channels keeps almost constant during planform transformations.

The differences between fluvial and tidal meanders appear to be even more evident considering subtidal channels. These channels are common close to the inlets that connect lagoons with the open sea, and form a complex tributary system, which can connect its landward reaches with the intertidal channel network. Differently from alluvial plains, which can be

inundated only during exceptional floods, subtidal meanders and related overbank areas are constantly submerged. Hydrodynamic of these channels is extremely complex, since both minimum and maximum velocities of tidal currents are experienced when both the channel and related overbanks are flooded. Flow distribution within the channel can be influenced by currents developed in overbank areas, promoting a hydrodynamic configuration which can control times and modes of channel planform evolution. In subaqueous setting, water-saturation of the point bar deposits decreases the intergranular friction and promotes collapses along the bar flanks (Bridges and Leeder, 1976; Choi et al., 2013). Moreover, where subtidal platforms hosting channels occur in wide and shallow lagoons, inter-channel areas can be affected by strong wind-induced wave winnowing, which can influence sediment distribution along the channels draining the platforms. Although the combination of the aforementioned features can sign the stratal patterns and sedimentary facies distribution of subtidal point bars, specific facies models for these bars are missing, and documentation of these deposits in the fossil record is limited to their occurrence on top of coarsening-upward successions associated with tidal flood deltas.

Towards the goal of providing new insight into the morphodynamic evolution and sedimentology of subtidal meander bends, the present study investigates a submerged meander, located in the southern Venice Lagoon (Adriatic Sea, Italy). A multidisciplinary approach was chosen in order to reconstruct the meander bend evolution and its internal architecture. The planform evolution of the study bend during the last century was obtained through the comparison between detailed historical maps, aerial photos and satellite images. High-resolution geophysical investigations along with the analysis of sedimentary cores allowed to depict the sedimentary facies and internal architecture of the point bar deposits and outer bank region. Integration between the aforementioned datasets allowed to depict a facies model for subtidal channel developed in lagoons affected by micro-tidal regimes.

4.2.3 Geological Setting

4.2.3.1 The Venice Lagoon

The Venice Lagoon, located in the NE sector of Italy (Fig. 4.1A), is situated in the Venetian foreland basin, which developed between the South-Alpine and the Apennine chains since the Late Oligocene (Massari et al., 2009). During the Early Pleistocene, the basin experienced deep-water deposition; afterwards it was filled up with about 750 m of shallowing-upward deposits, spanning from turbidites to shallow marine (Massari et al., 2004). The Venice Lagoon formed during the last 7500 years as a consequence of the Holocene transgression, which promoted the formation of lagoon – estuarine – barrier systems in the Northern epicontinental Adriatic shelf, through the flooding of the Late Pleistocene alluvial-plain (Zecchin et al., 2009). The modern Venice Lagoon (Fig. 4.1B), forms an elongated, NE-SW oriented basin, which represents the largest Mediterranean brackish water body (roughly 550 km^2), with a length of about 50 km and 10 km width. The lagoon average depth is of about 1.5-2 m. It is connected to the Adriatic Sea through three inlets (Lido, Malamocco and Chioggia; Fig. 4.1B) and is subjected to a semidiurnal tidal regime, with an average tidal range of about 1.0 m and peak tidal amplitudes of about 0.75 m (D'Alpaos et al., 2013) around Mean Sea Level (MSL).

4.2.3.2 The study site

This study focuses on the Portosecco channel, which is located in the southern Venice Lagoon, about 3 km east of the Malamocco inlet (Fig. 4.1B, C). The Portosecco subtidal channel ranges in width between 70 and 100 m, shows a wavelength of about 1 km and a radius of curvature of 260 m (Fig. 4.1D). The channel bend axis trend about EW. The channel develops on a subtidal platform, locally covered by widespread seagrass meadows. Average water depth on the subtidal platform is about 1 m below the mean sea level (MSL), whereas the channel thalweg

ranges between 4 and 5 m below the MSL. The width to depth ratio of the channel is around 19. In the southernmost reach of the study bend (Fig. 4.1D), the channel branches around a relief that is about 1.7 m high from the channel floor. This relief has an elongated planform shape, and is 60 m wide and 300 m long.

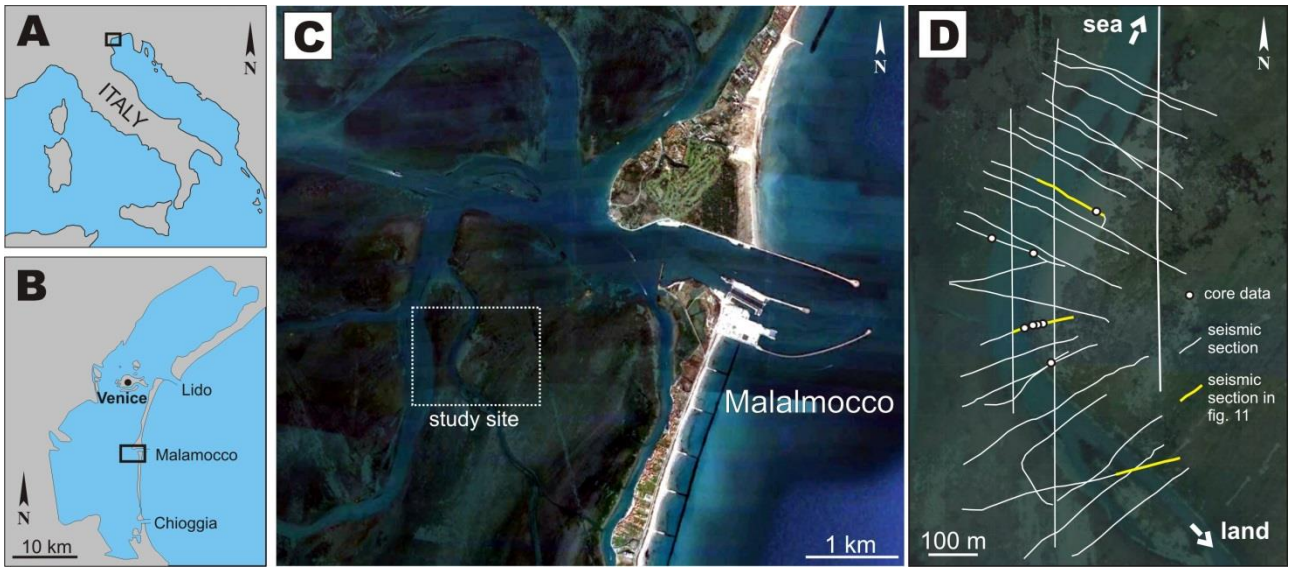

Figure 4.1: Geographic location of the study site. (A) Location of the Venice Lagoon in the Mediterranean Sea. (B-C) Position of study site in the central part of the Venice Lagoon. (D) Satellite image (from Google™ Earth) showing the study meander bend and acquisition scheme of sub bottom profiles. Yellow dots show location of sedimentary cores.

4.2.4 Methods

The present work is based on coupling of remote sensing, sedimentological and geophysical analyses. The terms used here to define different parts of the channel bend and related deposits (Fig. 4.2), are similar to those used for fluvial meanders and related deposits (Ielpi and Ghinassi, 2014). Considered the bidirectional nature of tidal currents along the meander bend, the upstream and downstream sides of the point bar are named here landward and seaward side, respectively (Fig. 4.2). The point bar brink (Fig. 4.2) is named here as the rim separating the top of the bar from its slope.

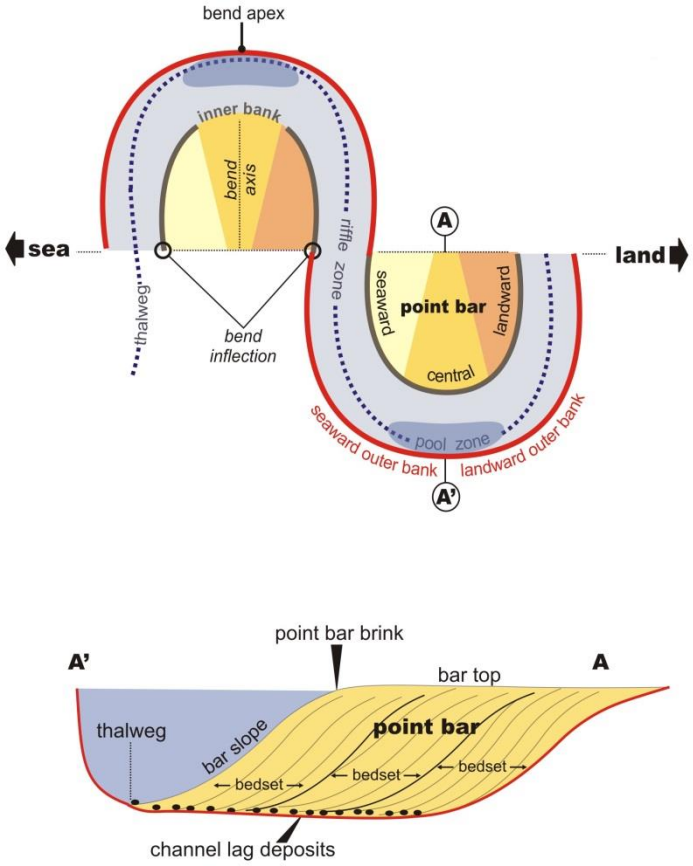

Figure 4.2: Descriptive terminology for tidal meander bends and related point-bar architecture.

4.2.4.1 Historical data analyses

The historical planform evolution of the study area was recovered using georeferenced CTR map (1900), aerial photo (1962) and satellite image (2015), which offer a cover for an overall time-span of about 100 years (Fig. 4.3A). The subtidal channel banks were digitized for each year using ArcGIS, to determine the distribution and the size of areas in which erosion and/or deposition took place, as consequence of channel migration. The planform evolution of the Portosecco channel has been defined through the comparison between maps of its boundaries: 1900 vs 1962 (Fig. 4.3B); 1962 vs. 2015 (Fig. 4.3B) and 1900 vs. 2015 (Fig. 4.3C). These maps allow to define the maximum rates of bank shifts, for each study time interval.

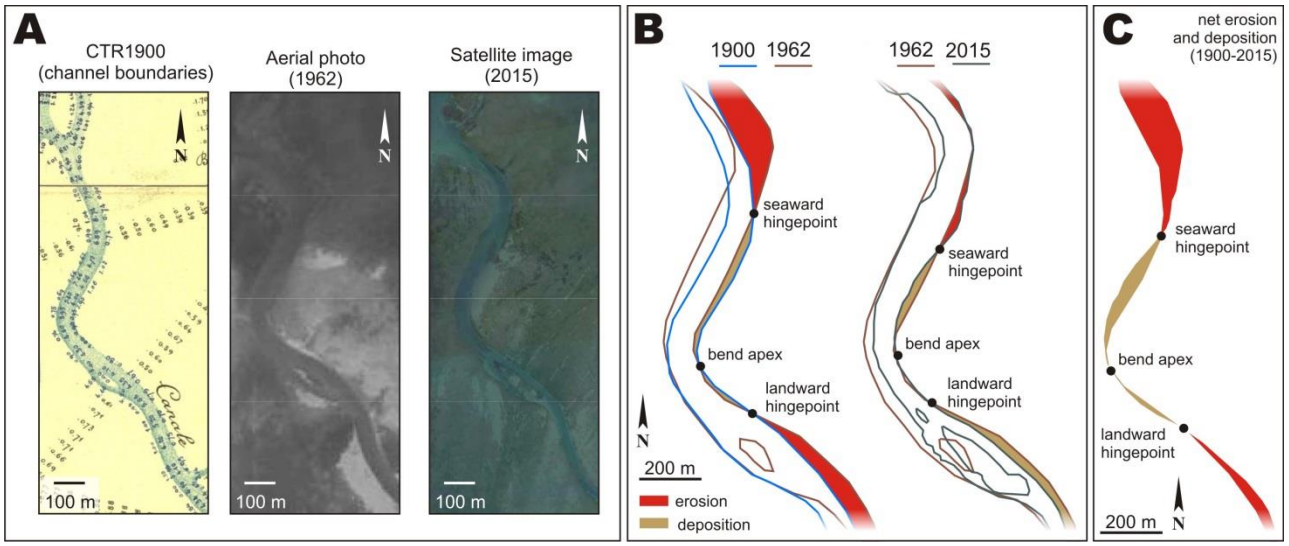

Figure 4.3: Planform evolution of the study bar. A) Historical maps and aerial photos used for comparing different stages of channel bend evolution. B) Distribution of erosion and deposition during different stages (1900 vs. 1962 and 1962 vs. 2015) of channel development. C) Net erosion and deposition occurred along the eastward bank of the study channel between 1900 and 2015.

4.2.4.2 Sedimentary core analysis

Using a hand auger coring sampler, which prevents sediment compaction, eight georeferenced cores were recovered in selected sites (Fig. 4.1D), in order to calibrate the sub-bottom sections and define sedimentary features of point bar and overbank deposits. Coring depth spans from 1 to 3 m and cores are 3.5 cm in diameter. Collected cores were kept humid in PVC liners and successively cut longitudinally, measured and photographed. Core logging was carried out following the basic principles of facies analyses, highlighting sediment color and grain size, presence of sedimentary structures, vertical grain-size trends, degree of bioturbation and presence of vegetal and/or shell remains.

4.2.4.3 Sub bottom profiles

In order to analyze the point bar internal architecture, sub-bottom profiler investigations were carried out boating over the channel and related overbank areas. Data acquisition took place in ultra-shallow water conditions, with an average water level lower than 1 m deep. Seismic data

were acquired along 28 transects, oriented both parallel to the North (3) and perpendicular (25) to the channel of the meander (Fig. 4.1D). Profiles were acquired by using a sub-bottom profiler that during the acquisition worked with acoustic pulses in Continuous Waveform (CW) mode, using a 3.5 kHz frequency and short pulses (0.5-3 msec). Low frequencies were used to investigate the subsurface architectures. Processing was carried out by means of Seisprho software, using a signal velocity of 1500 m/s. Position data and acquisition tracks were registered through GPS (two TOPCON GR-3 receivers – dual frequency (L1/L2) and dual constellation (NavStar/Glonass), with integrated Tx/Rx UHF radio were used) and then processed through the Geo Office software of Leica. The diffuse seagrass meadows, together with ultra-shallow water conditions and presence of gas, locally prevented acquisition of high-resolution data.

Three representative sections, located in the landward, central and seaward side of the channel bend respectively (Fig. 4.1D), were analyses integrating planform evolution of the bend (Fig. 4.3A) with seismic data. Specifically, by means of a 3D modelling software (Move 2014.2^{TM}), the position of the inner bank of the bend in 1900 and 1962 was projected in these specific section, allowing detection of stratal architectures developed over the past century.

4.2.5 Results

4.2.5.1 Planform evolution

The comparison between the historical CTR map (1900) and the aerial photo acquired in 1962 (Fig. 4.3B) shows that the bar slightly accreted laterally, with a maximum shift of about 24 m along its seaward side that occurred with a rate of ca. 40 cm/yr. A slight migration rate characterized the landward side of the bar, whereas the bend apex remained almost stable. In parallel, erosion occurred north and south of the study bar along the eastern bank of the channel

(Fig. 4.3B). The maximum of bank retreat occurred North of the bar, where the bank shifted 109 m eastward, with a migration rate of ca. 175 cm/yr.

Between 1962 and 2015, most of the eastern bank of the channel accreted, and erosion was limited to its northern reach (Fig. 4.3B). The maximum accretion occurred in the southern reach of the channel, where erosion dominated between 1900 and 1962. Here the eastern bank of the channel shifted westward of 23 m, with a rate of about 43 cm/yr. Erosion decreased in the northern areas, where the eastern bank retreated of 24 m, with a rate of 45 cm/yr. The bend apex remained almost stable during this stage.

A comparison between the historical CTR map (1900) and the 2015 configuration (Fig. 4.3C) shows that the overall morphology of the study bar did not vary significantly over the past 115 years. Over this time span, the bar slightly accreted laterally, with a total shift of about 50 m along its seaward side. The landward side shifted laterally of about 16 m, whereas the bend apex remained almost stable. Seaward of the study bar, where erosion was dominant, the eastern bank of the channel retreated of about 126 m. The final result of the alternation between erosion and deposition in the southern reaches of the eastern bank, was an overall bank retreat of about 35 m. The overall effect of these planform changes was an increase of the radius of curvature from 220 to 280m, without any relevant shift of the bend apex.

4.2.5.2 Sedimentary features

Point bar deposits

Point bar deposits consist of sub-horizontal beds that cover a clinostratified interval (Fig. 4.4 and 4.5A). These deposits have been cored for about 2 - 2.5 m, although seismic data show that they are up to 5 m thick (Fig. 4.4) and that can be followed for about 80-90 m in dip direction.

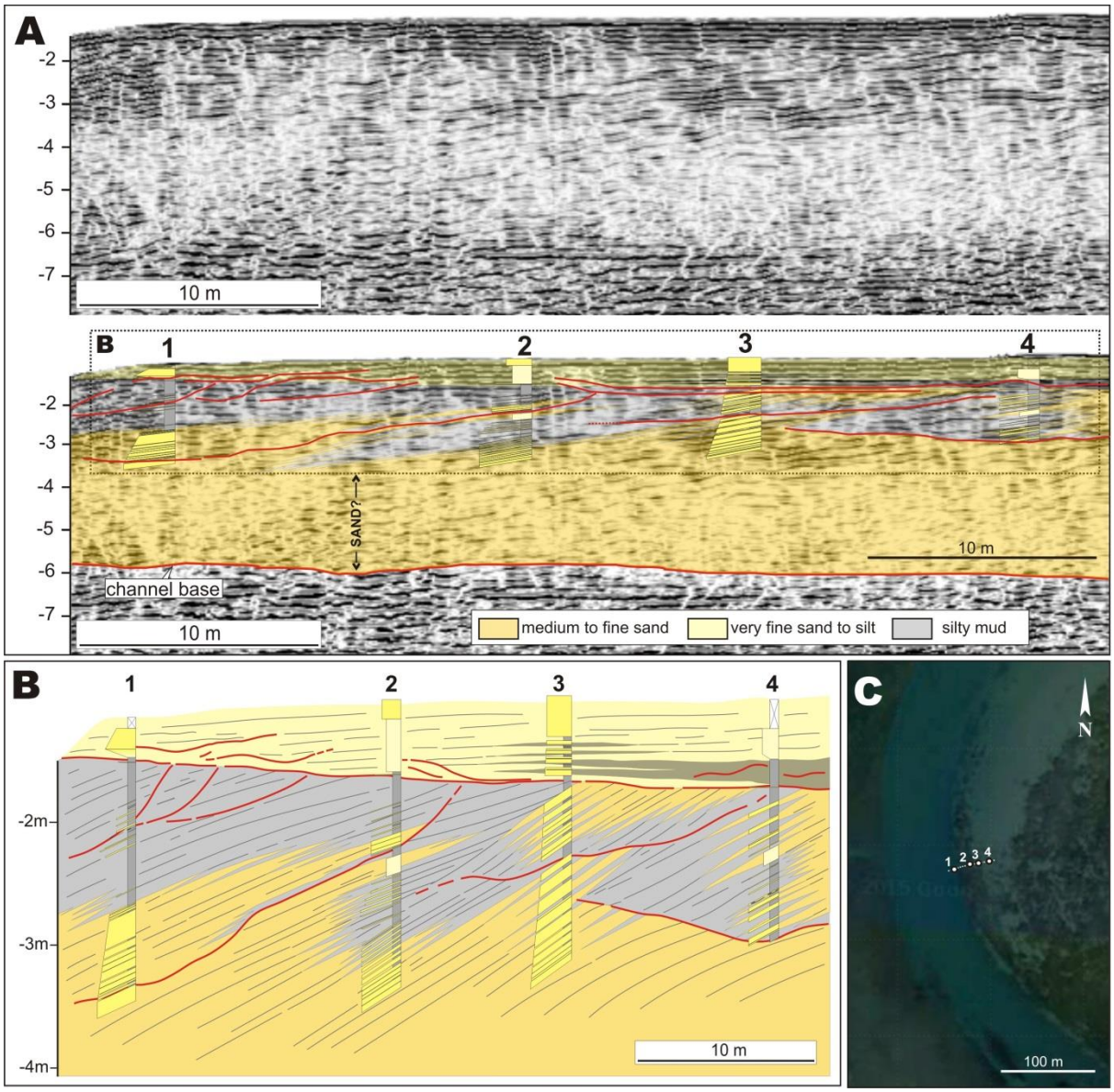

Figure 4.4: Clinostratified deposits. A) Sub-bottom profile along the point bar axis and relative interpretation coupled with core data. B) Close view of A showing correlation between cores with vertical exaggeration. C) Location of the study profile.

Clinostratified deposits are made of dark-colored, 0.5-3 cm thick heterolithic beds, consisting of alternating mud and fine to medium sand, with abundant plant and shell debris (Fig. 4.5A, B). The uppermost 1.8 m of these deposits show a clear fining-upward grain size trend, that is commonly associated with a thinning of beds. Inclined beds dip between 10° and 3°, and they flatten out moving upward (Fig. 4.4B). Mud is generally massive, although plane parallel laminations are locally preserved and highlighted by the presence of millimetric, dark, organic

laminae (Fig. 4.5B, D). Sandy layers are commonly normal graded (Fig. 4.5B) with a sharp, erosive base (Fig. 4.5E). Sand is well-sorted, mud-deprived and contains millimetric shell fragments and rare gastropods. Plant debris are very abundant in these sandy layers (Fig. 4.5C), and can be concentrated in the upper part of the normal graded beds (Fig. 4.5B, C), where a subtle plane parallel stratification occurs. Bioturbation is not common, and isolated, sub-vertical, cylindrical burrows (Fig. 4.5E) have been detected in some cores. Integration between core and seismic data shows that changes in grains size and dipping angle can occur in adjacent bedsets (Fig. 4.4).

Horizontal-bedded deposits sharply overlay the clinostratified sand and mud (Fig. 4.4A and 4.5A) and thin from 80 to 10 cm moving toward the bend apex (Fig. 4.4B). They consist of poorly-defined, 3-5 cm thick beds of grey sandy silt to fine sand with subordinate mud. Sandy and silty beds are massive and contain scattered plant debris or shell fragments (Fig. 4.5G, K). The basal boundary of sandy beds is commonly sharp, and marked by accumulations of shell fragments (Fig. 4.5F, H). Bivalve shells from these layers are commonly abraded (Fig. 4.5I). Muddy silt can show a subtle lamination, commonly marked by plant detritus. Bioturbation is diffuse and causes local deformation of the thinner layers (Fig. 4.5F). Horizontal-bedded deposits show an overall, coarsening-upward grain-size trend from silt to medium-fine sand; although correlation between adjacent cores shows that also lateral changes in grain size occur over distances of few tens of meters.

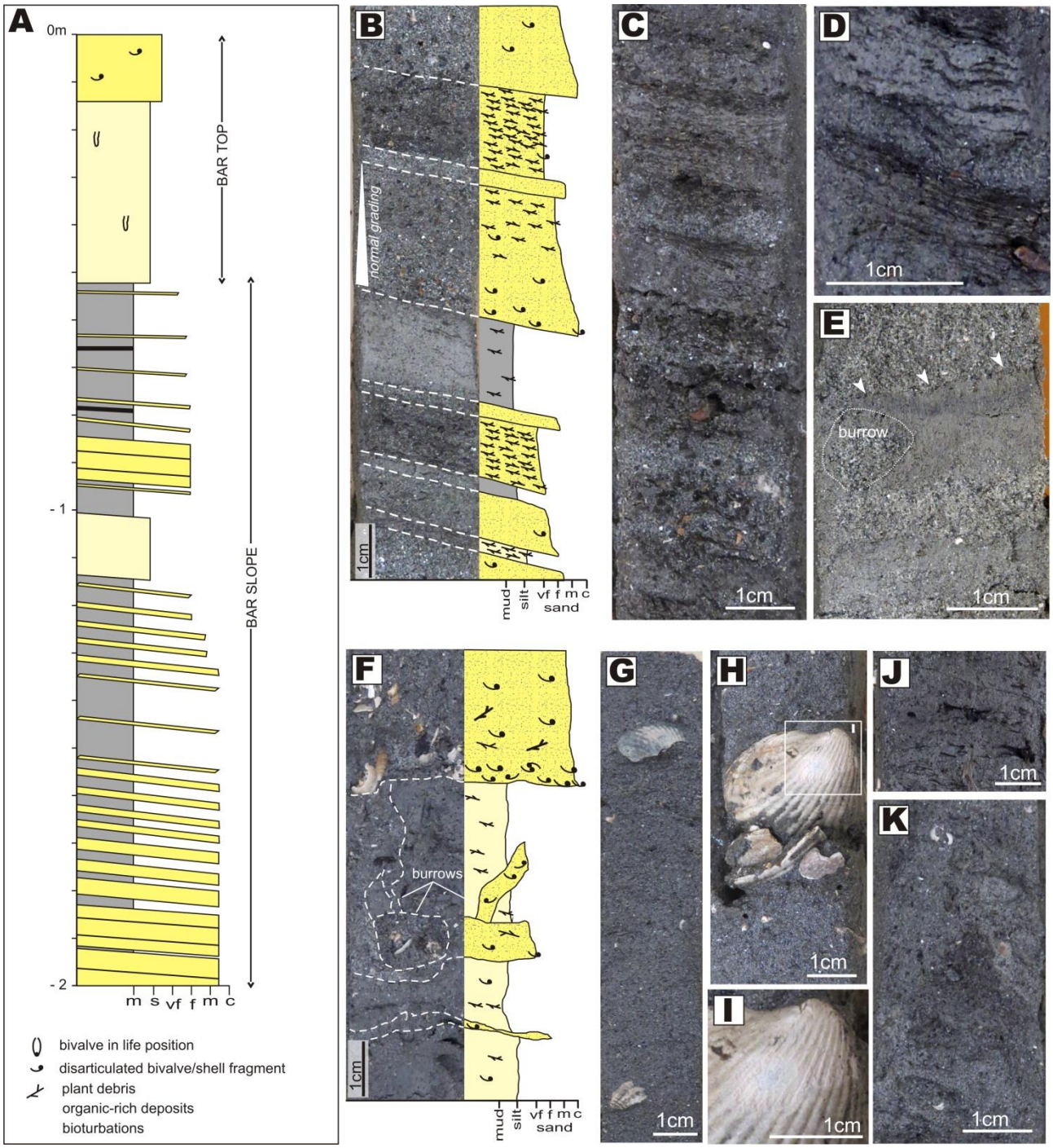

Figure 4.5: Core data from clinostratified and horizontally-bedded bar deposits. A) Sedimentological log from core 2 of figure 4.4A. B) Inclined heterolithic deposits and related sedimentological log. Note the clear normal grading characterizing some of the sandy layers. C) Plant-debris rich, laminated sandy deposits. D) Plant-debris laminae in muddy layers. E) Normal-graded sandy layer abruptly overlaying a muddy interval. F) Horizontally-bedded deposits and related sedimentological log. G) Structureless sand with scattered shell fragments. H) Shell rich layer within sandy deposits. I) Detail of H showing abrasion of a Cerastoderma edule shell. J) Dispersed plant debris in muddy deposits. K) massive sand with dispersed plant debris.

Overbank deposits

Overbank deposits are horizontally bedded and have been cored up to a depth of 3 m below the lagoon floor, in the bend apex zone (Fig. 4.6A). They consist of bioturbated, dark grey, mud, muddy silt and sand, which form beds ranging in thickness between 5 and 100 cm (Fig. 4.6B). In the upper portion of the core, muddy silt is massive and dark gray, and contains abundant shells and shell fragments (Fig. 4.6D). Irregular, organic-rich layers with abundant small gastropod shells can be interbedded within the muddy silt (Fig. 4.6C). Sandy deposits can occur as 1-2 cm thick irregular layers within the silt (Fig. 4.6F), or form 10-15 cm thick structureless beds (Fig. 4.6E). This sand can be slightly laminated, although it is commonly massive because of the intense bioturbation. Wood fragments and plant debris (Fig. 4.6E) are common.

Overbank deposits appear to be similar to those cored in the uppermost part of the inner bank, although the latter are sandier and show a lower content in organic matter. These deposits do not show any significant vertical grain size trend, although the uppermost part of the cored deposits is made of shell-rich silty sand deposits.

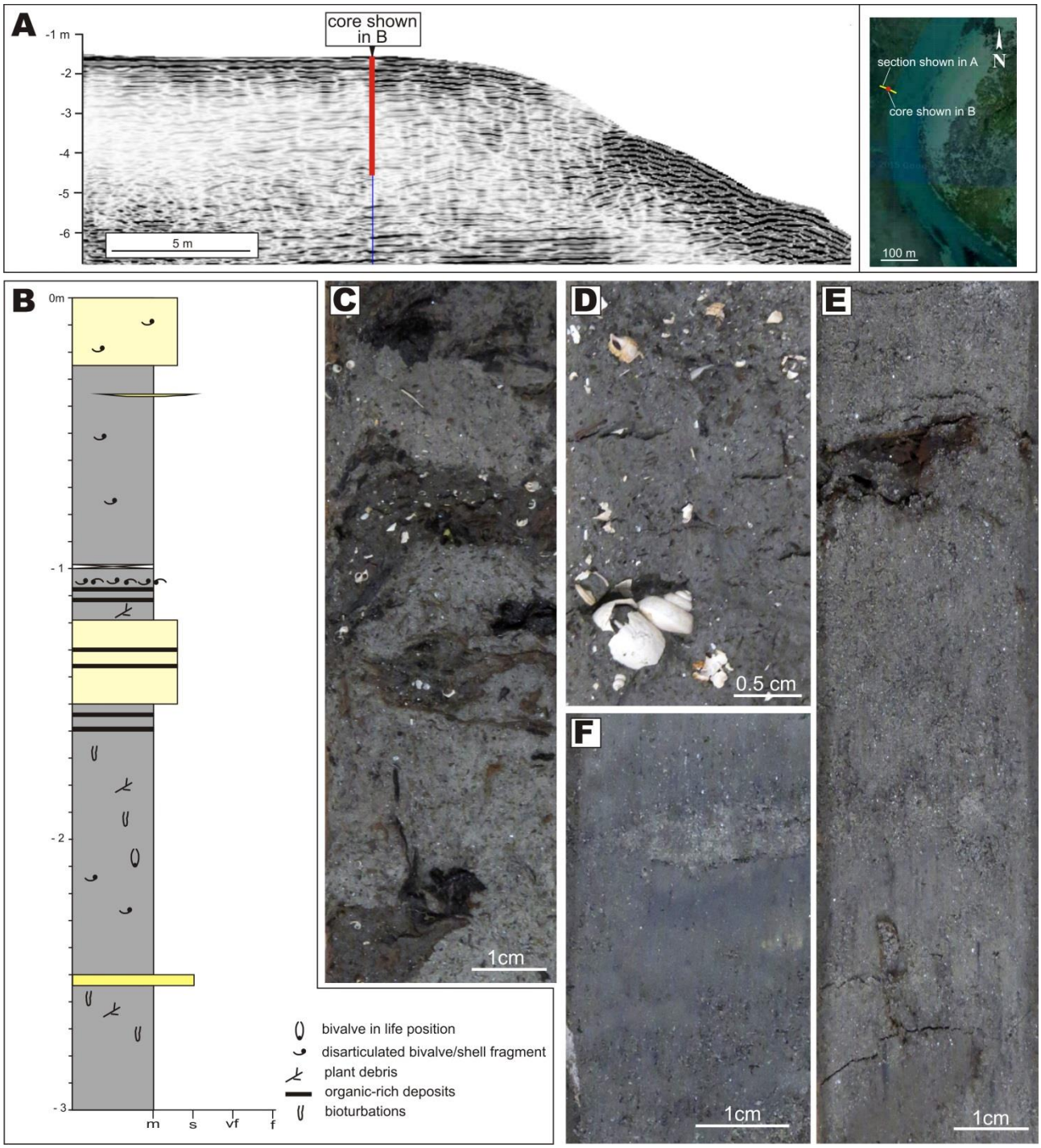

Figure 4.6: Overbank deposits. A) Sub-bottom profile from the bend apex zone showing location of the sedimentary core shown in B. B) Sedimentological log across the horizontally-bedded outer bank deposits. C) Deformed, organic-rich layers with abundant gastropod shells. D) Shell-rich sandy layer. F) Irregular sandy layer within massive mud. E) Massive sand with plant debris.

4.2.5.3 Stratal geometries

Seismic sections from both point bar and overbank areas provided insights to detect definite architectural features, basing on the occurrence of truncations, erosive surfaces and changes in dip angle of beds. Seven main types of stratal geometries (SG1 - 7) were defined (Fig. 4.7, 4.8 and 4.9) and briefly summarized in figure 4.10. The first four types of stratal geometries (SG1 – 4) occur within the clinostratified point bar deposits. SG5 characterizes the horizontally-bedded sediments occurring either on point bar top and in the overbank areas. SG6 was identified along the outer bank zone, whereas SG7 occurs at the toe of both inner and outer bank.

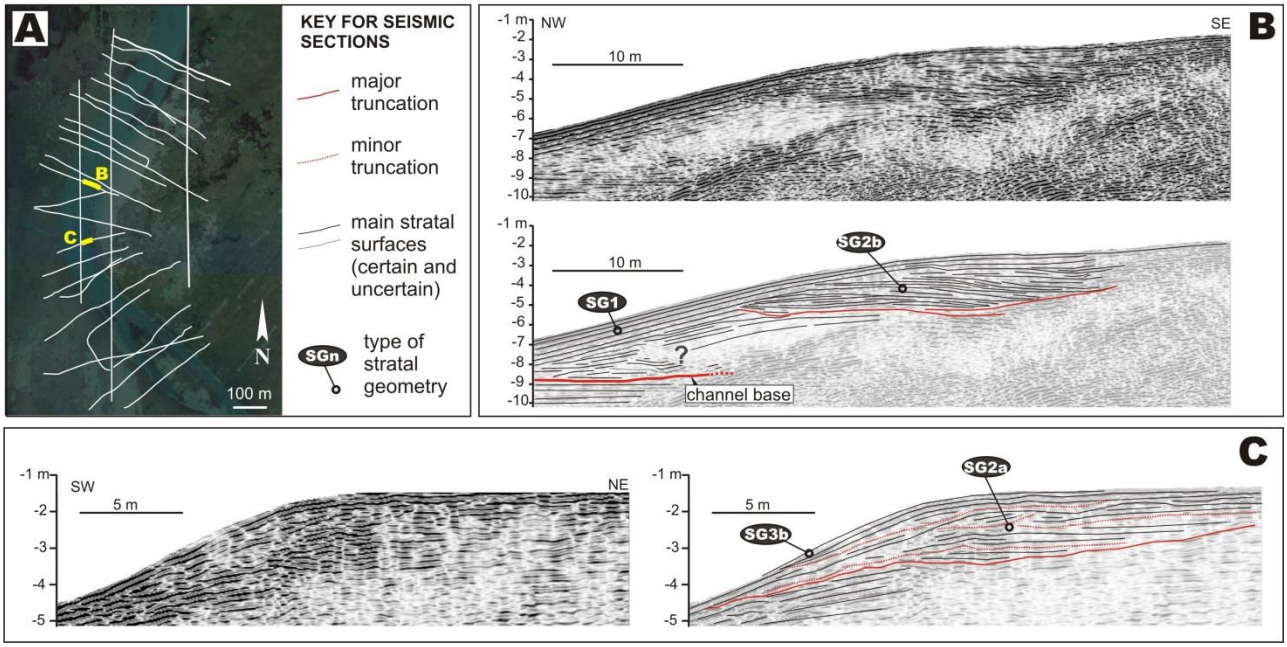

Figure 4.7: Clinostratified point-bar deposits. A) Location of sections shown in B and C. B-C) Mounded (B) and (C) sub-horizontal clinostratified deposits filling a collapse scour in the upper part of the bar.

SG1 – Regularly-bedded clinostratified point bar deposits, consisting of conformably stacked beds dipping between 10° and 3° with a gently convex profile (Fig. 4.7B, 4.8B and 4.10). They form bedsets up to 4-5 m thick. Core data show that the upper 1.8 m of these deposits are characterized by a clear fining-upward grain size trend (Fig. 4.4B).

SG2 – Clinostratified deposits are cut by a surface dipping channelward about 3-10° and showing a concave-upward profile. The surface has an overall erosional relief of about 1.5 – 2 m

and is covered by 0.5-1 m thick deposits that merge channelward with clinoforms. These deposits show two main stratal patterns, which define an overall fining-upward grain size trend. The first pattern (SG2a) is represented by sub-horizontal beds that are locally cut by minor truncations with an erosional relief of about 0.3 – 0.5 m (Fig. 4.7C, 4.8C and 4.10). The second pattern (SG2b) is defined by beds that show an overall convex-upward profile, with minor truncations (Fig. 4.7B and 4.10). SG2 deposits characterize the upper, mud-rich part of the clinostratified deposits, and are common along the seaward portion of the point bar and close to the bend apex.

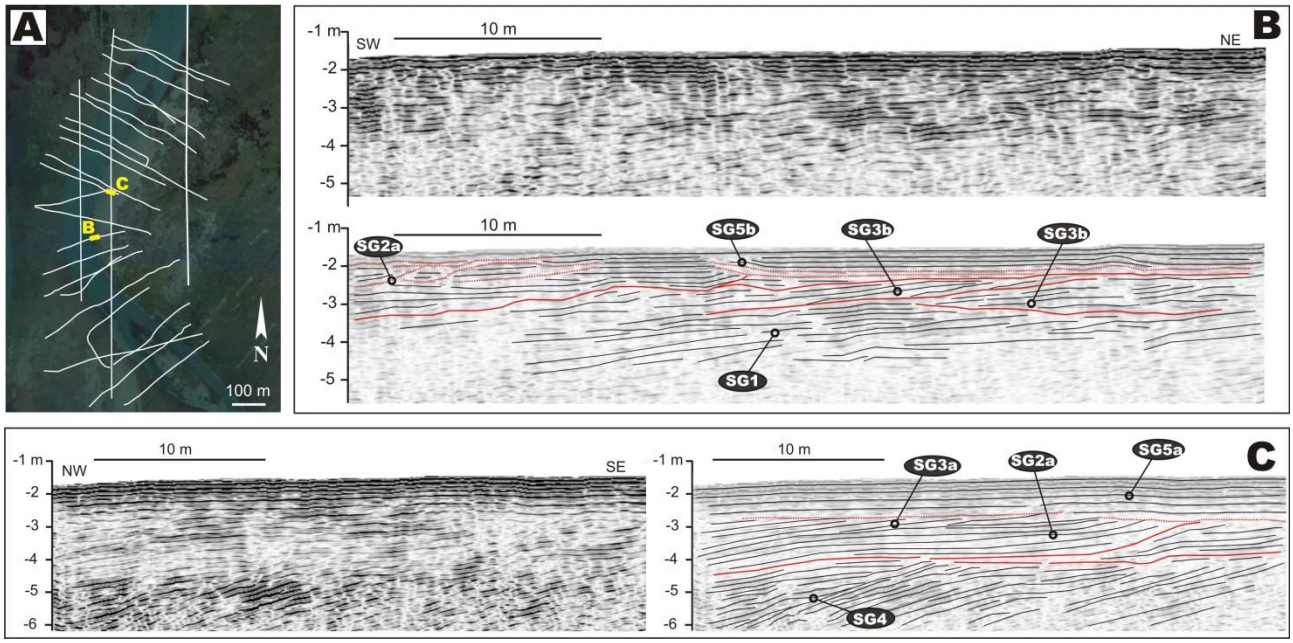

Figure 4.8: Clinostratified point-bar deposits. A) Location of sections shown in B and C. B-C) Different stratal geometries characterizing the uppermost part of the clinostratified deposits and overlying horizontally-bedded sediments.

SG3 – Clinostratified deposits downlapping: i) more inclined beds (ca. 4°) without clear evidence of erosion (SG3a; Fig. 4.8C and 4.10) or ii) a channelward-dipping, concave-upward surface (SG3b; Fig. 4.8B and 4.10). Bedsets with downlapping beds show a vertical grain size trend that ranges from undefined to slightly coarsening upward (Fig. 4.4B).

SG4 – Clinostratified deposits are onlapped by less-inclined beds (ca. 4°) without any evidence of truncations (Fig. 4.8C). This stratal pattern marks the boundary between two adjacent bedsets and mainly occurs in the middle-upper part of the clinostratified interval.

SG5 – Horizontally-bedded sediments forming either the uppermost part of the point bar succession or the overbank areas. They are up to 80 cm and at least 10 m thick in point bar and overbank areas respectively. SG5a show a laterally continuous bedding and lack any evidence of internal truncations (Fig. 4.8C, 4.9C and 4.10). Stratal surfaces can be followed for long distances without any significant change in attitude or geometry. SG5b shows local truncations (Fig. 4.8B, 4.9B and 4.10) with an erosional relief of about 15-30 cm. These truncations define minor depressions, which are commonly filled with regularly bedded deposits.

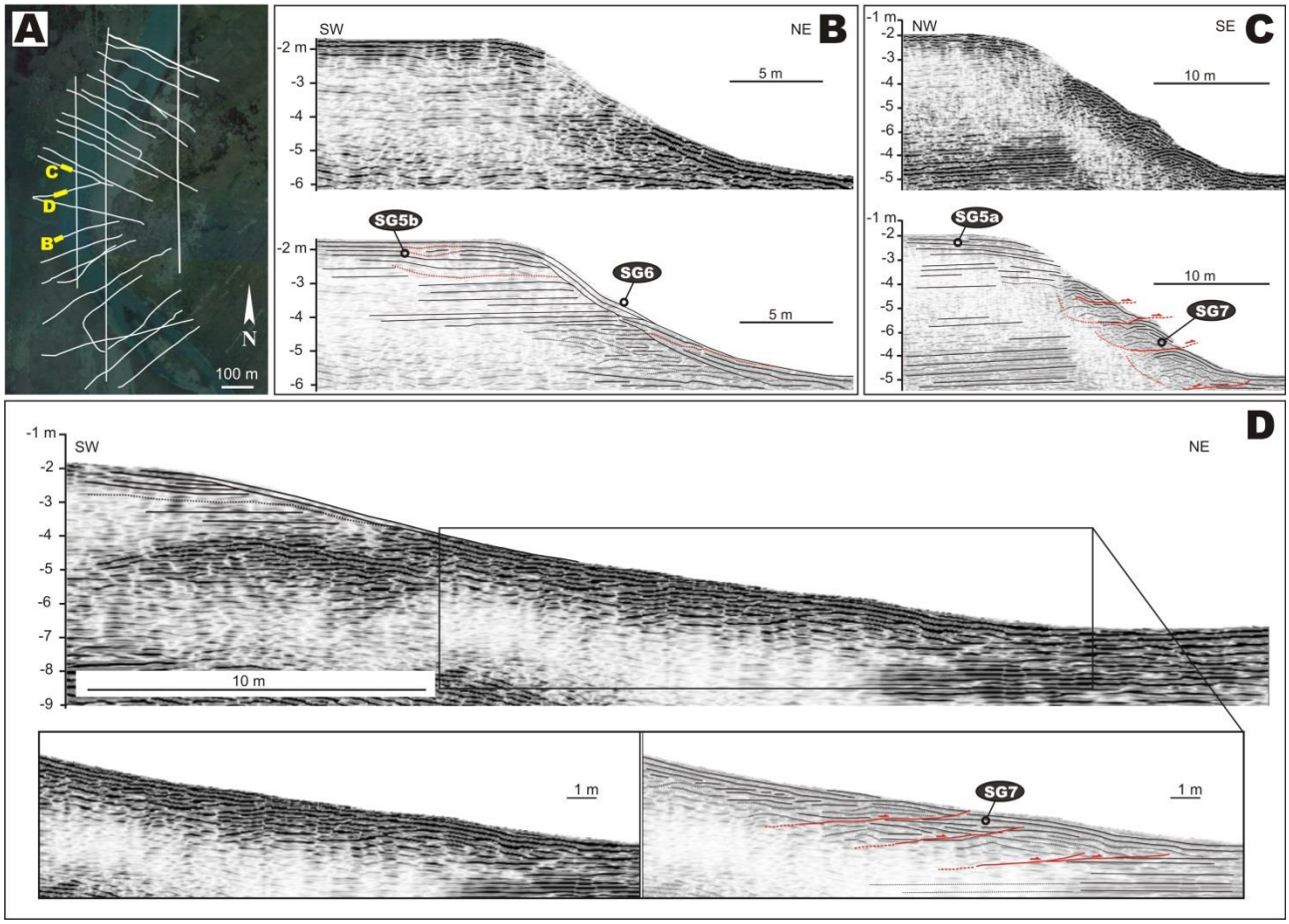

Figure 4.9: Outer bank deposits. A) Location of sections shown in B, C and D. B) Horizontally-bedded deposits and downlapping beds occurring in the outer bank zone. C-D) Collapse deposits developed at the toe of the outer (C) and (D) inner bank.

SG6 – Inclined beds dipping between 5and 10° channelward and forming sets no more than 50 cm thick. Commonly, these beds drape and downlap the outer bank of the channel, pinching out before reaching the thalweg (Fig. 4.9B and 4.10). Made exception for their location along the outer bank and their steeper depositional angle, these deposits are similar to those of SG3a.

SG7 – Deformed deposits occurring in the lower part of the inner and outer bank. Internal stratal pattern defines mounded units, with a relief spanning from 10 to 100 cm (Fig. 4.9C, D and 4.10). These mounds are locally separated by minor truncations.

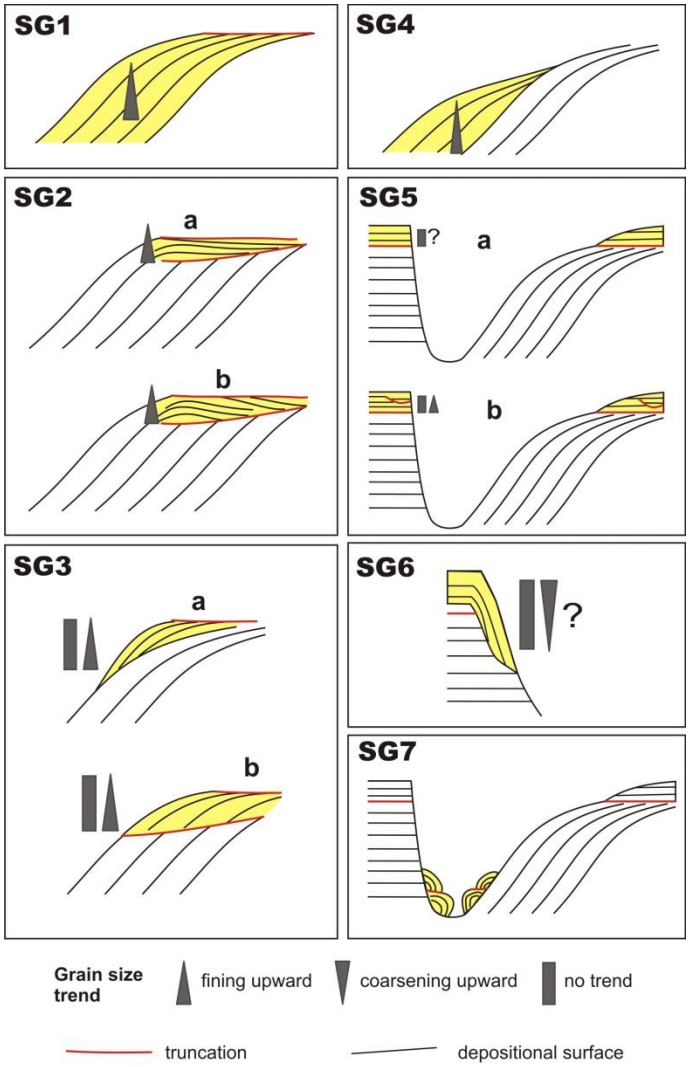

Figure 4.10: Summary of the different geometries and related grain-size trend.

4.2.5.4 Linking channel planform evolution with bar architecture

The channel planform evolution of the channel bend was linked with point bar stratal architecture, placing the position of the inner bank (i.e. point bar brinkpoint) during 1900 and 1962 (Fig. 4.11A) above selected seismic lines (Fig. 4.11B, C, D), which are located in the seaward (line V56), central (line V51) and landward (line V45) sector of the channel bend respectively (Fig. 4.11A).

The seaward section (V56) is located in a zone which registered the higher amount of lateral accretion (Fig. 4.3B, C). Specifically, along this section, the inner bank migrated laterally of ca. 25 m between 1900 and 1962 and 20 m between 1962 and 2015 (yellow, white and blue arrows in Fig. 4.11C), with an overall shift of ca. 45 m. Seismic images show that lateral migration occurred in parallel with a rise of the point bar brinkpoint, that climbed up for about 100 cm following a gently flattening rising trajectory (blue dashed line in Fig. 4.11C). The flattening of the brinkpoint trajectory during bank migration is even more evident considering also the deposits older than 1900 (Fig. 4.11C). Stratal geometries show also that ca. 100 cm of sediments accumulated over the bar since 1900, and that ca. 60 cm of them was deposited between 1962 and 2015.

The bend apex section (V51) is located in the most stable zone of the bend, since the bend apex seems to have occupied the same position since 1900 (Fig. 4.3B, C). Horizontal bedded deposits accumulated in the brink zone are about 0.5 m thick, and represent the maximum thickness of sediment accumulated since 1900 (Fig. 4.11B). Horizontal-bedded deposits can be followed downdip into the channel, where they are affected by numerous minor truncations (Fig. 4.11B).

The landward section (V45) crosses a zone where the inner bank retreated between 1900 and 1962, and successively accreted from 1962 to 2015 (Fig. 4.3B, C). In this section, the location

of the 1962 bank (white arrow in Fig. 4.11D) corresponds with the updip termination of an erosive surface, that is covered by clinostratified beds accumulated between 1962 and 2015 (Fig. 4.11D). During accumulation of clinostratified beds, the bar brinkpoint shifted laterally and rose up of about 30 m and 0.4 m respectively, defining a slightly rising trajectory comparable with that of section V56.

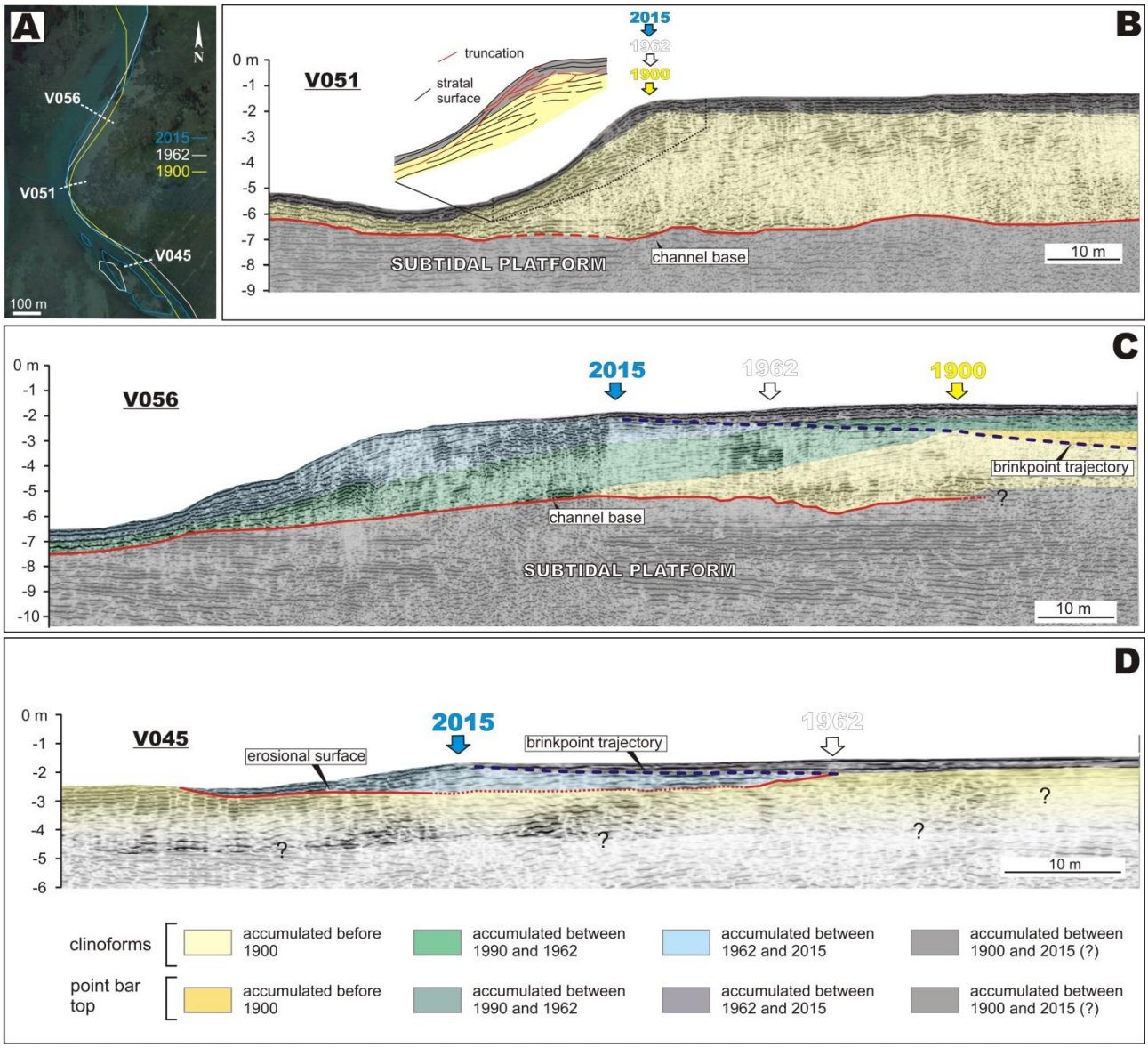

Figure 4.11: Evolution of the study bar over the past century. A) Location of section shown in B, C and D. B) Seismic section showing stratal architecture in the bend-apex zone. Note that about 1 m of sediments aggraded on the brink zone after the 1900, whereas no sedimentation occurred on the bar slope. C) Seismic section across the seaward side of the bar. Note concurrence of bar migration and aggradation, as highlighted by the rising bar brink point trajectory. D) Seismic section across the landward side of the bar. Bank retreat occurred between 1900 and 1962 is documented by an erosive surface (red line).

4.2.6 Discussion

4.2.6.1 Sedimentary processes

Principles of flow and sediment distribution along curved channels has been mainly derived from fluvial bends (e.g., Hooke, 1975; Dietrich et al., 1979; Dietrich and Smith, 1983; Dietrich, 1987). These models point to the occurrence of a cross-stream pressure gradient towards inner channel banks (Bathurst et al., 1977), which was associated to water super-elevation along outer channel banks, caused by centrifugal force. This pressure gradient induces the development of helical flow that causes the formation of asymmetric channel profiles, with erosion on the outer bank, and concomitant sediment transport towards the inner bank (Bluck, 1971). This basic mechanism of flow distribution have been widely used also to approach the study of point bar deposits developed in tidal (e.g. de Mowbray, 1983; Bridges and Leeder, 1976; Choi et al., 2004; Santos and Rossetti, 2006) and turbiditic channel bends (Peakall et al., 2000; Kneller, 2003; Kolla et al., 2007; Janocko et al., 2013).

However in subtidal cases, the study bend is constantly submerged and its sedimentary features are expected to differ from those characterizing intertidal and supratidal channels, which provided the most popular facies models for tidal point bars (Bridges and Leeder, 1976; Barwis, 1978; de Mowbray, 1983; Choi et al., 2004). Beyond tidal modulation of water discharge, the hydrodynamic of the study bend is influenced by the water column overlying the bend. This setting slightly resembles fluvial meanders during extreme floods, when considerable amount of water overpass the main channel (Naish and Selling, 1996; Shiono and Muto, 1998; Ishigaki et al., 2000; Loveless et al., 2000; Wormleaton et al., 2004). Laboratory and field studies show that in these conditions the overbank flow interacts with the main channel flow, causing: i) a reduction in magnitude of the helical flow, preventing the development of the a cross-stream pressure gradient (Wormleaton et al., 2004); ii) sediment accumulation where the overbank flow re-enters

the main channel (Naish and Selling, 1996; Wormleaton et al., 2004; Ghinassi et al., 2013). A further relevant consequence due to the constant presence of water above the channel bend is associated with sediment remobilization due to wave winnowing. The elongated shape of the Venice Lagoon increases the wind fetch, and during winter time, strong winds from NE (Bora) can generate string waves. Such waves are particularly effective in the central and southern lagoon, where they are able to stress the lagoon bottom remobilizing a considerable amount of sediments (Carniello et al., 2011; Marani et al., 2011).

Wave- and tide-generated currents acting on the inter-channel areas are, therefore, taken in account analyzing the study deposit. Wave signature in the horizontally-bedded bar top and overbank deposits (SG5) is represented by the shell-floored sandy beds, which developed during storm events, when waves suspended fine sediments concentrating shells and sandy deposits. Inter-storm, fair-weather conditions allowed settling of fine sediments and promoted bioturbation, which obliterated the primary sedimentary structures, possibly developed during storm events. The lack of root traces or oxidations is consistent with this interpretation model. Minor erosive surfaces, characterizing horizontal-bedded deposits (SG5b), developed where wave action, possibly modulated by tidal currents, scoured the bottom. From the hydrodynamic point of view this configuration resembles the offshore transition zone of open coasts (cf. Clifton, 1976; Reading and Collinson, 1996; Clifton, 2006), where mud background sedimentation is interrupted by seafloor winnowing during storm events.

The occurrence of clinostratified deposits indicates that in-channel sedimentation was mainly controlled by a secondary circulation, which causes across-stream sediment transport and accumulation of fine-grained deposits in the upper part of the bar (Leopold and Wolman, 1960; Nanson, 1980). The occurrence of a clear fining-upward grain size trend in SG1 deposits supports this interpretation. Onlap SG4 geometries, commonly develop in this setting as consequence of

channel bend reorientation, as demonstrated by architectural studies from fluvial point bars (Ielpi and Ghinassi, 2014; Durkin et al., 2015). Maximum efficiency of the secondary circulation occurred during ebb stages, when most of the water occupying the interchannel areas was conveyed into the channel, causing a considerable increase in water discharge and efficiency of the helicoidal flow.

Nevertheless, several features highlight that the study bar differs from the classical tidal point bars. A first relevant difference is represented by the numerous channelward-dipping truncations, cutting in the upper part of the clinostratified deposits (SG2a, b and SG3b). These truncations formed as detachment surfaces for sediment collapses, induced by wave loading on the brink zone of the bar, which was effortlessly destabilized due to water-saturation of sediments that decreased the intergranular friction (cf. Bridges and Leeder, 1976; Choi et al., 2013). Once these collapse scours were generated, different modes of infill gave rise to different stratal geometries. Where cross-stream circulation was effective, infill of the collapse scours was driven by a flux of sediment from the channel. In this case, SG2a and SG2b stratal geometries developed. Specifically, SG2b deposits formed where the secondary circulation pushed upbar a considerable amount of sediments, which filled up the collapse scour forming mounded accumulations. Where the amount of sediment transported from the channel was limited, the scour was filled up with sub-horizontal beds, forming SG2a geometries. Downlap geometries of SG3b deposits indicate that deposits filling the scour were sourced from the bar top zone, where the sediment was remobilized by wave action and drifted to the bar brink by tidal currents. Sediment, remobilized by the interaction between wave and tidal currents, were delivered to the channel also in the outer bank and bar brink zones, where generated downlap geometries of SG6 and SG3a deposits, respectively. The coarsening-upward grain size trend of these deposits is consistent with these geometries.

Location of mounded deposits of SG7 at the toe of the banks, suggest they represent deposits collapsed both from the outer bank and from the bar top. The lack of collapse scour surfaces along the outer bank deposits is due to their progressive dismantling caused by lateral channel migration. The preservation of collapsed blocks at the toe of the channel margins is consistent with scarce erosive power of tidal currents due to the minimal tidal excursion affecting the Venice Lagoon.

4.2.6.2 Planform evolution and bar aggradation

The occurrence of channelward-dipping beds below the inner bank zone demonstrates that the, all in all, the study bar progressively increased its sinuosity, as commonly occur in most tidal (e.g. Bridges and Leeder, 1976; Choi et al., 2004; Santos and Rossetti 2006; McClennen and Housley, 2006) or fluvial (e.g. Edwards et al., 1983; Willis, 1993; Ielpi and Ghinassi, 2014; Durkin et al., 2015) channel bends. Migration rates and morphodynamics for the whole lifespan of the bend are unknown, although its planform evolution and related stratigraphic architectures have been recognized for the last century. The main points arising from the analyses of historical maps and aerial photos, and from their comparison with the stratigraphic record are: i) the bend apex remained almost stable; ii) maximum migration rates of the channel were of the order of dm/yr; iii) during channel migration, bar top surface locally aggraded up to 1 m (aggradation rate ca. 1cm/yr).

i) Planform evolution of the study bar is associated with changes from erosion to deposition in different bar sectors (Fig. 4.11). Alternation between erosion and deposition along channel bends follows changes in flow dynamics and variation in sediment supply (Seminara, 2006). In the present case, an overall accretion along the seaward side of the bar (Fig. 4.3C) would be linked with dominance of ebb flows (Hughes, 2012), which promoted bypass-erosion along the

landward and central part of the bar (e.g. 1900-1962). Nevertheless, planform stability of the bend apex zone indicated a decrease in efficiency of the secondary helical flow, which, in turn, induced a reduction of outer bank retreat. A decrease of secondary circulation is consistent with a progressive increase of water depth over the subtidal platforms, of the Venice Lagoon, during the past century (Carniello et al., 2009). The increase of water thickness above the meander bend caused a reduction in magnitude of the cross-stream pressure gradient and related helical flow (Wormleaton et al., 2004), which was not able to induce outer bank retreat.

ii) Maximum migration rates of the order of dm/yr are consistent with other studies (Garofalo, 1989; Gabet, 1998), and specifically with rates obtained from channels of the Venice Lagoon (McClennen and Housley, 2006; Finotello et al., 2015), but are almost an order of magnitude lower than values characterizing fluvial meanders (e.g. Moody and Meade, 2014; van de Lageweg et al., 2015). Among the features which can contribute to slow the lateral shift of the study subtidal channel can be listed: i) muddy composition of the deposits forming the outer bank (cf. Marani et al., 2002); ii) presence of seagrass cover in the outer bank zone; ii) occurrence of large collapsed blocks that armor at the toe of the outer bank (cf. Gabet, 1998); iv) lack of long-lasting, extreme events characterized by high water discharge; v) location of the channel in subtidal realm, that prevents funneling of ebb waters within the channel, contributing to decrease its erosive power; vi) reduction in magnitude of the cross-stream pressure gradient and related helical flow due to the presence of a constant volume of water above the bend (Wormleaton et al., 2004). The slight increase of the radius of curvature occurred over the past century, highlights that the channel is increasing its efficiency, possibly in order to drain a large volume of water associate with a local increase in tidal prism. The occurrence of different values of migration rates along the channel bend remarks the importance of local constrains in controlling planform evolution. For example, the high-migration rate affecting the northern reach of the study bend

(Fig. 4.3C) would be consistent with the occurrence of an erodible bank, made of non-cohesive sediments (e.g. older sandy bar). Similar changes are demonstrated to play a key role in controlling local planform evolution of fluvial point bars (Smith et al., 2009; 2011; Ghinassi and Ielpi, 2015).

iii) Beyond establishment of depositional or erosional conditions along the bar, a common process that affected landward, central and seaward sectors of the bar was represented by accumulation of horizontal-bedded bar top deposits. This process was less effective in the landward sector, but allowed accumulation of about 1 m of deposits along the seaward side of the bar, where sedimentation was continuous since 1900. The sharp basal surface of the horizontal-bedded, bar top deposits corresponds to a wave-generated truncation, and its rising trajectory indicates a progressive upward shift of the point bar brink zone during lateral migration of the channel. The steepness of the brink zone trajectory (Fig. 4.11C) defines the amount of aggradation, affecting the bar top area during channel migration. In this case, the progressive flattening of the brink point trajectory is consistent with the progressive decline in sediment supplied to the lagoon over the past century (Carniello et al., 2009).

4.2.7 Conclusions

Planform evolution, stratal architecture and sedimentary features of a subtidal meander bend in the central Venice Lagoon provided new insights to understand the sedimentology of tidal point bars. The main results from the present study can be listed as follows:

1) Sedimentation in the study subtidal point bar stemmed out from the interaction between the in-channel secondary helical flow and wave winnowing occurring in overbank areas. The secondary circulation controlled sediment redistribution from the channel thalweg to the bar top, and contributed to form the “classical” fining-upward grain size trend of point bar deposits. Wave-winnowing of the overbank areas caused development of an abrupt truncation between

clinostratified bar core deposits and overlying horizontally-bedded sediments. Sediment remobilized from overbank areas by wave winnowing was drifted into the channel, forming peculiar apron-like accumulations both along the outer and inner bank.

2) Wave loading caused frequent collapses of the channel bank deposits. Along the inner bank, collapse scours are well preserved and show different patterns of infill, which vary if the sediment is sourced from the channel (i.e. helical flow) or from bar top (i.e. wave winnowing).

3) Progressive increase in water depth, affecting the Venice Lagoon over the past century, reduced the effect of helical flow developed in the bend apex zone, with consequent reduction of lateral migration rate of the channel bend. Values of migration rate (dm/yr), nevertheless, are still in the range of those measured for tidal channels.

4) Although sedimentation was not uniform in different sectors of the meander bend, the bar slightly grew increasing its radius of curvature, contributing to a subtle decrease in channel sinuosity. The sectors of the bar affected by a greater lateral shift were also interested by vertical aggradation (ca. 1 cm/yr), that occurred through sediment storage on the bar top area. In this zone, the rising and flattening bar brink point trajectory reflects the progressive decrease in aggradation rate, which is associated with reduction of sediment supply affecting the lagoon over the past century.

CHAPTER 5

CONCLUSIONS

Using a multidisciplinary approach, that couples remote sensing, sedimentological and geophysical analyses with numerical and 3D modeling, the present study focused on three main topics: i) the role of low order tributaries in controlling the evolution of tidal meander bend; ii) the influence of salt marsh aggradation in shaping geometries of tidal point bars, iii) sedimentary process and morphodynamics changes acting on subtidal point bars.

The main results stemmed out from this research can be summarized as follow:

i) Minor lateral tributaries exert a critical role on tidal meander evolution, controlling the amount of water and sediment provided to the main channels. When the sediment discharge of tributaries, in correspondence of the outer bank, exceeds the sediment transport capability of the main channel, sedimentation can occur at the outlet of tributary channels, forming prograding lobate units. In such cases, flux concentration against the inner bank can generate erosion, where both fluvial and tidal classical facies models predict deposition.

ii) Tidal meanders draining salt-marshes, are characterized by well-developed, sand-rich levee deposits that, develop thanks to limited range of flowing discharge, which prevents levee breaching and formation of crevasse splays.

In symmetric tidal meander bend the seaward and landward sides of the tidal point bar act as upstream and downstream bar sectors, experiencing bed shear stresses of similar magnitude during a tidal cycle. In the study case, this causes an overall symmetric distribution of sediment grain size along the bar. Bi-directionality of tidal currents causes secondary circulations to cut an elongated pool scour, which can be characterized by two minor depressions possibly associated to flood and ebb secondary cells.

Lateral migration occurs in parallel with an increase in cross-sectional area, that stems out from both lifting up of the banks and scouring of the channel base. The combination between lateral migration (8-10 cm/yr) and vertical aggradation (2.5-3 mm/yr) provided a spoon-shaped geometry to the bar top surface. Although meandering rivers can be affected by comparable rates of floodplain aggradation, development of similar geometries is hindered by their high lateral migration rate, that allows the cutoff to be reached before that a significant thickness of deposits is accumulated on the bar top.

iii) Sedimentation in the subtidal point bars stemmed out from the interaction between the in-channel secondary helical flow and wave winnowing, occurring in overbank areas. The "classical" fining-upward grain size trend of point bar deposits is due to the secondary circulation, which controlled sediment redistribution from the channel thalweg to the bar top, while wave-winnowing of the overbank areas caused development of an abrupt truncation between clinostratified bar core deposits and overlying horizontally-bedded sediments. Sediment remobilized from overbank areas by wave winnowing was drifted into the channel, forming peculiar apron-like accumulations both along the outer and inner bank. Wave loading caused frequent collapses of the channel bank deposits that generated collapse scours, well preserved along the inner bank, where they show different patterns of infill that vary if the sediment is sourced from the channel (i.e. helical flow) or from bar top (i.e. wave winnowing).

Values of migration rate (dm/yr) of the study bend are in the range of those measured for other tidal channels, even though progressive increase in water depth, affecting the Venice Lagoon over the past century, reduced the effect of helical flow developed in the bend apex zone, with consequent reduction of lateral migration rate of the channel bend. Over the last century, the study bar slightly grew increasing its radius of curvature, contributing to a subtle decrease in channel sinuosity, even though sedimentation was not uniform in different sectors of the bend.

Overall, the sectors affected by a greater lateral shift were also interested by vertical aggradation (ca. 1 cm/yr), which occurred through sediment storage on the bar top area. In this zone, the rising and flattening bar brink point trajectory reflects the progressive decrease in aggradation rate, associated with reduction of sediment supply affecting the lagoon over the past century.

REFERENCES

Allen, J.R.L. (1963). The classification of cross-stratified units with notes on their origin. *Sedimentology* **2**, 93-114.

Allen, J.R.L. (1982). Sedimentary structures. Developments in sedimentology. Elsevier.

Allen, J.R.L. (2000). Morphodynamics of Holocene salt marshes: a review sketch from the Atlantic and Southern North Sea coasts of Europe. *Quaternary Science Reviews*, **19**(12), 1155-1231.

Ashley, G.M. and **Zeff**, **M.L**. (1988). Tidal channel classification for a low-mesotidal salt marsh. *Marine Geology*, **82**(1), 17-32.

Bartholdy, J. (2012). Salt marsh sedimentation. In *Principles of tidal sedimentology* (pp. 151-185). Springer Netherlands.

Bathurst, J.C., **Thorne, C.R.** and **Hey, R.D.** (1977). Direct measurements of secondary currents in river bends. *Nature* **269**, 504-506.

Barwis, J.H. (1978). Sedimentology of some South Carolina tidal creek point bars and a comparison with their fluvial counterparts. *Fluvial sedimentology, Canadian Society of Petroleum Geologists Memoir 5* (pp. 129–160). Eds Miall AD(Canadian Society Petroleum Geologists, Calgary).

Barwis, J.H. and **Hayes, M.O.** (1979). Regional patterns of modern barrier island and tidal inlet deposits as applied to paleoenvironmental studies. In*Carboniferous Depositional Environments in the Appalachian Region* (pp. 472-498). Carolina Coal Group, University of South Carolina Columbia, SC.

Bayliss-Smith, T.P., **Healey, R.**, **Lailey, R.**, **Spencer, T.** and **Stoddart, D.R.** (1979). Tidal flows in salt marsh creeks. *Estuarine and Coastal Marine Science*, **9**(3), 235-255.

Bellucci, L.G., **Frignani, M.**, **Cochran, J.K.**, **Albertazzi, S.**, **Zaggia, L.**, **Cecconi, G.** and **Hopkins, H.** (2007). ^{210}Pb and ^{137} Cs as chronometers for salt marsh accretion in the Venice Lagoon–links to flooding frequency and climate change. *Journal of Environmental Radioactivity*, **97**(2), 85-102.

Biron, P., Roy, A.G., Best, J.L. and **Boyer, C.J.**, (1993). Bed morphology and sedimentology at the confluence of unequal depth channels. *Geomorphology*, **8**,115–129.

Bluck, B.J. (1971). Sedimentation in the meandering River Endrick. *Scottish Journal of Geology*, **7**, 93-138.

Brice, J.C. (1974). Evolution of meander loops. *Geological Society of America Bulletin*, **85**, 581-586.

Brierley, G.J. (1991). Bar sedimentology of the Squamish River. British Columbia: definition and application of morphostratigraphic units. *J Sed Res*, **61**,211–225.

Brice, J.C. (1977). Lateral migration of the middle Sacramento River, California (No. 77-43). *US Geological Survey. Water Resources Division*.

Bridges, P.H., and **Leeder, M.R.** (1976). Sedimentary model for intertidal mudflat channels, with examples from the Solway Firth. *Scotland.Sedimentology*, **23**(4), 533-552.

Carniello, L., Defina, A. and **D'Alpaos, L.** (2009). Morphological evolution of the Venice Lagoon: evidence from the past and trend for the future. *J Geophys Res – Earth Surface*, 114:F04002.

Carniello, L., D'Alpaos, A. and **Defina, A.** (2011). Modeling wind waves and tidal flows in shallow micro-tidal basins. *Estuarine Coastal Shelf Sci*, **92**(2):263–276.

Carniello, L., Defina, A. and **D'Alpaos, L.** (2012). Modeling sand-mud transport induced by tidal currents and wind waves in shallow microtidal basins: Application to the Venice Lagoon (Italy). *Estuarine Coastal Shelf Sci*, 102–103:105–115.

Choi, K.S., Dalrymple, R.W., Chun, S.S., and **Kim, S.P.** (2004). Sedimentology of modern, inclined heterolithic stratification (IHS) in the macrotidal Han River delta, Korea. *Journal of Sedimentary Research*, **74**(5), 677-689.

Choi, K. (2011). External controls on the architecture of inclined heterolithic stratification (IHS) of macrotidal Sukmo channel: wave versus rainfall. *Marine Geology*, **285**(1), 17-28.

Choi, K., Hong, C.M., Kim, M.H., Oh, C.R., and **Jung, J.H.** (2013). Morphologic evolution of macrotidal estuarine channels in Gomso Bay, west coast of Korea: Implications for the architectural development of inclined heterolithic stratification. *Marine Geology*, **346**, 343-354.

Choi, K. and **Jo, J.H.** (2015). Morphodynamics of Tidal Channels In the Open Coast Macrotidal Flat, Southern Ganghwa Island In Gyeonggi Bay, West Coast of Korea. *J Sed Res*, **85**(6),582–595.

Coco, G., Zhou, Z., van Maanen, B., Olabarrieta, M., Tinoco, R. and **Townend, I.** (2013). Morphodynamics of tidal networks: Advances and challenges. *Mar Geol*, **346**,1–16.

D'Alpaos, L. and **Defina, A.** (2007). Mathematical modeling of tidal hydrodynamics in shallow lagoons: A review of open issues and applications to the Venice lagoon. *Comput. Geosci*, **33**,476–496.

D'Alpaos, A., Lanzoni, S., Marani, M., and **Rinaldo, A.** (2007). Landscape evolution in tidal embayments: modeling the interplay of erosion, sedimentation, and vegetation dynamics. *Journal of Geophysical Research: Earth Surface (2003–2012)*, 112(F1).

D'Alpaos, A., Lanzoni, S., Marani, M. and **Rinaldo, A.** (2010). On the tidal prism–channel area relations. *J Geophys Res*, 115:F01003.

Dalrymple, R.W., Makino, Y., and **Zaitlin, B.A.** (1991). Temporal and spatial patterns of rhythmite deposition on mud flats in the macrotidal Cobequid Bay-Salmon River estuary. Bay of Fundy, Canada.

De Mowbray, T. (1983). The genesis of lateral accretion deposits in recent intertidal mudflat channels, Solway Firth, Scotland. *Sedimentology*, **30**,425–435.

Dietrich, W.E., Smith, J.D. and **Dunne, T.** (1979). Flow and sediment transport in a sand bedded meander. *Journal of Geology*, **87**, 305-315.

Dietrich, W.E. and **Smith, J.D.** (1983). Influence of the point bar on flow through curved channels *Water Resour*, **19,** 1173–1192.

Dietrich, W.E. (1987). Mechanics of flow and sediment transport in river bends. In: Richards, K.S. (Ed.), River Channels: Environment and Process. Institute of British Geographers. Special Publication, **18**,179-227.

Díez-Canseco, D., Arz, J.A., Benito, M.I., Díaz-Molina, M. and **Arenillas, I.** (2014). Tidal influence in redbeds: A palaeoenvironmental and biochronostratigraphic reconstruction of the Lower Tremp Formation (South-Central Pyrenees, Spain) around the Cretaceous/Paleogene boundary. *Sedimentary Geology*, **312**, 31-49.

Durkin, P.R., Hubbard, S.M., Boyd, R.L. and **Leckie, D.A.** (2015). Stratigraphic Expression of Intra-Point-Bar Erosion and Rotation. *Journal of Sedimentary Research*, **85**, 1238-1257.

Edwards, M.B., Eriksson, K.A and**, Kier, R.S.** (1983). Paleochannel geometry and flow patterns determined from exhumed Permian point bars in north-central Texas. *Journal of Sedimentary Petrology*, **53**, 1261-1270.

Fagherazzi, S., Bortoluzzi, A., Dietrich, W.E., Adami, A., Lanzoni, S., Marani, M. and **Rinaldo, A.** (1999). Tidal networks 1. Automatic network extraction and preliminary scaling features from digital terrain maps. *Water Resources Research*, **35**(12), 3891-3904.

Fagherazzi, S., Hannion, M. and **D'Odorico, P.** (2008). Geomorphic structure of tidal hydrodynamics in salt marsh creeks. *Water resources research*, **44**(2).

Fagherazzi, S., Gabet, E.J. and **Furbish, D.J.** (2004). The effect of bidirectional flow on tidal channel planforms. *Earth Surf Process Landforms*, **29**,295–309.

Fagherazzi, S., Carniello, L., D'Alpaos, L. and **Defina, A.** (2006). Critical bifurcation of shallow microtidal landforms in tidal flats and salt marshes. *Proc Natl AcadSci USA*, **103**(22), 8337–8341.

Fagherazzi, S., et al. (2012). Numerical models of salt marsh evolution: ecological, geomorphic, and climatic factors. *Rev Geophys*, **50**(1),RG1002.

Fenies, H. and **Faugères, J.C.** (1998). Facies and geometry of tidal channel-fill deposits (Arcachon Lagoon, SW France). *Marine Geology*, **150**(1), 131-148.

Frothingham, K.M. and **Rhoads, B.L.** (2003). Three-dimensional flow structure and channel change in an asymmetrical compound meander loop, Embarras River, Illinois. *Earth Surface Processes and Landforms*, **28**(6), 625-644.

Fruergaard, M., et al. (2011). Punctuated sediment record resulting from channel migration in a shallow sand-dominated micro-tidal lagoon, Northern Wadden Sea, Denmark. *Marine Geology*, **280**(1), 91-104.

Gabet, E.J. (1998). Lateral migration and bank erosion in a salt marsh tidal channel in San Francisco Bay, California. *Estuaries*, **21**(4B),745–753.

Garofalo, D. (1980). The influence of wetland vegetation on tidal stream channel migration and morphology. *Estuaries*, **3**(4), 258-270.

Garotta, V., Pittaluga, M.B. and **Seminara, G.** (2006). On the migration of tidal free bars. *Physics of Fluids (1994-present)*, **18**(9), 096601.

Ghinassi, M., Billi, P., Libsekal, Y., Papini, M. and **Rook, L.** (2013). Inferring fluvial morphodynamics and overbank flow control from 3D outcrop sections of a Pleistocene point bar, Dandiero Basin, Eritrea. *Journal of Sedimentary Research*, **83**, 1066-108411.

Ghinassi, M., Nemec, W., Aldinucci, M., Nehyba, S., Özaksoy, V. and **Fidolini, F.** (2014). Plan-form evolution of ancient meandering rivers reconstructed from longitudinal outcrop sections. *Sedimentology*, **61**, 952-977.

Ghinassi, M. and **Ielpi, A.** (2015). Stratal Architecture and Morphodynamics of Downstream-Migrating Fluvial Point Bars (Jurassic Scalby Formation, UK). *Journal of Sedimentary Research*, **85**, 1123-1137.

Hickin, E.J. and **Nanson, G.C.** (1975). The character of channel migration on the Beatton River, northeast British Columbia, Canada. *Geological Society of America Bulletin*, **86**(4), 487-494.

Hickin, E.J. and **Nanson, G.C.** (1984). Lateral migration rates of river bends. *Journal of Hydraulic Engineering,* **110**, 1557-1567.

Hooke, R. (1975). Distribution of sediment transport and shear stress in a meander bend. *Journal of Geology*, **83**, 543–565.

Hooke, J.M. (1997). Styles of channel change. *Applied fluvial geomorphology for river engineering and management*, 237-268.

Hooke, J.M. (2013). River meandering. In: Wohl, E. (Ed.), Treatise on Geomorphology. Academic Press, San Diego (California, United States). *Fluvial Geomorphology*, **9**,260–288.

Hubbard, S.M., Smith, D.G., Nielsen, H., Leckie, D.A., Fustic, M., Spencer, R.J. and **Bloom, L.** (2011). Seismic geomorphology and sedimentology of a tidally influenced river deposit, Lower Cretaceous Athabasca oil sands, Alberta, Canada. *American Association of Petroleum Geologists Bulletin*, **95**, 1123-1145.

Hughes, Z.J. (2012). Tidal Channels on Tidal Flats and Marshes*. Principles of Tidal Sedimentology*, (pp. 269–300). Eds Davis Jr. RA, Dalrymple RW (Springer, Dordrecht Heidelberg London New York).

Ielpi, A. and **Ghinassi, M.** (2014). Planform architecture, stratigraphic signature and morphodynamics of an exhumed Jurassic meander plain (Scalby Formation, Yorkshire, UK). *Sedimentology,* **61**, 1923-1960.

Ikeda, S., Parker, G. and **Sawai, K.** (1981). Bend theory of river meanders. 1. Linear development. *J Fluid Mech*, **112**:363–377.

Ishigaki, T., Shiono, K., Rameshwaran, P., Scott, C.F. and **Muto, Y.** (2000). Impact of Secondary Flow on Bed Form and Sediment Transport in a Meandering Channel for Overbank Flow. *Proceedings of Hydraulic Engineering*, **44**, 849-854.

Jackson, R.G. (1976). Depositional Model of Point Bars in the Lower Wabash River. *J Sed Petrol*, **46**(3),579–594.

Janocko, M., Nemec, W., Henriksen, S. and **Warchoł, M.** (2013). The diversity of deep-water sinuous channel belts and slope valley-fill complexes. *Marine and Petroleum Geology*, **41**, 7-34.

Kasvi, E., Vaaja, M., Alho, P., Hyyppä, H., Hyyppä, J., Kaartinen, H. and **Kukko, A.** (2013). Morphological changes on meander point bars associated with flow structure at different discharges. *Earth Surface Processes and Landforms,* **38**, 577-590.

Kolb, C.R. (1963). Sediments forming the bed and banks of the lower Mississippi River and their effect on river migration. *Sedimentology*, **2**(3), 227-234.

Kolla, V., Posamentier, H.W. and **Wood, L.J.** (2007). Deep-water and fluvial sinuous channels—Characteristics, similarities and dissimilarities, and modes of formation. *Marine and Petroleum Geology*, **24**(6), 388-405.

Labrecque, P.A., Jensen, J.L., Hubbard, S.M. and **Nielsen, H.** (2011). Sedimentology and stratigraphic architecture of a point bar deposit, Lower Cretaceous McMurray Formation, Alberta, Canada. *Bullettin of Canadian Petroleum Geology*, **59**,147–171.

Land, L.S. and **Hoyt, J.H.** (1966). Sedimentation in a Meandering ESTUARY1. *Sedimentology*, **6**(3), 191-207.

Lanzoni, S. and **Seminara, G.** (2002). Long-term evolution and morphodynamic equilibrium of tidal channels. *Journal of Geophysical Research: Oceans (1978–2012)*, **107**(C1), 1-1.

Leopold, L.B. and **Wolman, M.G.** (1960). River meanders. *Geological Society of America Bulletin*, **71**, 769-793.

Li, C., Chen, C., Guadagnoli, D. and **Georgiou, I.Y.** (2008). Geometry induced residual eddies in estuaries with curved channels: Observations and modeling studies. *J Geophys Res*, 113:C01005.

Loveless, J.H., Sellin, R.H.J., Bryant, T.B., Wormleaton, P.R., Catmur, S. and **Hey, R.** (2000). The Effect of Overbank Flow in a Meandering River on its Conveyance and the Transport of Graded Sediments. *Water and Environment Journal*, **14**, 447–455.

Marani, M., Lanzoni, S., Zandolin, D., Seminara, G. and **Rinaldo, A.** (2002). Tidal meanders. *Water Resour Res*, **38**(11),1225.

Marani, M., Belluco, E., D'Alpaos, A., Defina, A., Lanzoni, S. and **Rinaldo, A.** (2003). On the drainage density of tidal networks. *Water Resources Research*, **39**(2).

Marani, M., D'Alpaos, A., Lanzoni, S., Carniello, L. and **Rinaldo, A.** (2007). Biologically-controlled multiple equilibria of tidal landforms and the fate of the Venice lagoon. *Geophysical Research Letters*, **34**(11).

Marani, M., d'Alpaos, A., Lanzoni, S. and **Santalucia, M.** (2011). Understanding and predicting wave erosion of marsh edges. *GeophysicalResearch Letters*, **38**(21).

Massari, F., Rio, D., Barbero, R.S., Asioli, A., Capraro, L., Fornaciari, E. and **Vergerio, P.P.** (2004). The environment of Venice area in the past two million years. *Palaeogeography, Palaeoclimatology, Palaeoecology*, **202**(3), 273-308.

Massari, F., Grandesso, P., Stefani, C. and **Jobstraibizer, P.G.** (2009). A small polyhistory foreland basin evolving in a context of oblique convergence: the Venetian basin (Chattian to Recent, Southern Alps, Italy). *Foreland basins. Oxford: Blackwell Scientific*, 141-168.

McClennen, C.E. and **Housley, R.A.** (2006). Late-Holocene channel meander migration and mudflat accumulation rates, Lagoon of Venice, Italy. *Journal of Coastal Research*, 930-945.

McGowen, J.H and **Garner, L.E.** (1970). Physiographic features and stratification types of coarse-grained point bars: modern and ancient examples. *Sedimentology*, **14**,77-111.

Middelkoop, H. and **Asselman, N.E.** (1998). Spatial variability of floodplain sedimentation at the event scale in the Rhine–Meuse delta, The Netherlands. *Earth Surface Processes and Landforms*, **23**(6), 561-573.

Mjos, R., Walderhaug, O. and **Prestholm, E.** (2009). Crevasse splay sandstone geometries in the Middle Jurassic Ravenscar Group of Yorkshire, UK. *Alluvial Sedimentation, International Association of Sedimentologists, Special Publication*, **17**, 167-184.

Moody, J.A. and **Meade, R.H.** (2014). Ontogeny of point bars on a river in a cold semi-arid climate. *Geological Society of America Bulletin*, **126**(9-10), 1301-1316.

Morris, J.T., Sundareshwar, P.V., Nietch, C.T., Kjerfve, B. and **Cahoon, D.R.** (2002). Responses of coastal wetlands to rising sea level. *Ecology*, **83**(10), 2869-2877.

Mudd, S.M., D'Alpaos, A. and **Morris, J.T.** (2010). How does vegetation affect sedimentation on tidal marshes? Investigating particle capture and hydrodynamic controls on biologically mediated sedimentation. *Journal of Geophysical Research: Earth Surface (2003–2012)*, **115**(F3).

Naish, C. and **Sellin, R.H.J.** (1996). Flow structure in a large-scale model of doubly meandering compound channel. In: Ashworth, P.J., Bennet, S.J., Best, J.L., McLelland, S.J. (pp. 631–654). Eds. Coherent Flow Structures in Open Channels. John Wiley & Sons, Chichester (United Kingdom).

Nanson, G.C. (1980). Point bar and floodplain formation of the meandering Beatton River, northeastern British Columbia, Canada. *Sedimentology*, **27**,3-29.

Nanson, G.C. and **Hickin, E.J.** (1983). Channel migration and incision on the Beatton River. *Journal of Hydraulic Engineering*, **109**(3), 327-337.

Parker, G., Shimizu, Y., Wilkerson, G.V., Eke, E.C., Abad, J.D., Lauer, J.W., Paola, C., Dietrich, W.E. and **Voller, V.R.** (2011). A new framework for modeling the migration of meandering rivers. *Earth Surf Process Landforms*, **36**:70–86.

Peakall, J., McCaffrey, B. and **Kneller, B.** (2000). A process model for the evolution, morphology, and architecture of sinuous submarine channels. *Journal of Sedimentary Research*, **70**(3), 434-448.

Peakall, J., Ashworth, P.J. and **Best, J.L.** (2007). Meander-Bend Evolution, Alluvial Architecture, and the Role of Cohesion in Sinuous River Channels: A Flume Study. *Journal of Sedimentary Research*, **77**,197-212.

Reading, H.G. and **Collinson, J.D.** (1996). Clastic coasts. *Sedimentary environments: processes, facies and stratigraphy*, 154-231.

Rinaldo, A., Dietrich, W.E., Rigon, R., Vogel, G.K. and **Rodrlguez-Lturbe, I.** (1995). Geomorphological signatures of varying climate. *Nature,* **374**(6523),632–635.

Rizzetto, F. and **Tosi, L.** (2011). Aptitude of modern salt marshes to counteract relative sea-level rise, Venice Lagoon (Italy). *Geology*, **39**(8), 755-758.

Rizzetto, F. and **Tosi, L.** (2012). Rapid response of tidal channel networks to sea-level variations (Venice Lagoon, Italy). *Global and Planetary Change*, **92**, 191-197.

Roner, M., D'Alpaos, A., Ghinassi, M., Marani, M., Silvestri, S., Franceschinis, E. and **Realdon, N.** (2015). Spatial variation of salt-marsh organic and inorganic deposition and organic carbon accumulation: Inferences from the Venice lagoon, Italy. *Advances in Water Resources*.

Seminara, G. (2006). Meanders. *J Fluid Mech*, **554**,271–297.

Shiono, K. and **Muto, Y.** (1998). Complex flow mechanisms in compound meandering channels with overbank flow. *Journal of Fluid Mechanics*, **376**, 221-261.

Smith, D.G., Hubbard, S.M., Leckie, D. and **Fustic, M.** (2009). Counter point bar deposits: Lithofacies and reservoir significance in the meandering modern Peace River and ancient McMurray Formation, Alberta, Canada. *Sedimentology*, **56**,1655–1669.

Smith, D.G., Hubbard, S.M., Lavigne, J., Leckie, D.A. and **Fustic, M.** (2011). Stratigraphy of counter-point-bar and eddy-accretion deposits in low-energy meander belts of the Peace-Athabasca Delta, northeast Alberta, Canada. In: Davidson, S.K., Leleu, S., North, C.P. (pp. 143-152). Eds. River to Rock Record: The Preservation of Fluvial Sediments and Their Subsequent Interpretation. SEPM Special Publication 97.

Solari, L., Seminara, G., Lanzoni, S., Marani, M. and **Rinaldo, A.** (2002). Sand bars in tidal channels, part two, Tidal meanders. *J Fluid Mech*, **451**,203–238.

Terwindt, J.H.J. (1988). Palaeo-tidal reconstructions of inshore tidal depositional environments. In *Tide-influenced sedimentary environments and facies* (pp. 233-263). Reidel Dordrecht.

Thomas, R.G., Smith, D.G., Wood, J.M., Visser, J., Calverley-Range, E.A. and **Koster, E.H.** (1987). Inclined heterolithic stratification -Terminology, description, interpretation and significance. *SedGeol*, **53**,123–179.

Van de Lageweg, W.I., Schuurman, F., Cohen, K.M., van Dijk, W.M., Shimizu, Y. and **Kleinhans, M.G.** (2015). Preservation of meandering river channels in uniformly aggrading channel belts. *Sedimentology*, doi: 10.1111/sed.12229

Willis, B.J. (1993). Bedding geometry of ancient point bar deposits. In: Marzo, M., Puigdefabregas, C. (pp. 101–114). Eds. Alluvial Sedimentation. *International Association of Sedimentologists, Special Publication*, 17.

Wormleaton, P.R., Sellin, R.H.J., Bryant, T., Loveless, J.H., Hey, R.D. and **Catmur, S.E.** (2004). Flow structures in a two-stage channel with a mobile bed. *Journal of Hydraulic Research*, **42**, 145-162.

Zecchin, M., Baradello, L., Brancolini, G., Donda, F., Rizzetto, F. and **Tosi, L.** (2008). Sequence stratigraphy based on high-resolution seismic profiles in the late Pleistocene and Holocene deposits of the Venice area. *Mar Geol*, **253**,185–198.

Zecchin, M., Brancolini, G., Tosi, L., Rizzetto, F., Caffau, M. and **Baradello, L.** (2009). Anatomy of the Holocene succession of the southern Venice lagoon revealed by very high-resolution seismic data. *Continental Shelf Research*, **29**(10), 1343-1359.

ACKNOLEGMENTS

I wish to thanks all people that believe and believed in me, that supported and helped me during the last three years.

A special thanks goes to my supervisor Massimiliano Ghinassi, he is always present and gave me great support during all the PhD. He is a wonderful teacher, I've learnt so much from him and I hope to learn much more.

Another special thanks goes to my co-supervisor Andrea D'Alpaos, he always helped and supported me, giving me different perspective (an engineering perspective).

I am very grateful to both for the wonderful experience I had.

Thanks to my family. To my mum, my dad, my sister and brother. They are always there for me, maybe not physically but in every way they can. They support me every day, they believe in me and inspire me to give my best every day.

Thanks to all my friends, to those near and far. You are always with me and you make me feel at home, even when I'm not.

Thanks.